Dynamics of chromatin remodelling during plant cell differentiation

BREWER, GRACE,ELIZABETH

Dynamics of chromatin remodelling during plant cell differentiation

Grace Elizabeth Brewer

Thesis submitted for the qualification of Master of Science (MSc) by Research at The Department of Biosciences

Durham University

2017

Abstract

Cell differentiation is the process by which a pluripotent cell acquires a determined, specialised state. This process relies on the precise spatiotemporal control of gene expression, which is partly regulated at the level of chromatin architecture. Chromatin is a complex of nucleic acids and histone proteins which compresses DNA to fit in the cell nucleus. The structure of chromatin modulates the ability of eukaryotic cells to respond to developmental cues. It does so by regulating the accessibility of DNA to transcription factors and the RNA polymerase transcriptional machinery. Histone post-translational modifications are key contributors to the regulation of chromatin architecture during development.

This thesis investigates the key histone modifications associated with plant cell differentiation, and the role of auxin, cytokinin and brassinosteroids in guiding chromatin changes during plant cell differentiation. This entailed conducting numerous experiments on the model plant *Arabidopsis thaliana,* including observing the effect of loss of function of histone-modifying enzymes on root cell differentiation and cytokinin response. In addition, this thesis examined the effect of disturbing the balance of phytohormones on VASCULAR-RELATED NAC-DOMAIN 7 (VND7)-induced xylem transdifferentiation. Finally, protein-protein interaction assays were conducted to identify molecular interactions between hormone signalling genes and histone-modifying enzymes.

These experiments revealed that some loss-of-function mutants had a significantly different root meristem size to the wildtype and an impeded cytokinin response. This highlights the regulatory role of chromatin architecture in cell differentiation and indicates that hormone signals may guide histone-modifying enzymes during cell differentiation. Furthermore, disrupting the phytohormone balance resulted in defective VND7-induced xylem transdifferentiation, suggesting that a specific hormonal framework may be necessary to promote VND7 activity. Finally, the negative regulator of brassinosteroid signalling, BR-INSENSITIVE 2 (BIN2), was found to interact with histone methyltransferases SU(VAR)3–9-RELATED 5 (SUVR5), SU(VAR)3–9 HOMOLOG 5 (SUVH5) and CURLY LEAF (CLF).

Table of Contents

List of Figures

List of Tables

Statement of copyright

Acknowledgements

I wish to express my sincere gratitude to my supervisor, Dr Miguel de Lucas, who was abundantly helpful and offered invaluable support and guidance.

It also gives me great pleasure in acknowledging the support of Joey Nelson for all his help in the lab.

I would like to convey thanks to N8 Agrifood and Durham University for providing the financial means and laboratory facilities to support my studies.

1. Introduction

1.1 Cell differentiation

Cell differentiation is the process of a cell changing from one pluripotent cell type to another more specialised cell type (Stange, 1965). This process plays an essential and ongoing role throughout the course of development in multicellular organisms. Fundamentally, the many functionally specialised cell types produced as a result of cell differentiation, are organised into the diverse tissues and organs that make up multicellular organisms (Cooper, 2000).

When a cell differentiates it must make two sequential decisions. The first is when to stop proliferating and start undergoing differentiation, and the second is what cell fate to attain. Hormones play a major role in regulating the initiation of differentiation as well as cell type identity (Dello Ioio et al., 2008; Sabatini et al., 1999). Both of these processes rely on precise spatiotemporal gene expression patterns which determine cell morphology, biochemistry, and physiology. Such patterns of gene expression are controlled at multiple levels, one of which being chromatin architecture (Ralston and Shaw, 2008; Lelli et al., 2012).

1.2 Chromatin remodelling

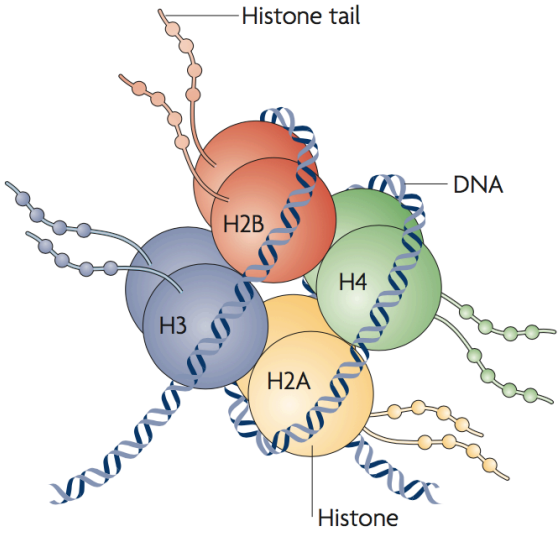

Figure 1: The nucleosome. The nucleosome consists of a length of DNA wrapped around a histone octamer. Figure taken from Tsankova et al. (2007).

Eukaryotic cells tightly package their DNA into a nucleoprotein complex called chromatin. A fundamental subunit of chromatin is the nucleosome (Figure 1). The nucleosome consists of 147 base pairs of DNA wrapped around a histone octamer comprising of two copies of each of the four core histone proteins H2A, H2B, H3 and H4 (Morales et al., 2001; Kouzarides, 2007). These four core histones have a C-terminal fold domain and an N-terminal tail (Davey et al., 2002). The C-terminal fold domain primarily mediates interactions between core histones (Arents et al., 1991; Arents et al., 1995) whilst the N-terminal tails protrude from the nucleosome core particle and are subject to a number of post-translational modifications that modulate chromatin architecture (reviewed in Kouzarides, 2007).

Chromatin architecture regulates the accessibility of DNA for various genomic processes including DNA replication, repair, recombination and transcription (Morales et al., 2001; Berr et al., 2011). Epigenetic determinants, such as DNA methylation and histone post-translational modifications, make dynamic and reversible changes to DNA and associated histones. These changes do not affect the DNA sequence yet alter chromatin structure (reviewed in Goldberg et al., 2007). Histone post-translational modifications occur on different amino acid residues on N-terminal histone tails or sometimes within the globular histone core (Bannister and Kouzarides, 2011). These modifications modulate transcription both directly and indirectly. This involves moderating DNA accessibility to transcription factors and RNA polymerase transcriptional machinery as well as recruiting effector protein complexes to the nucleosome surface (Berger, 2007).

Numerous studies have shown that specific histone modifications are associated with open chromatin and actively transcribed genes, whilst other histone modifications are linked to chromatin condensation and transcriptional repression (Berger, 2007). For example, histone acetylation is activating (Zentner and Henikoff, 2013), whilst histone methylation can be both activating and repressive depending on the number of methyl groups added (Bannister et al., 2002) and the amino acid residue modified (Kouzarides, 2002). These post-translational histone modifications are regulated by enzymes which either add (“writers”) or remove (“erasers”) histone marks (Srivastava et al., 2016). According to the histone code hypothesis (Jenuwein and Allis 2001;

Strahl and Allis, 2000), histone writers and erasers mediate combinations of histone marks, which synergistically and antagonistically interact with one another to dynamically modulate chromatin compaction and gene expression.

1.3 The *Arabidopsis* root and xylem differentiation pathway as model systems

Plants are ideal systems for research into epigenetic regulation of development. As sessile organisms, plants have remarkable developmental plasticity and form most organs post-embryonically. This requires continuous epigenetic reprogramming and enables plants to adapt to dynamic growth environments. Furthermore, many plant epigenetic regulators are well conserved amongst metazoans (Geisler and Paro, 2015). *Arabidopsis thaliana,* in particular, has been widely recognised in plant research as a good model system. This is due to its small diploid genome, short generation time, small size, its ability to generate a lot of seed through self-pollination and it is easy to transform (Koornneef and Meinke, 2010).

In plants, growth occurs through a combination of cell division and cell elongation which take place in meristems. Apical meristems located at the tip of shoots and roots give rise to primary growth, which increases the length of shoots and roots. On the other hand, lateral meristems, which include the vascular cambium and cork cambium, are responsible for increasing plant width, known as secondary growth (Nieminen et al., 2015; McManus and Veit, 2002). In the root apical meristem, stem cell initials give rise to all cell types of the root. These initials are located adjacent to the quiescent centre (QC), which is responsible for maintaining initials in an undifferentiated state (Dolan et al., 1993; van den Berg et al., 1997). Cell lineages can be easily identified in the root as continuous files of cells emerging from repeated transverse divisions in daughter cells of stem cell initials, called transit amplifying cells (Dolan et al., 1993; Perilli et al., 2012). The robust cellular organisation and simple structural and functional organisation of the *Arabidopsis* root make it an excellent model system to study developmental processes (Scheres and Wolkenfelt, 1998).

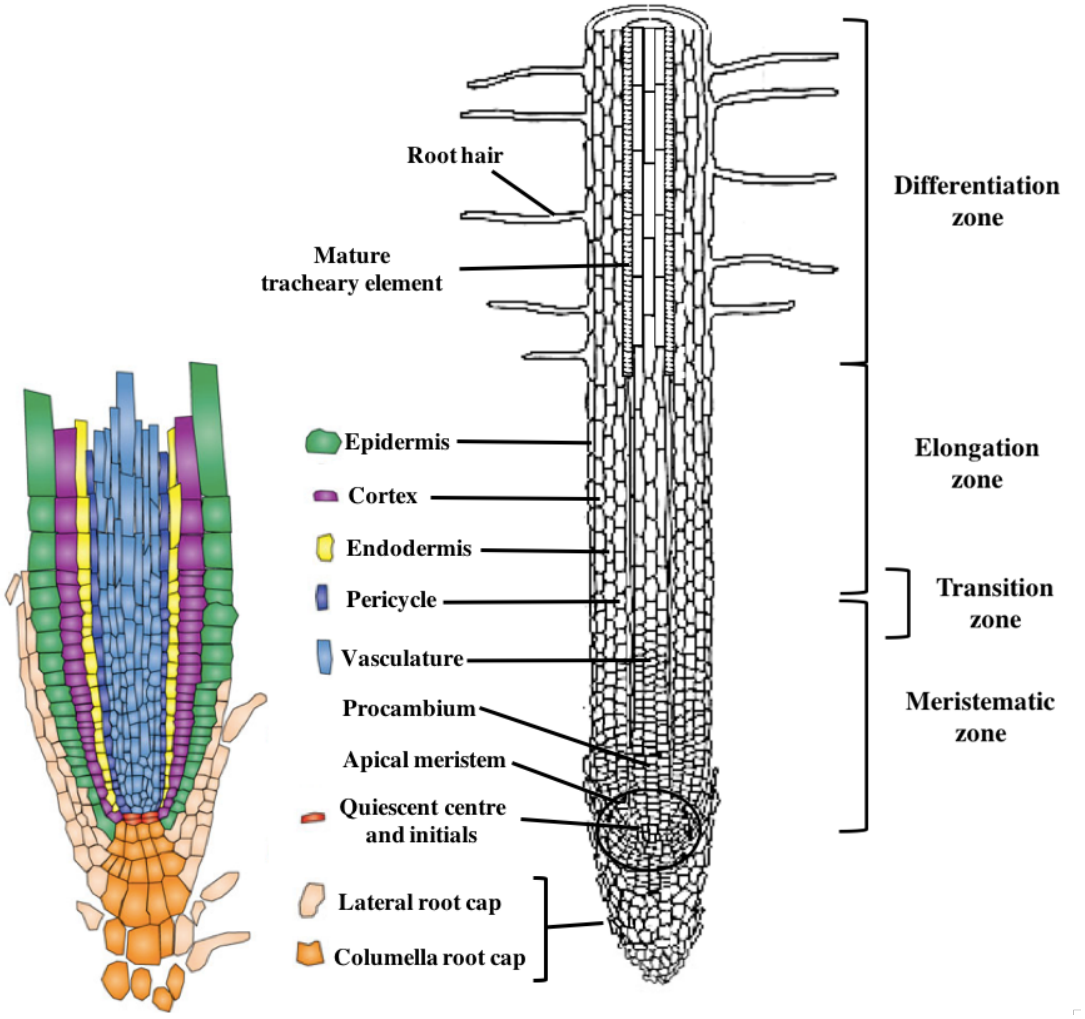

Figure 2: Structure of *Arabidopsis* primary root. Figures adapted from Jaillais and Chory (2010) and Thies and Grossman (2006).

The *Arabidopsis* root consists of concentric cell layers of epidermis, cortex, endodermis, pericycle and finally vascular tissue in the centre of the root (Figure 2). Along the longitudinal axis, typical plant roots contain four distinct developmental zones which reflect a temporally ordered series of developmental events that are easy to track. In the meristematic zone, the transit amplifying cells undergo rapid mitotic division. In the transition zone, cells stop dividing and increase slowly in length. In the zone of elongation, cells undergo rapid elongation. Finally, in the zone of differentiation, elongated cells become specialised mature cells. This differentiation zone is easily recognised by the formation of epidermal root hairs (Dolan et al., 1993).

The xylem differentiation pathway in roots, in particular, offers a tractable system to study chromatin remodelling processes during cellular differentiation. Xylem is part of the vascular system of plants which transports water and minerals through the plant body and also provides mechanical support (reviewed at Lucas et al., 2013). Tracheary elements (TEs) are one of three types of highly specialised cells which make up xylem. They undergo a well-defined differentiation process from meristematic cells of the procambium, which involves patterned secondary cell wall deposition, lignification, programmed cell death and autolysis (Fukuda, 1996). The establishment and utilisation of experimental systems for induced TE differentiation have enabled the discovery of many factors and key genes involved in their differentiation (Fukuda, 1997; Ye, 2002). Therefore, there is a variety of experimental tools and extensive transcriptional data available to study this process.

1.4 Histone modifications and plant cell differentiation

Cell differentiation is accompanied by dynamic chromatin remodelling. In mammalian systems, it has been shown that pluripotent stem cells are typically associated with a more open chromatin configuration that is accessible for transcriptional activation. On the other hand, differentiated cells have a more condensed and repressive chromatin configuration (Meshorer and Misteli, 2006; Mattout and Meshorer, 2010). In both mammalian and plant systems, this dynamic chromatin remodelling during cell differentiation has been linked to the deposition or removal of different sets of active and repressive chromatin marks. In differentiated cells, net genomic coverage of repressive chromatin marks increases (Aoto et al., 2006; Bartova et al., 2008; De Lucas, 2016), yet decreases for transcriptionally active chromatin marks (Lee et al., 2004; Krejci et al., 2009; De Lucas, 2016).

A variety of histone post-translational modifications exist that modulate chromatin compaction, including acetylation, methylation, phosphorylation, ubiquitination, amongst others (Huang et al., 2014). Of these, histone acetylation and histone methylation are the most studied in relation to chromatin remodelling and transcription and will therefore be focused upon in this study.

1.4.1 Histone acetylation

Histone acetylation is a major histone modification whereby an acetyl group is added to lysine residues on amino-terminal tails of histones. This neutralises the positive charge of lysines and weakens histone interactions with negatively charged DNA, which subsequently leads to an open, permissive chromatin configuration and active transcription (Zentner and Henikoff, 2013). Histone acetylation is regulated by histone acetyltransferases (HATs) and histone deacetylases (HDAs) that add and remove acetyl groups, respectively (Struhl, 1998).

Research has shown that histone acetylation can play a key role in maintaining meristem activity and controlling the transition from cell division to cell differentiation. Histone acetylation levels decrease as cells progress from mitotically active, undifferentiated meristematic cells to fully differentiated cells in the *Arabidopsis* root (Rosa et al., 2014). Moreover, loss of function of the histone H3 acetyltransferase GENERAL CONTROL NONDEREPRESSIBLE 5 (GCN5), results in shorter roots and reduced meristem size (Kornet and Scheres, 2009). On the other hand, inhibition of certain HDAs using Trichostatin A (TSA) leads to hyperacetylation, which delays cell differentiation and induces the expression of a meristem marker in cells from the differentiation zone (Rosa et al., 2014).

It has recently been shown that other HDAs, that are not inhibited by TSA treatment, namely HDT1 and HDT2, regulate the transition from cell division to cell elongation. Knockdown of *HDT1/2* resulted in a premature switch from cell division to cell elongation and a reduction in root meristem cell number (Li et al., 2017). This is because HDT1/2 negatively regulate the acetylation levels and expression of *C_{19}-GIBBERELLIN 2-OXIDASE 2* (*GA2ox2*), which encodes for a major gibberellin (GA) inactivating pathway in *Arabidopsis* (Rieu et al., 2008). GA promotes mitotic activity (Ubeda-Tomas et al., 2009; Achard et al., 2009) and delays the developmental switch from cell division to cell elongation (Moubayidin et al., 2010). Thus HDT1/2 control GA metabolism to regulate cell progression in roots.

Histone deacetylation also plays a crucial role in maintaining stem cell fate in the root apical meristem. WUSCHEL-RELATED HOMEOBOX 5 (WOX5) transcription factor is a key regulator of the root apical meristem stem cell niche. *WOX5* is expressed in the QC cells and the protein moves to surrounding stem cells initials where it recruits the co-repressor TOPLESS (TPL) and HDA19 to differentiation-promoting factor gene *CYCLING DOF FACTOR 4* (*CDF4*). Thus, WOX5-mediated histone deacetylation represses *CDF4* to maintain stem cells in their undifferentiated state (Pi et al., 2015).

1.4.2 Histone methylation

Histone methylation is defined as the transfer of one, two or three methyl groups to lysine (K) or arginine (R) residues on amino-terminal tails of histones (reviewed in Ng et al, 2009). The effect of histone methylation on gene expression is complex and varies according to which amino acid residue is modified (Kouzarides, 2002), and also how many methyl groups are added (Bannister et al., 2002). Whilst methylation of histone H3 at lysine 9 (H3K9) or lysine 27 (H3K27) correlates with transcriptional repression (Ikeuchi et al., 2015a; Schubert et al., 2006), methylation at H3K4 or H3K36 is activating (Jenuwein and Allis, 2001; Zhang et al., 2009). Arginine methylation also dynamically regulates transcription. Whilst methylation of histone H3 at arginine 17 (H3R17) has been associated with transcriptional activation (Niu et al., 2008), methylation at H4R3 has been associated with repressing target gene expression (Wang et al., 2007; Yue et al., 2013; Cho et al., 2012).

Polycomb group (PcG) and trithorax group (trxG) proteins are key regulators of developmental gene expression, which mediate histone methylation deposition via a catalytic Su(var) 3-9, Enhancer of zeste and Trithorax (SET) domain (Jenuwein et al., 1998). PcG proteins exist in two separate complexes, one of which, Polycomb Repressive Complex 2 (PRC2), is recruited to DNA via Polycomb response elements (PREs) (Xiao et al., 2017) and catalyses trimethylation of H3K27 (H3K27me3) (Kuzmichev et al., 2002; Cao et al., 2002; Muller et al., 2002). TrxG proteins on the other hand can counteract PcG function and catalyse methylation of H3K4 and H3K36. This activates gene expression by mediating chromatin decondensation (Byrd

and Shearn, 2003; Wysocka et al., 2005; Dorighi and Tamkun; 2013). Such histone marks can be removed by jumonji domain C (JmjC domain) containing demethylases (Tsukada et al., 2006; Chen et al., 2006).

A trxG protein, SET DOMAIN GROUP2 (SDG2), controls the H3K4me3 mark in most genes (Guo et al., 2010). Loss-of-function of SDG2 results in reduced root growth due to impaired mitotic activity in the meristem zone (Yao et al., 2013). Furthermore, another H3K4 histone methyltransferase, ARABIDOPSIS TRITHORAX 1 (ATX1)/SDG27, is known to play an important role in modulating cell proliferation and the transition to elongation such that *atx1-1* mutants also show defects in root growth (Napsucialy-Mendivil et al., 2014).

H3K27me3-mediated gene silencing is catalysed by homologs of *Drosophila* core subunit Enhancer of zeste [E(z)] in the *Arabidopsis* PRC2 complex, namely CURLY LEAF (CLF), SWINGER (SWN) and MEDEA (MEA) (Goodrich et al., 1997; Chanvivattana et al., 2004; Grossniklaus et al., 1998). PRC2 is known to target the H3K27me3 repressive mark to specific genomic regions in response to developmental cues (Boland et al., 2014) and De Lucas et al. (2016) found that H3K27me3 repressive mark is more prevalent in cells that have started the differentiation process. H3K27me3 may be responsible for restricting meristematic activity as Aichinger et al. (2011) found that loss of function of CLF resulted in larger meristem size and longer roots. Furthermore, loss-of-function mutants in multiple PRC2 subunits fail to retain mature somatic root hair cells in their differentiated state, resulting in dedifferentiation and the generation of a callus, an unorganised pluripotent cell mass (Ikeuchi et al., 2015b). Together, these studies demonstrate the importance of PRC2-mediated H3K27me3 in establishing and maintaining the differentiated status of cells.

1.5 Hormonal regulation of plant cell differentiation

Plant hormones have essential roles in controlling diverse growth and developmental processes in the plant root. Extensive crosstalk occurs between phytohormones to co-ordinately control specific developmental processes in roots including cell division, elongation and differentiation (Takatsuka and Umeda, 2014). In particular, the role of

auxin, cytokinin (CK) and brassinosteroid (BR) signalling in controlling cellular decisions during differentiation has been the subject of much research.

1.5.1 Hormone signals and cell differentiation initiation

In root cells, the first cell differentiation decision of when to switch from cell division to cell differentiation, is modulated by hormonal signals. Auxin is known to promote cell division in the root meristematic zone (Dello Ioio et al., 2008) such that exogenous application of auxin causes an increase in meristem size due to an increase in the rate of cell division (Dello Ioio et al., 2007). On the other hand, mutants in the auxin efflux carrier, PIN-FORMED 2 (PIN2), show a reduction in root meristem size as a result of a decrease in cell division (Blilou et al., 2005). CK promotes meristematic cell differentiation and delimits the transition zone in root meristems (Dello Ioio et al., 2008; Perilli and Sabatini, 2010). Dello Ioio et al. (2007) found that exogenous application of CK results in a decrease in the number of meristematic cells, and therefore reduction in meristem size. It was also found that CK-deficient plants with mutations in CK receptor ARABIDOPSIS HISTIDINE KINASE 3 (AHK3) and the ARABIDOPSIS TYPE B CK-RESPONSE REGULATORS (ARRs), ARR1 and ARR12 (Dello Ioio et al., 2007), exhibit an increased meristem size due to progressive accumulation of meristematic cells.

The root meristem size is thought to be established and maintained by a balance between CK and auxin signalling. CK has been found to directly antagonise auxin action in the transition zone. It does so, in part, by regulating the expression of *SHORT HYPOCOTYL 2* (*SHY2*), a member of the AUXIN/INDOLE-3-ACETIC ACID (AUX/IAA) family of transcriptional repressors and *GH3.17*, a member of the GRETCHEN HAGEN 3 (GH3) group II family of auxin-inducible acyl-acid-amido synthetases. ARR1, a transcription factor produced downstream of CK signalling, promotes *SHY2* expression. *SHY2* represses *PIN* auxin efflux carrier genes and inhibits polar auxin transport (Dello Ioio et al., 2008; Ruzicka et al., 2009). Furthermore, recent research has shown that ARR1 transcriptionally activates *GH3.17* which induces auxin catabolism (Di Mambro et al., 2017). CK control of both polar auxin transport, via *SHY2*, and auxin degradation, via *GH3.17*, defines the auxin

minimum. This CK-dependant auxin minimum controls the switch from cell division to cell differentiation to establish the position of the root transition zone and subsequently monitor meristem size (Di Mambro et al., 2017).

In addition to auxin and CK, BRs also play a crucial role in regulating meristem activity. BR perception is required in the epidermis to promote cell division of transit amplifying cells, which increases the meristem size (Hacham et al., 2011; Vragović et al., 2015). Vragović et al. (2015) showed that epidermal BR control of cell proliferation is mediated by auxin. Furthermore, BRs maintain the self-renewing capacity of the QC, which also determines the root meristem size (González-García et al., 2011). Throughout root development, endogenous BR levels are controlled spatiotemporally such that low levels of BRs maintain QC activity and meristem size, whilst higher BR concentrations promote cell elongation and differentiation in the transition zone (Chaiwanon and Wang, 2015; González-García et al., 2011).

1.5.2 Hormone signals and cell identity

Hormonal signals also play an essential role in determining cell identity. For example, many studies have demonstrated the importance of auxin, CK and BR signalling in cell fate determination during vascular development. Auxin plays an important role in the early stages of vascular patterning. Polar auxin flow is essential for continuous vascular formation such that mutants in the auxin transport protein PIN1 show excess vascularisation (Gälweiler et al., 1998). Furthermore, mutations in the *GNOM* gene, which encodes an ADP-ribosylation factor G protein (ARF GEF) required for polar localisation of PIN1 (Steinmann et al., 1999), have clustered TEs or scattered single TEs that are not interconnected to form strands (Jürgens et al., 1991; Mayer et al., 1991). Mutations in the *MONOPTEROS* (*MP*) gene, which encodes an auxin response factor, result in reduced vascular tissue due to formation of discontinuous vascular strands (Hardtke and Berleth, 1998). Reduced vasculature and severe vascular patterning defects are also observed in mutants with defects in perceiving auxin such as *axr6* (Hobbie et al., 2000). Alongside vascular patterning, Yoshida et al. (2005) demonstrated the importance of auxin for transdifferentiation into TEs using a *Zinnia elegans* cell culture system. They found that treating cultured *Zinnia* mesophyll cells

with the auxin transport inhibitor 1-N-naphthylphthalamic acid (NPA) inhibited transdifferentiation. The inhibitory effect of NPA on transdifferentiation could be overcome by treatment with a high concentration of auxin 1-naphthaleneacetic acid (NAA). Later, NAA was found to promote expression of genes associated with auxin signalling and transcriptional regulators of vascular cell differentiation (Yoshida et al., 2009).

CK has also been implicated in controlling specification of vascular cell files. In wildtype *Arabidopsis,* the root vascular cylinder constitutes phloem poles and procambial cell files flanking a central axis of xylem. In the xylem axis, metaxylem is typically located in central positions and protoxylem in marginal positions (Mähönen et al., 2006b). In mutants with defects in components of the CK signalling pathway, such as CK receptor WOODEN LEG (WOL) and ARR1, ARR10, and ARR12 transcription factors, all cells within the vasculature differentiate solely into protoxylem (Mähönen et al., 2000; Argyros et al., 2008). Moreover, treatment with CK inhibits protoxylem formation (Mähönen et al., 2006a). Together, these results suggest that CK negatively regulates protoxylem differentiation, such that in developing protoxylem, ARABIDOPSIS HISTIDINE PHOSPHOTRANSFER PROTEIN 6 (AHP6) down-regulates CK signalling (Mähönen et al., 2006b).

CK signalling has been shown to integrate with auxin signalling to specify vascular patterning in the root meristem. *AHP6* expression is auxin-dependent and loss of function of AHP6 expands CK-related gene expression domains from procambium into protoxylem position, which prevents protoxylem differentiation (Mähönen et al., 2006b). Moreover, CK signalling in the procambium promotes the bisymmetric distribution of the PIN auxin efflux proteins which channel auxin into the central xylem axis (Bishopp et al., 2011). CK is also thought to increase the sensitivity of cambial initials to auxin, which promotes initials to differentiate into TEs, as CK induces TE formation acropetally in the presence of auxin IAA (Baum et al., 1991).

BRs also play an essential role in vascular patterning. BR biosynthesis mutants such as *dwarf7-1* have fewer vascular bundles which are irregularly spaced and the size and number of xylem cells is greatly reduced (Choe et al., 1999). Another BR

biosynthesis mutant, *cpd,* was found to show unequal division of the cambium such that more phloem cells were present at the expense of the xylem (Szekeres et al., 1996). The BR perception mutant *bri1* shows a similar phenotype of increased phloem relative to xylem per vascular bundle (Caño-Delgado et al., 2004). Iwasaki and Shibaoka (1991) and Yamamoto et al. (1997) demonstrated that BRs are also necessary for TE differentiation. Transdifferentiation of mesophyll cells into TEs was inhibited when *Zinnia* cell cultures were treated with the BR biosynthesis inhibitor, uniconazole, whilst addition of brassinolide (BL) overcame this inhibitory effect (Iwasaki and Shibaoka, 1991).

1.6 Histone modifications and plant hormone signalling

Numerous studies have revealed a direct link between hormone signalling and histone modifications during plant development. TOPLESS (TPL)/TPL-RELATED (TPR) belongs to the plant Groucho corepressor family (Causier et al., 2012) and has been shown to repress the expression of numerous hormone-related genes by recruiting HDAs (Szemenyei et al., 2008; Causier et al., 2012). For example, TPL/TPR has been shown to recruit HDA19 to repress BR signalling positive regulator BRASSINAZOLE-RESISTANT 1(BZR1) target genes (Wang et al., 2013), AUXIN RESPONSE FACTOR (ARF) target genes (Long et al., 2006) and abscisic acid (ABA) signalling genes targeted by BZR2/BRI1-EMS-SUPPRESSOR 1 (BES1) (Ryu et al., 2014). Furthermore, it has recently been shown that BES1-mediated control of root meristem activity relies on TPL/TPR repressive function and the recruitment of HDA19 (Espinosa-Ruiz et al., 2017).

Asides from TPL/TPR/HDA19 control of hormone signalling, Zhang et al. (2014a) demonstrated an interaction between BR and GA signalling and chromatin remodelling factor PICKLE (PKL). PKL controls BR and GA signalling and inhibits the H3K27me3 modification of cell elongation–related genes in the dark to promote hypocotyl growth (Zhang et al., 2014a). Other studies have shown that recruitment of HATs increases the expression of auxin-responsive genes (Weiste and Dröge-Laser, 2014). A final example is that BES1 interacts with two JmjN/C domain-containing

proteins, thought to be histone demethylases that target H3K9me3, to regulate BR-related gene expression and obtain the optimal BR response (Yu et al., 2008).

In the context of cell differentiation, mutants in genes encoding chromatin remodelling enzymes have defects in cell differentiation (Ikeuchi et al., 2015a) and share characteristics with auxin and CK mutants (Dello Ioio et al., 2008). This suggests that hormone signalling components may interact with chromatin remodelling enzymes during differentiation. Much further investigation is required however to elucidate the mechanisms by which hormones integrate with chromatin remodelling during cellular differentiation.

1.7 Experimental aims and hypothesis

In light of previous research, I present the hypothesis that hormone signalling guides histone modifications during plant cell differentiation.

To test this hypothesis, this study aims to answer the following questions:

- What are the principal histone modifications associated with plant cell differentiation?
- How does hormone signalling regulate TE differentiation?
- What are the molecular interactions between hormone signalling genes and histone modifying enzymes and what is the context and biological meaning of these interactions?

Firstly, loss-of-function mutants in histone modifying enzymes were treated with differentiation-promoting CK and the root meristem size was measured. This identified the key histone modifying enzymes associated with cell differentiation initiation that are regulated by CK.

Next, a TE trans-differentiation experimental system was used which utilised estradiol-inducible overexpression of the master regulator *VASCULAR-RELATED NAC-DOMAIN* 7 (*VND7*). Hormones were applied to *VND7* inducible seedlings, and

the impact of perturbing hormone levels on TE induction was identified by looking at secondary cell wall deposition.

Finally, to identify the molecular interactions between hormone signalling genes and histone modifying enzymes, a yeast two-hybrid (Y2H) protein-protein interaction assay was performed. Positive interactions were validated *in vivo* by bimolecular fluorescence complementation (BiFC) before the context and biological meaning of these interactions was investigated using a number of different methods. These included analysing the expression of candidate genes in hormone-treated loss-of-function mutants using quantitative real time (qRT)-PCR and investigating the effect of loss of function of histone modifying enzymes on hormone response.

2. Materials and methods

2.1 Chemical suppliers

Details of the suppliers of all chemicals and reagents used in this study are described in Appendix 1.

All restriction enzymes and respective buffers were purchased from Thermo Fisher Scientific unless an alternative supplier is stated.

2.2 Plant materials and growth conditions

2.2.1 Plant material

The wildtype *Arabidopsis thaliana* seeds were obtained from laboratory stocks of Columbia ecotype (Col0). All seeds used in this study were in Col0 ecotype background.

Histone modifying enzyme loss-of-function mutants *ash1 homolog 3* (*ashh3,* AT2G44150, SALK_131218.49.35.n), *ash1-related 1* (*ashr1,* AT2G17900, SALK_018048.35.40.x), *homologue of trithorax 1* (*atx1,* AT2G31650, SALK_149002.50.05.x), *arabidopsis trithorax-related protein 5* (*atxr5,* AT5G09790.1, SALK_130607.54.85.x), *curly leaf 29* (*clf29,* AT2G23380, SALK_021003.55.50.x), *arabidopsis lysine-specific histone demethylase 1* (*ld1,* AT1G62830, SALK_034869.39.40.x), *homolog of su(var)3-9 1* (*suvr1,* AT1G04050, SALK_021874.47.35.x), *jumonji domain-containing protein 22* (*jmj22,* AT5G06550, SAIL_680_G02), *swinger 7* (*swn7,* At4g02020, SALK_109121), *su(var)3-9 homolog 8* (*suvh8,* AT2G24740, SALK_123140.21.25.x), and *su(var)3–9-related 5* (*suvr5*, AT2G23740, SALK_026224.41.90.x) (Alonso et al., 2003; Sessions et al., 2002) were obtained from SALK and SAIL collections of T-DNA insertion lines courtesy of Nottingham Arabidopsis Stock Centre (NASC).

The *VND7* conditional overexpression (VND7ox) line (Coego et al., 2014) was obtained from NASC. The HISTONE 2B::YELLOW FLUORESCENT PROTEIN (H2B::YFP) line (Boisnard-Lorig et al., 2001) was kindly donated by Dr. Peng Wang (Durham University). VND7ox plants were crossed with H2B::YFP plants to obtain the VND7ox;H2B::YFP line. The XVE::GUS line was obtained courtesy of Prof. Salomé Prat (CNB-CSIC, Madrid. Spain).

2.2.2 Seed sterilisation

Seeds were sterilised in 1.5ml Eppendorf tubes first with 500µL of sterilisation solution (70% ethanol (EtOH), 0.1% Tween 20) for 15 minutes with constant shaking using an orbital shaker. 500µL of 100% EtOH was then added to the tubes which were shaken for a further 5 minutes before repeating this step once again. The next stage of seed sterilisation was carried out in sterile conditions under a laminar flow hood. All liquid was removed from the seeds and 500µL of fresh 100% EtOH was added to each tube followed by a further 5 minutes of constant shaking. After removal of the 100% EtOH, the seeds were left to air dry in the laminar flow hood and stored at room temperature until used for experiments.

2.2.3 Plant growth medium

1X Murashige and Skoog (MS) medium was made up to contain 4.3g/l of MS basal salt mixture, 10g/l sucrose, 0.5g/l 2-(N-morpholino)ethanesulfonic acid (MES), and 10g/l agar for vertical plates or 8g/l agar for horizontal plates. The pH was adjusted to pH 5.8 using a 0.1M KOH solution before the addition of agar. Media was autoclaved for 20 min at 121°C.

Table 1: Hormone stock solution preparation

Hormone	Stock solution
3-Indolacetic Acid (IAA)	10mM in EtOH
Bikinin	10mM in dimethylsulfoxide (DMSO)
Brassinazole (BRZ)	1mM in DMSO
Epibrassinolide (BL)	10mM in DMSO
ß-estradiol	100mM in EtOH
Trans-zeatin	30mM in 1M NaOH

Hormones were filter sterilised through 0.22µm nylon syringe filters and added to cooled MS media after autoclaving. Stock solutions were prepared according to Table 1, aliquoted and stored at -20ºC.

2.2.4 Plant growth conditions

In a laminar flow hood, sterilised seeds were sown onto square plates or petri dishes containing 1X MS medium. To synchronise germination, seeds were stratified for 2-3 days at 4ºC before being grown vertically or horizontally in a growth chamber with a 16h light/8h dark cycle at 21ºC.

For seeds sown onto soil, seeds were stratified in distilled water (dH_2O) at 4ºC for 2-3 days and then transferred to soil in pots. Pots were then covered with a plastic lid and placed in a greenhouse with a 16h light at 22ºC/8h dark at 18ºC growth cycle.

2.3 Plant genotyping

2.3.1 Plant genomic DNA extraction

Sample material was placed in 1.5ml tubes along with two stainless steel grinding balls and 100µL of 1X extraction buffer (stock 10X extraction buffer: 200mM TRIS HCl pH 7.5, 250mM NaCl, 25mM Ethylenediaminetetraacetic acid (EDTA), and 0.5% Sodium Dodecil Sulfate (SDS) diluted to 1X with dH_2O). The tubes were placed into grinding blocks and the samples were ground for 2 minutes at 25Hz. The samples were then centrifuged for 5 minutes at maximum speed and 50µL of the supernatant containing genomic DNA was added to new tubes along with 50µL water.

2.3.2 Genotyping PCR

Table 2: Genotyping PCR reaction mix

Reagent	**Volume/reaction (µL)**
Taq Mix	6
Forward Primer (10µM)	0.1
Reverse Primer (10µM)	0.1
dH_2O	3.8
DNA	2

Table 3: Genotyping PCR cycling conditions

Temperature (°C)	**Time**	**Number of cycles**
95	2min	1
95	15s	41
50	30s/Kb	
72	1min	
72	5min	1
12	∞	

The genotyping PCR reaction mix was set up according to Table 2 and performed according to the PCR cycling conditions detailed in Table 3. All genotyping PCR primers used are listed in Appendix 2.

2.3.3 Agarose gel electrophoresis

PCR products were tested using agarose gel electrophoresis. Agarose gels were prepared from 1g agarose dissolved in 100ml 1X TAE buffer (40mM Tris pH 7.6, 20mM acetic acid, 1mM EDTA) and ethidium bromide was added to a final concentration of 0.5µg/ml. 5µL of sample was loaded into wells with 6X DNA loading buffer (60% glycerol, 0.25% bromophenol blue, 0.25% xylene cyanol FF, 150mM Tris pH 7.6). Each gel also had a separate well containing 5µL hyperladder for fragment size determination. Gels were run at 150V for approximately 20 minutes. Gels were imaged using a Syngene InGenius gel documentation system controlled by GeneSnap software.

2.4 Root meristem size analysis

Seedlings were grown on vertical MS agar plates for 5 days as described under section 2.2.4. 5-d-old seedlings were transferred using hooked forceps onto vertical MS agar plates supplemented with 0.1μM trans-Zeatin or 0.1μM DMSO as a control and incubated in a growth chamber for 16 hours. After 16 hours of treatment, a blade was used to cut away the shoot from the seedlings and only the root was placed on a glass slide containing 10μg/ml propidium iodide. The stained roots were imaged immediately using a Zeiss 510 Meta confocal laser scanning microscope.

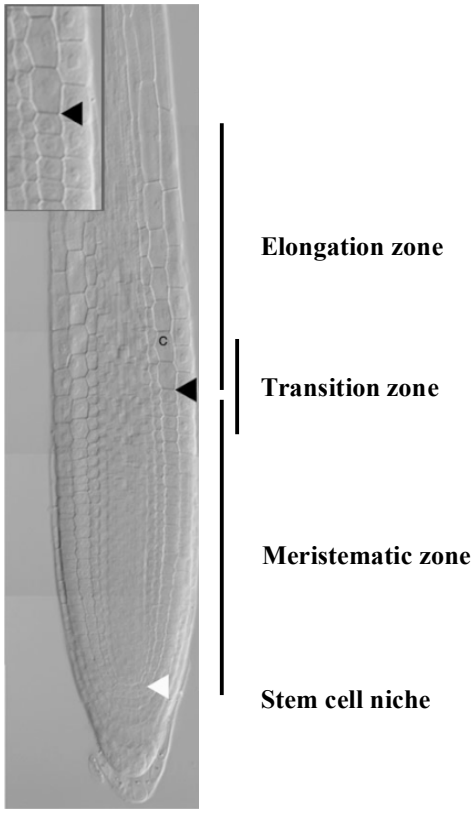

Figure 3: Root meristem size. The root meristem size was calculated as the number of cortex cells in a file (c) between the QC (white arrowheads) and the first elongated cortex cell (black arrowheads). Figure taken from Perilli and Sabatina (2010).

The root meristem size was measured from the microscopy images using the ImageJ (NIH) software to count the number of meristematic cortex cells in a file extending from the QC to the first elongated cell excluded (from white to black arrowhead in Figure 3) (Perilli and Sabatina 2010).

2.5 Hormone treatment of conditional overexpression lines

Seedlings were grown on vertical MS agar plates for 5 days according to conditions described in section 2.2.4. 5-d-old seedlings were carefully transferred onto vertical MS agar plates supplemented with 10μM IAA, 10μM trans-Zeatin, 0.2μM BL or non-supplemented MS agar plates as a control and placed in a growth chamber for 24 hours. After 24 hours of pre-treatment, seedlings were carefully transferred onto vertical MS agar plates supplemented with either 10μM DMSO or 10μM estradiol as well as either 10μM IAA, 10μM trans-Zeatin, 0.2μM BL or non-supplemented MS agar plates and placed in a growth chamber for a further 72 hours.

VND7ox roots were stained with propidium iodide according to the protocol described in Coiro and Truernit (2017) and mounted in clearing solution (chloral hydrate/glycerol/water, 8:1:2, w/v/v) on glass slides. VND7ox;H2B::YFP roots were cleared using ClearSee (10% xylitol, 15% sodium deoxycholate, 25% urea) and stained with 1mg/ml Calcofluor White following the methods as found in Kurihara et al. (2015) and mounted in ClearSee solution on glass slides. VND7ox and VND7ox;H2B::YFP stained roots were imaged using a Zeiss 880 confocal laser scanning microscope.

XVE:GUS seedling roots were fixed in 90% acetone for 30 minutes, washed twice with water and submerged in GUS staining solution (50mM Phosphate buffer, 0.1% Triton TX-100, 1.5mM Potassium Ferrocyanide, 1.5mM Potassium Ferricyanide, 2mM 5-bromo-4-chloro-3-indolyl ß-D-glucuronide cyclohexamine salt dissolved in DMSO). After 5 mins of vacuum infiltration, samples were incubated at 37°C in the dark for 18 hours. XVE:GUS roots were then washed with increasing concentrations of diluted ethanol (70%, 50%, 30% and 10%) and then dH_2O before being mounted in clearing solution on glass slides. XVE:GUS roots were imaged using brightfield microscopy.

2.6 Xylem differentiation induction in *Arabidopsis* leaves

Arabidopsis leaf discs were co-cultured with auxin, cytokinin (CK) and bikinin for 3 days to induce ectopic transdifferentiation of mesophyll cells to tracheary elements (TEs) according to the protocol as in Saito et al. (2017). Images were taken of the leaf discs using brightfield microscopy.

2.7 Hot fusion cloning

2.7.1 Plasmid vectors

Genes of interest were cloned into pGBKT7 DNA-binding domain cloning vectors and pGADT7 activation domain cloning vectors (Clontech).

2.7.2 Primer design

Primer pairs were designed to incorporate 17bp homologous to the target site of the plasmid vector, followed by 22bp homologous to the gene of interest. A list of the hot fusion cloning primers used in this study can be found in Appendix 3.

2.7.3 PCR

Table 4: PCR reaction mix

Reagent	**Volume/reaction (μL)**
dH_2O	35.5
5X Phusion Buffer	10
Forward Primer (10μM)	1
Reverse Primer (10μM)	1
dNTPs (10mM)	1
Phusion DNA polymerase	0.5
cDNA template	1

Table 5: PCR cycling conditions

Temperature (ºC)	Time	Number of cycles
98	2min	1
98	15s	10
60	30s	
72	30s/Kb	
98	15s	30
65	30s	
72	30s/Kb	
72	7min	1
4	∞	

The PCR reaction was set up with the reaction mix and cycling conditions detailed in Tables 4 and 5.

2.7.4 PCR product purification

PCR products were analysed by agarose gel electrophoresis. If the band on the gel was unique and corresponded with the expected size, then 100µL of Ampure beads mix (carboxyl-modified Sera-Mag Magnetic Speed-beads in a PEG/NaCl buffer made according to Rohland and Reich (2012)) was added to the PCR product and left to incubate for 5 min at room temperature. The PCR tubes were then placed on a magnet, the supernatant was removed, the beads were washed twice with 80% EtOH, and left to dry out on the magnet for 5 min. The beads were next resuspended in 10µL dH_2O, placed back on the magnet and the supernatant containing the clean PCR product was recovered. The concentration of the clean PCR products was measured using a Labtech Nanodrop ND-1000 Spectrophotometer.

If multiple bands were present when the PCR products were analysed by agarose gel electrophoresis, bands of the expected size were cut out of the agarose gel and the DNA was extracted. The band of interest was cut out of the gel using an open UV box and sterile scalpel blade. The piece of gel was placed in a 1.5ml tube and 400µL NTI binding buffer was added to the tube which was incubated at 60ºC for 5 mins and then vortexed to ensure all the gel had dissolved. The total volume was added to a Macherey-Nagel™ NucleoSpin™ Gel and PCR Clean-up Column and centrifuged at maximum speed for 1 min and the liquid was discarded. The column was washed with

750µL of 80% EtOH, centrifuged at maximum speed for 1 min and the liquid was again discarded. Next, the column was placed in a new collection tube, 30µL of dH_2O was added to the column which was centrifuged at maximum speed for 1 min to collect the purified PCR product.

2.7.5 Vector preparation

Table 6: Restriction digest reaction mix for pGBKT7

Reagent	**Volume/reaction (µL)**
Plasmid DNA	8
dH_2O	9
10x Cut-smart Buffer	2
NdeI	0.5
PstI	0.5

Table 7: Restriction digest reaction mix for pGADT7

Reagent	**Volume/reaction (µL)**
Plasmid DNA	8
dH2O	9
10x Cut-smart Buffer	2
NdeI	0.5
XhoI	0.5

pGADT7 and pGBKT7 vectors were linearised by digestion with restriction enzymes purchased from New England Biolabs. The reaction mixes described in Tables 6 and 7 were incubated at 37ºC for 2h and the enzyme was then inactivated by incubating at 70ºC for 15 min.

Linearised plasmids were purified using 2x volume of Ampure beads Mix according to the method in section 2.7.4.

2.7.6 Hot fusion reaction

The hot fusion reaction was conducted according to the protocol in Fu et al. (2014).

2.7.7 *E. coli* transformation

Table 8: Antibiotic working concentrations and stock solution preparation.

Antibiotic	**Working concentration (µg/ml)**	**Stock solution**
Carbenicillin	100	100 mg/ml in dH_2O. Filter sterilised using 0.22µm nylon syringe filters and stored at -20°C.
Kanamycin	25	50 mg/ml in dH_2O. Filter sterilised and stored at -20°C.
Hygromycin	40	500 mg/ml in PBS. Filter sterilised and stored at 4°C.
Gentamycin	40	125 mg/ml in dH_2O. Filter sterilised and stored at -20°C.
Rifampicin	100	100 mg/ml in DMSO. Filter sterilised and stored at -20°C.

Plasmids were transformed into DH5α *Escherichia coli* (*E. coli*) cells using heat shock as follows: 20µL hot fusion reaction product was added to 100µL of *E. coli* Dh5α competent cells and incubated on ice for 30 minutes. The cells were then heat shocked for 2 minutes at 42ºC and were placed immediately on ice for 5 minutes. 200µL of liquid Luria-Bertani (LB) broth (25g per litre of dH_2O of LB Broth High Salt Granulated comprised of 10g/l Tryptone, 5g/l Yeast Extract and 10g/l NaCl; autoclaved for 20 minutes at 121ºC) was then added to each tube and the tubes were shaken at ~200 rpm for 1 hour at 37 ºC to allow recovery. Aliquots of each culture were then spread onto LB agar plates (37g per litre of dH_2O of LB Agar High Salt Granulated comprised of 10g/l Tryptone, 5g/l Yeast Extract, 10g/l NaCl and 12g/l Agar; adjusted to pH 7.2 and autoclaved for 20 minutes at 121ºC) containing the appropriate antibiotic for the selection of the plasmid (see Table 8 for working concentrations, all antibiotics were purchased from Melford). Plates were incubated at 37 ºC for 1 day to develop colonies.

2.7.8 Colony PCR

Table 9: Colony PCR reaction mix

Reagent	**Volume/reaction (μL)**
2x PCRBIO Taq Mix	6
Forward Primer T7_F (10uM)	0.2
Reverse Primer 3'AD or 2'BD (10uM)	0.2
dH_2O	3.6
Template DNA	2

Table 10: Colony PCR cycling conditions

Temperature (ºC)	**Time**	**Number of cycles**
94	5min	1
94	15s	40
50	30s	
72	30s	
72	5min	1
12	∞	

Positive colonies were screened by colony PCR. The PCR reaction was set up with the reaction mix and cycling conditions detailed in Tables 9 and 10. All colony PCR primers used in this study can be found in Appendix 4.

Positive colonies were selected and grown in liquid LB broth containing the appropriate antibiotic for the selection of the plasmid (ampicillin for pGADT7 and kanamycin for pGBKT7; see Table 8 for working concentrations) at 37ºC overnight.

2.7.9 Plasmid DNA extraction and validation by digestion

Plasmid DNA from two positive colonies was isolated from *E. coli* hosts using Wizard® *Plus* SV Minipreps DNA Purification System following Promega's instructions.

Table 11: Restriction digest reaction mix

Reagent	Volume/reaction (µL)
H_2O	12.5
Buffer	2
Restriction enzyme	0.5
Plasmid DNA	5

Plasmids were digested with restriction enzymes using a reaction mix described in Table 11 and this reaction mix was incubated at 37ºC for 2h. Digested plasmids were then checked by agarose gel electrophoresis as described under section 2.3.3.

If the result was positive, plasmids were sent for sequencing. All sequencing reactions were performed by the DNA Sequencing laboratory, School of Biological and Biomedical sciences, Durham University (DBS, Durham University). DNA sequence data was analysed using BLAST 2 sequencing tool (www.ncbi.nlm.nih.gov/blast/bl2seq) and APE software (http://biologylabs.utah.edu/jorgensen/wayned/ape/).

2.8 Yeast two-hybrid assay

2.8.1 Yeast strains

The two yeast (*Saccharomyces cerevisiae*) strains used in this two-hybrid assay were: AH109 (*MATa, trp1-901, leu2-3, 112, ura3-52, his3-200, gal4Δ, gal80Δ, LYS2::GAL1*$_{UAS}$*-GAL1*$_{TATA}$*-HIS3, GAL2*$_{UAS}$*-GAL2*$_{TATA}$*-ADE2, URA3::MEL1*$_{UAS}$*-MEL1*$_{TATA}$*-lacZ*) (Holtz, unpublished) and Y187 (*MATα, ura3-52, his3-200, ade2-101, trp1-901, leu2-3, 112, gal4Δ, met–, gal80Δ, URA3::GAL1*$_{UAS}$*-GAL1*$_{TATA}$*-lacZ*) (Harper et al., 1993).

2.8.2 Reporter genes

The reporter genes used in this yeast two-hybrid (Y2H) system were *ADE2*, *HIS3*, and *MEL1*. Expression of these reporter genes in response to two-hybrid interactions allowed cells to grow on plates lacking adenine and histidine and turned yeast colonies

blue in the presence of X-Gal, respectively. A Y2H interaction was considered positive if at least two of the reporter genes were activated.

2.8.3 Yeast transformation and mating

pGBKT7 and pGADT7 vectors that were generated according to the hot fusion protocol in section 2.7 were transformed into Y187 and AH109 cells, respectively. Pairs of positive interactions were identified by mating transformed Y187 and AH109. This was carried out according to the High-Throughput Transformations (96-Well Format) and Two-Hybrid Matrix protocols as in Walhout and Vidal (2001) with some minor adjustments.

2.8.4 β-galactosidase assay

β-galactosidase activity was qualitatively measured following a protocol similar to that in Möckli and Auerbach (2004). Colonies of mated transformants successfully grown on SD-Leu-Trp plates were resuspended in 200µL liquid SD-Leu-Trp and incubated overnight at 30ºC. Cells were pelleted by centrifugation at 2000rcf for 2 minutes, the supernatant was discarded and the pellet was resuspended in 10µL dH_2O. Cell lysis occurred through three cycles of flash freezing in liquid nitrogen followed by thawing at 30ºC. Cells were then mixed with 100µL of PBS buffer containing 500µg/mL X-gal, 0.5% agarose, and 0.05% β-mercaptoethanol and incubated overnight at room temperature. Pictures were taken when the blue α-galactosidase phenotype was optimal.

2.9 Bimolecular fluorescence complementation *(*BiFC)

2.9.1 Preparation of BiFC expression vectors encoding fusion proteins

Forward primer preparation for genes of interest and PCR amplification of the genes of interest were performed as mentioned in section 2.7. A list of the BiFC forward primers and universal reverse primer used in this study can be found in Appendix 5.

Table 12: Restriction digest reaction mix

Reagent	Volume/reaction (µL)
Plasmid DNA	10
dH_2O	6
10x Cut-smart Buffer	2
AscI	1
SpeI	1

BiFC plasmid vectors, pYFN43 and pYFC43 (Belda-Palazón et al., 2012) were linearised by digestion with restriction enzymes. The reaction mix was set up according to Table 12 and was incubated at 37ºC for 2h. Linearised plasmids were cleaned using Ampure beads according to the protocol as in section 2.7.4.

The hot fusion cloning reaction, *E. coli* transformation and plasmid validation that followed were also performed as mentioned in section 2.7.

2.9.2 Preparation of *Agrobacterium* cultures

BiFC plasmids, pBiYFPc and pBiYFPn, encoding the fusion proteins were transfected into GV3101 *Agrobacterium tumefaciens* cells as follows: 5µl of plasmid (100µg/µL) was added to 100µL of *A. tumefaciens* GV3101 competent cells, mixed and incubated on ice for 5 mins. The cells were then frozen for 5 mins in liquid nitrogen, followed by 5 mins of heat shock at 37ºC. After heat shocking the cells, 300µL of LB media was added and the cells were incubated for 2h at 28ºC with agitation. Finally, the culture was spread onto selective LB plates containing gentamycin, rifampicin and kanamycin for the selection of the plasmid (see Table 8 for working concentrations) and incubated for 2 days at 28ºC to develop colonies.

After 2 days, one single colony was picked and cultured over night at 30°C in 10ml of liquid LB broth containing the antibiotics gentamycin, rifampicin and kanamycin for the selection of the plasmid (see Table 8 for working concentrations). The OD600 was calculated and used to work out the volume of each culture to add into a new flask in order to start with an OD600 of 0.2. This new flask contained 50ml of liquid LB broth supplemented with antibiotics and 200µM Acetosyringone. Cultures were left to grow for approximately 3 hours at 30°C until an OD600=0.4-0.6 was reached. The

cells were then centrifuged at 4000g for 10 minutes and re-suspended into MMA buffer (MS 5g/L, MES 1,95g/L, Sucrose 20g/L, pH=5,6 NaOH) supplemented with 200µM Acetosyringone and shaken at room temperature for one hour in the dark. The volume of MMA buffer added was calculated using the culture volume and OD600 value. *Agrobacterium* cultures containing p19 plasmid and BiFC constructs were mixed into a new 1.5ml tube in the ratio 1:1:1. P19 was used to suppress gene silencing.

2.9.3 Infiltration

Nicotiana benthamiana plants were grown for 3-4 weeks at 21°C with 16-h light/8-h dark cycles. A small incision was made in the epidermal cell layer of the lower leaf surface of the plants. The tip of a syringe containing the resuspended *Agrobacterium* mixture was placed against this incision and the liquid mixture was slowly infiltrated into the leaf. Plants were then placed in a greenhouse for 3 days.

2.9.4 Observation of the fluorescent signal

A segment of leaf tissue in the infiltrated zone of *Nicotiana benthamiana* leaves was excised and mounted in water onto a glass microscope slide. The fluorescence was examined using a Zeiss 880 confocal laser scanning microscope.

2.10 Measuring hypocotyl length in response to brassinosteroid treatment

Seedlings were grown on vertical MS agar plates for 2 days according to the methods described in section 2.2.4. After 2 days, seedlings were carefully transferred onto vertical MS agar plates supplemented with either 0.2µM BL, 0.2µM BRZ or non-supplemented MS agar plates as a control and placed in the growth chamber for a further 3 days. Photographs were taken of each plate and hypocotyl length was measured using ImageJ (NIH) software.

2.11 Quantitative PCR (qPCR) analysis

2.11.1 Brassinosteroid treatment

Seedlings were grown on vertical MS agar plates for 5 days according to conditions described in section 2.2.4. 5-d-old seedlings were carefully transferred into liquid MS media supplemented with 0.2µM BL, 0.2µM BRZ, or non-supplemented liquid MS media as a control and placed in a growth chamber for 16 hours.

2.11.2 RNA extraction

RNA was extracted according to the protocol in Townsley et al. (2015), which includes a number of steps previously described in Kumar et al. (2012). A few minor alterations were made to the protocol: (A) Tissues were lysed by adding 3-4 Zirconia/Silica beads to 2ml tubes containing ~20mg tissue and ground for 1min. (B) TE cells were not ground. (C) The lysate from ground tissues was split in two with ~200μl in each tube and one of these tubes was put aside at -80ºC before proceeding to mRNA isolation. (D) Volumes of all wash buffers were 200μl each. (E) A secondary wash was performed on the mRNA sample.

2.11.3 cDNA synthesis

Table 13: Reaction mixes and incubation times for cDNA synthesis

RNA mix	**Volume (µL) per reaction**	**Incubation**
RNA	5.75	
Random primers (100pMol)	0.5	
TOTAL	6.25	65ºC for 5 minutes
cDNA synthesis mix		
5X First Reaction Buffer	2	
10mM dNTP	1	
RevertAid Reverse Transcriptase	0.5	
RNase Inhibitor	0.25	
Incubated RNA mix	6.25	
TOTAL	10	25ºC for 10 minutes 42ºC for 60 minutes 70ºC for 10 minutes

For cDNA synthesis, reaction mixes were set up and incubated according to Table 13. cDNA solutions were then diluted 5-fold and stored at -20°C until required for qPCR.

2.11.4 qPCR reaction

Table 14: qPCR reaction mix

qPCR mix	**Volume/reaction (µl)**
2X SYBR Green PCR Mix Lo-ROX	10
Forward Primer (100µM)	0.1
Reverse Primer (100µM)	0.1
sterile dH_20	4.8
cDNA (1:10 dilution)	5

Table 15: qPCR cycling conditions

Temperature (°C)	**Time**	**Number of cycles**
94	3min	1
94	15s	40
55	30s	
72	30s – signal acquisition	

qPCR analysis was conducted on three biological replicates for each sample and three technical replicates for each biological replicate using a Rotorgene Q. The qPCR reaction mix and cycling conditions are detailed in Tables 14 and 15. All qPCR primers used are listed in Appendix 6.

Gene expression levels were calculated from the average of the three technical repeats relative to the expression levels of a reference gene (*UB10*) and analysed using the comparative Ct method (ΔΔCt method) as described in Applied Biosystems User Bulletin No. 2.

2.12 Statistical analysis

The data collected in this study was tested for normality of distribution using the Kolgomorov-Smirnov test and data sets were also assumed approximately normally distributed when sample size (N) > 30 according to the central limit theorem. None of

the distributions were significantly deviating from the normal distribution and therefore parametric independent-samples T tests were applied to the means of all data sets and the type 1 error probability (α) was set to 0.05. All statistical analysis was carried out using IBM SPSS Statistics.

3. Results

3.1 The effect of loss of function of histone modifying enzymes on meristem size and cytokinin response

The *Arabidopsis* root apical meristem comprises of stem cells surrounding the quiescent centre (QC), which together form the stem cell niche. These stem cells give rise to transit amplifying cells which undergo division in the proximal meristem before entering the elongation/differentiation zone whereby they differentiate into all cell types of the root (Dolan et al., 1993). The number of cells in the root meristem depends on stem cell activity and the rate of transition of transit amplifying cells from cell division to cell elongation (Li et al., 2017). This is co-ordinately controlled, in part, by two hormones, auxin and cytokinin (CK).

CK is known to antagonise auxin and promote cell differentiation such that exogenous application of CK reduces the number of meristematic cells and therefore the meristem size (Dello Ioio et al., 2007; Dello Ioio et al., 2008; Perilli and Sabatini, 2010). It was hypothesised that if chromatin structure does guide cell differentiation, differences in meristem size and CK response should be observed when studying mutants impaired in chromatin remodelling processes. To test this hypothesis, loss-of-function mutants in histone modifying enzymes (Table 16) were pre-treated with CK and the root meristem size was measured.

Table 16: Information on the histone modifying enzymes included in the root meristem size analysis

Accession Number	Name	Function	Potential role in transcription	Reference(s)
AT2G44150	ASHH3	Histone lysine methyltransferase	Unknown	
AT2G17900	ASHR1	Histone lysine methyltransferase	Unknown	
AT2G31650	ATX1	H3K4 tri-methyltransferase	Active	Alvarez-Venegas et al., 2003; Fromm and Avramova, 2014; Napsucialy-Mendivil et al., 2014; Pien et al., 2008
AT5G09790	ATXR5	H3K27 mono-methyltransferase	Repressive	Hale et al., 2016; Jacob et al., 2009
AT2G23380	CLF	H3K27 tri-methyltransferase	Repressive	Goodrich et al., 1997; Wang et al., 2016; De Lucas et al., 2016; Chanvivattana et al., 2004; Schubert et al., 2006; Jiang et al., 2008
AT1G62830	LDL1	H3K4 demethylase	Repressive	Jiang et al., 2007; Shi et al., 2004
AT1G04050	SUVR1	Histone lysine methyltransferase	Unknown	
AT5G06550	JMJ22	H4R3 demethylase	Active	Cho et al., 2012
AT4G02020	SWN	H3K27 tri-methyltransferase	Repressive	Chanvivattana et al., 2004
AT2G24740	SUVH8	Histone lysine methyltransferase	Unknown	
AT2G23740	SUVR5	H3K9 di-methyltransferase	Repressive	Caro et al., 2012

Table 17: Descriptive statistics for root meristem size of mock-treated and trans-Zeatin-treated wildtype and histone modifying enzyme mutant seedlings.

Plant line	Treatment	Sample size (N)	Mean	Standard Error of the Mean (SEM)
Col0	Mock	14	32.0	1.04
	trans-Zeatin	13	24.1	1.00
ashh3	Mock	15	28.1	1.07
	trans-Zeatin	14	28.6	1.02
ashr1	Mock	8	27.8	1.33
	trans-Zeatin	8	29.5	0.926
atx1	Mock	13	31.8	0.545
	trans-Zeatin	12	27.2	0.534
atxr5	Mock	15	27.8	0.718
	trans-Zeatin	15	27.6	0.616
clf29	Mock	11	28.5	1.13
	trans-Zeatin	9	30.2	1.52
jmj22	Mock	10	25.2	0.940
	trans-Zeatin	13	25.5	0.676
ldl1	Mock	6	27.7	1.20
	trans-Zeatin	4	25.0	1.83
suvr1	Mock	12	35.8	0.968
	trans-Zeatin	16	28.1	0.800
suvh8	Mock	18	34.2	1.04
	trans-Zeatin	13	30.0	0.913
suvr5	Mock	6	37.2	1.08
	trans-Zeatin	10	37.7	1.07
swn7	Mock	17	34.5	0.944
	trans-Zeatin	14	30.4	1.06

Table 18: T-test statistics for the effect of loss of function of histone modifying enzymes on mean root meristem size

Mutant	T critical value	Degrees of freedom (df)	p-value
ashh3	2.59	27	$P < 0.05$
ashr1	2.50	20	$P < 0.05$
atx1	0.197	19.5	$P = 0.846$
atxr5	3.37	27	$P < 0.05$
clf29	2.30	23	$P < 0.05$
jmj22	4.64	22	$P < 0.001$
ldl1	2.44	18	$P < 0.05$
suvr1	-2.67	24	$P < 0.05$
suvh8	-1.49	30	$P = 0.147$
suvr5	-2.96	18	$P < 0.05$
swn7	-1.76	29	$P = 0.089$

Table 19: T-test statistics for the effect of cytokinin treatment on mean root meristem size of wildtype and histone modifying enzyme mutant seedlings

Plant line	**T critical value**	**Degrees of freedom (df)**	**p-value**
Col0	5.48	25	$P < 0.001$
ashh3	-0.296	27	$P = 0.770$
ashr1	-1.08	14	$P = 0.299$
atx1	6.02	23	$P < 0.001$
atxr5	0.211	28	$P = 0.834$
clf29	-0.953	18	$P = 0.353$
jmj22	-0.232	21	$P = 0.819$
ldl1	1.28	8	$P = 0.236$
suvr1	6.18	26	$P < 0.001$
suvh8	2.92	29	$P < 0.05$
suvr5	-0.330	14	$P = 0.746$
swn7	2.91	29	$P < 0.05$

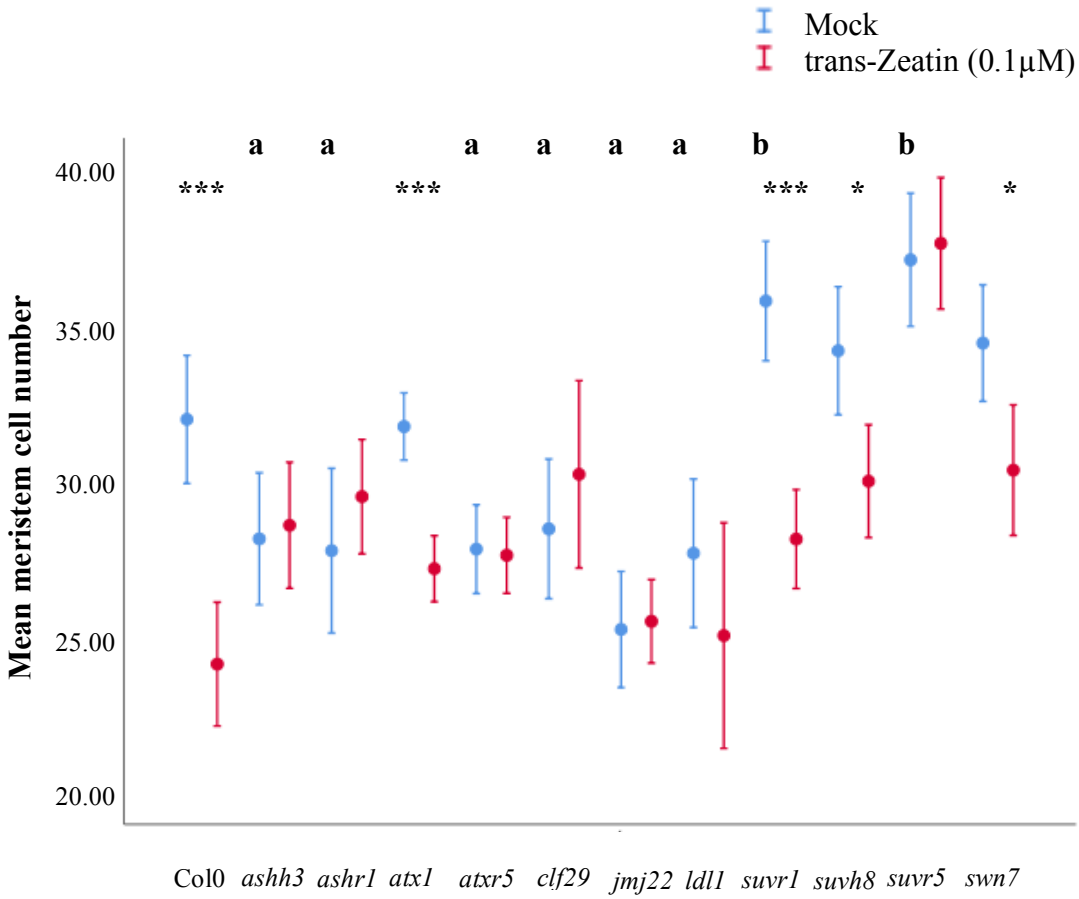

Figure 4: The mean meristem cell number of mock-treated and cytokinin-treated wildtype and histone modifying enzyme mutant seedlings. Mean number of root meristem cells in 5-d-old wildtype and histone modifying enzyme mutant seedlings after 16h of treatment with mock or trans-Zeatin (0.1μM). Error bars represent ± 1 SEM. Mock-treated groups denoted by 'a' have a mean meristem cell number that is significantly lower than the wildtype and mock-treated groups denoted by 'b' have a mean meristem cell number that is significantly higher than the wildtype. Groups denoted by '*' or '***' have a significant difference ($p < 0.05$ or $p < 0.001$, respectively) between mean meristem cell number of mock-treated and trans-Zeatin-treated roots. See Table 17 for sample sizes (N).

Statistical analysis showed that the mean meristem cell number was significantly lower in mock-treated *ashh3*, *ashr1*, *atxr5*, *clf29*, *jmj22*, and *ldl1* seedlings compared to mock-treated wildtype seedlings and significantly higher in mock-treated *suvr1* and *suvr5* seedlings compared to mock-treated wildtype seedlings (Tables 17 and 18,

Figure 4). There was no significant difference between mean meristem cell number in mock-treated *atx1, swn7* and *suvh8* seedlings and mock-treated wildtype seedlings (Tables 17 and 18, Figure 4).

Statistical analysis showed that the mean meristem cell number was significantly lower in trans-Zeatin-treated seedlings compared to mock-treated seedlings in wildtype, *atx1*, *suvr1*, *suvh8* and *swn7* (Tables 17 and 19, Figure 4). On the other hand, there was no significant difference between mean meristem cell number in mock-treated and trans-Zeatin-treated *ashh3*, *ashr1*, *atxr5*, *clf29*, *jmj22, ldl1* and *suvr5* seedlings (Tables 17 and 19, Figure 4).

3.2 The effect of auxin, cytokinin and brassinosteroid treatment on tracheary element differentiation

Tracheary element (TE) differentiation is a well-defined process which provides a perfect model system to study cytodifferentiation in plants (Fukuda and Komamine, 1980; Kondo et al., 2015; Kubo et al., 2005; Oda et al., 2010; Oda et al., 2005; Ohashi-Ito et al., 2010; Pesquet et al., 2010). TE differentiation is characterised by the deposition of a patterned secondary cell wall with annular, spiral, reticulate, or pitted wall thickenings, autolysis and programmed cell death whereby TEs are emptied of all cell contents and nuclei to form a hollow, tubular vascular system (Fukuda, 1996). This TE differentiation process is regulated by a number of factors (Turner et al., 2007; Ohashi-Ito and Fukuda, 2010) and auxin, cytokinin (CK), and brassinosteroids (BRs) are perhaps the most important regulators (Fukuda, 2004; Yoshida et al., 2005; Iwasaki and Shibaoka, 1991; Yamamoto et al., 1997).

Many of the experimental systems that have been developed to study TE differentiation require the manipulation of the phytohormones auxin, CK and BRs (Fukuda and Komamine, 1980; Kubo et al., 2005; Oda et al., 2005; Pesquet et al., 2010; Kondo et al., 2015; Saito et al., 2017). This poses issues when wanting to investigate the contribution of these hormones to the chromatin rearrangement that occurs during xylem differentiation. Yet this problem can be overcome by utilising experimental systems that induce TE differentiation by activating master transcription

factors (Oda et al., 2010; Ohashi-Ito et al., 2010; Yamaguchi et al., 2010a), rather than relying on application of hormones.

Several NAC domain proteins have been identified as master switches of xylem cell differentiation. Specifically, *VND6* and *VND7* have been found to be expressed more in differentiating xylem vessels (Kubo et al., 2005; Yamaguchi et al., 2008). Moreover, overexpression of *VND7* induces ectopic transdifferentiation of various non-vascular cells into protoxylem with secondary cell wall thickenings and repression of *VND7* reduces xylem vessel formation (Kubo et al., 2005; Yamaguchi et al., 2008; Yamaguchi et al., 2010a). In undifferentiated procambial cells, VND-INTERACTING 2 (VNI2) transcriptional repressor binds to VND proteins and inhibits VND7-mediated xylem-specific gene expression. Yet VNI2 is targeted for degradation when active VND7 is required to induce TE differentiation (Yamaguchi et al., 2010b).

Knowing that VND7 is a master regulator of TE differentiation has resulted in the development of experimental systems where *VND7* is expressed under the control of an estradiol-inducible promoter (Zuo et al., 2000; Coego et al., 2014) to induce xylem cell transdifferentiation without exogenous application of hormones. In this study, this system was used to determine whether specific hormonal contexts are required for proper TE differentiation. Firstly, XVE:GUS plant lines were treated with estradiol to check if estradiol induction is equally distributed in the root. Secondly, VND7ox plant lines were induced with estradiol to analyse the spatiotemporal pattern of VND7-induced xylem differentiation by looking at secondary cell wall deposition across different root cell types and along the root longitudinal axis. Next, VND7ox plant lines were pre-treated with auxin, CK and BRs before induction with estradiol and the effect on VND7-induced xylem differentiation (depicted by secondary cell wall deposition) was studied. Finally, in an attempt to better identify the effect of disturbing the balance of phytohormones on VND7-induced xylem differentiation at the cell type specific level, VND7ox;H2B::YFP plant lines were used. H2B::YFP is a protein fusion of the histone 2B (H2B) protein and the yellow fluorescent protein (YFP) under the control of the cauliflower mosaic virus promoter (CaMV 35S) and can be used as a marker for nuclei. TE differentiation consists primarily of

programmed cell death and autolysis, which involves nuclear degradation. Transcriptional master switches VND7 and VND6 have been shown to directly control this programme of programmed cell death and autolysis (Escamez and Tuominen, 2014). Therefore, it was hypothesised that it will be possible to determine which specific cell types have successfully undergone VND7-induced xylem transdifferentiation by the absence of the nucleus and thus absence of a fluorescent signal from YFP. So VND7ox;H2B::YFP plant lines pre-treated with auxin, CK and BRs before induction with estradiol and the spatial domains (cell types) in which VND7-induced xylem differentiation occurs were identified by looking at the fluorescent signal from YFP.

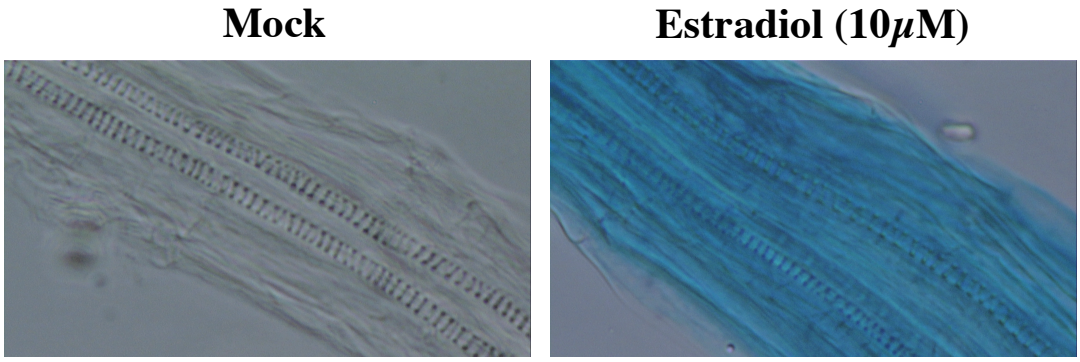

Figure 5: Estradiol-induced GUS expression in a root. GUS expression in 5-d-old XVE:GUS roots in which GUS expression is induced by estradiol treatment. XVE:GUS roots were treated with mock or estradiol (10μM) for 3 days.

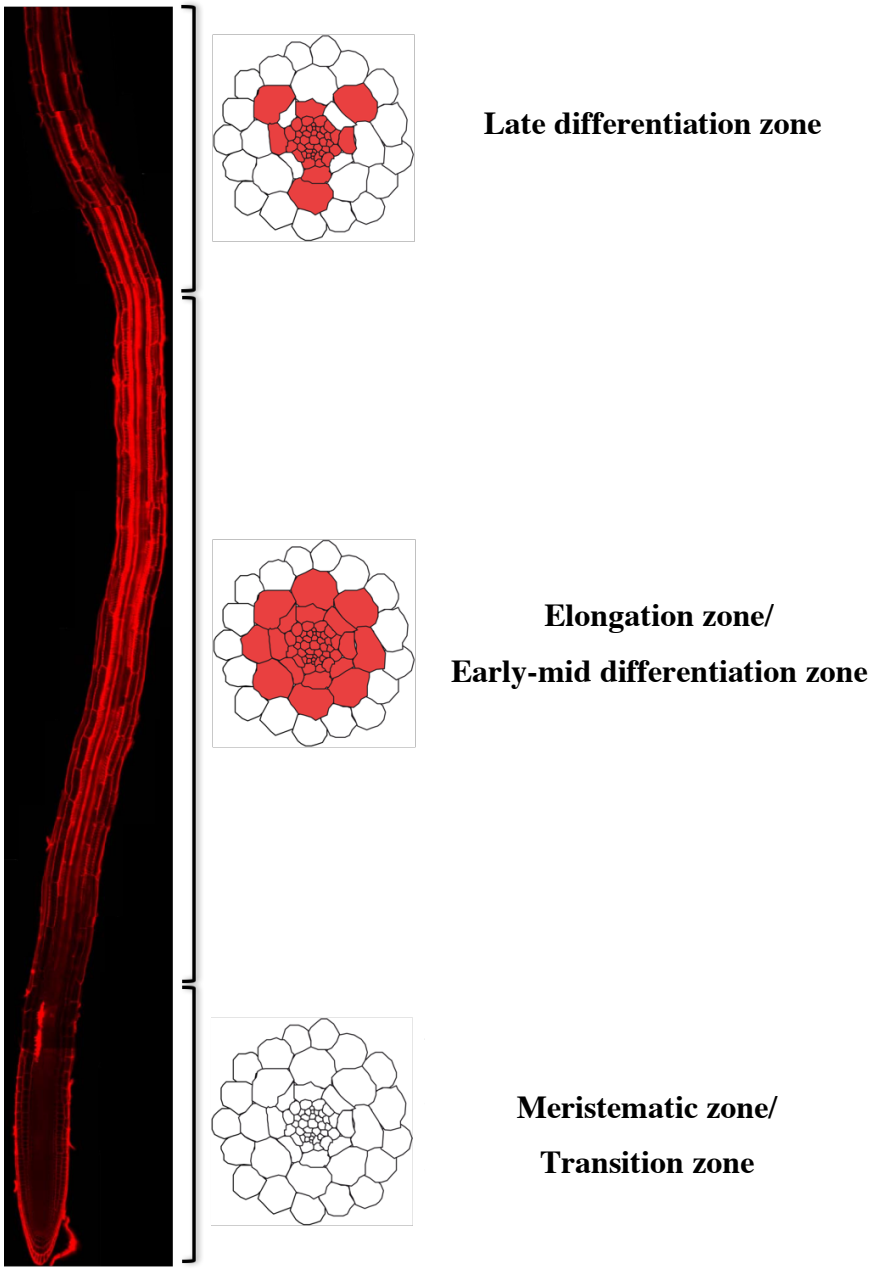

Figure 6: Spatio-temporal pattern of xylem transdifferentiation in VND7ox plant whole root. Xylem transdifferentiation in a 5-d-old VND7ox seedling whole root in which VND7 expression was induced by treatment with estradiol (10μM) for 3 days. Figure taken from M. de Lucas (personal communication).

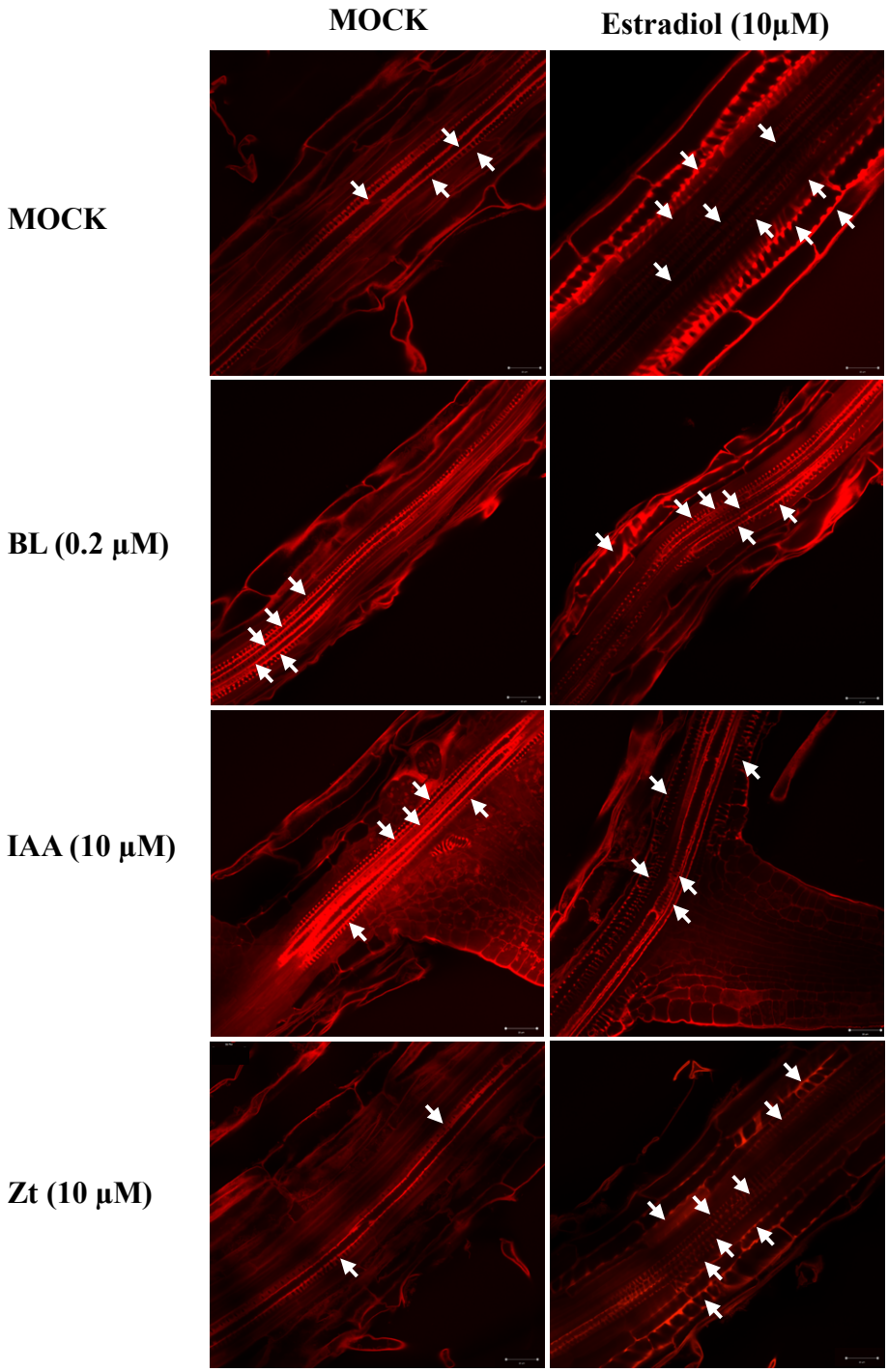

Figure 7: The effect of phytohormone treatment on xylem transdifferentiation in VND7ox roots. Xylem transdifferentiation in 5-d-old VND7ox roots in which VND7 expression was induced by estradiol treatment. Un-induced mock or estradiol (10μM) -induced VND7ox roots were treated for 3 days with brassinolide (BL) (0.2μM), indole-3-acetic acid (IAA) (10μM) or trans-Zeatin (Zt) (10μM) and hormone-free control. Red indicates cell walls and white arrows indicate secondary cell wall thickenings. Scale bars = 20µM.

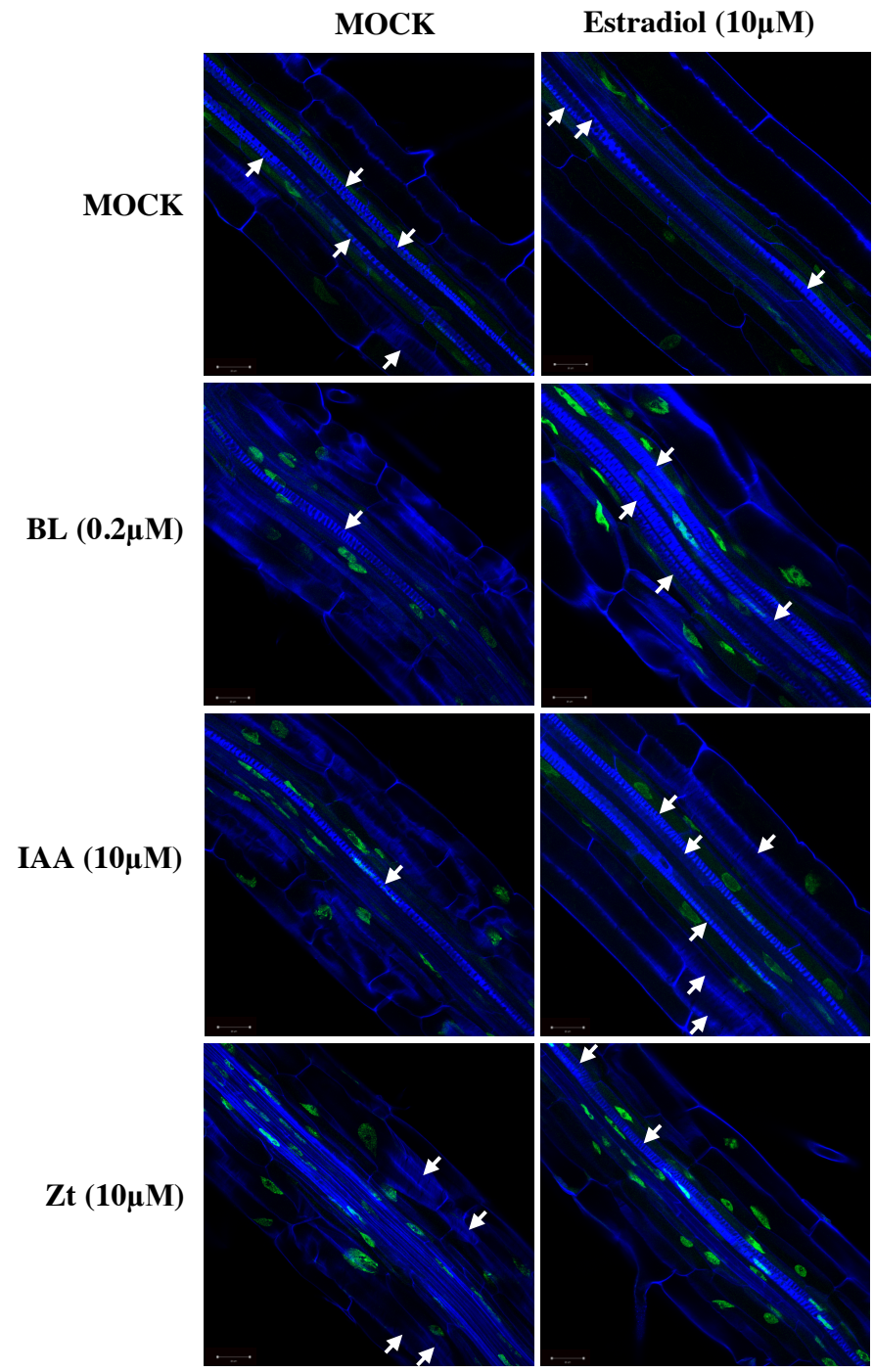

Figure 8: The effect of phytohormone treatment on xylem transdifferentiation in VND7ox;H2B::YFP roots. Xylem transdifferentiation in 5-d-old VND7ox;H2B::YFP roots in which VND7 expression was induced by estradiol treatment. Un-induced mock or estradiol (10μM)-induced VND7ox;H2B::YFP roots were treated for 7 days with brassinolide (BL) (0.2μM), indole-3-acetic acid (IAA) (10μM) or trans-Zeatin (Zt) (10μM) and hormone-free control. Blue indicates cell walls, green indicates nuclei and white arrows indicate secondary cell wall thickenings. Scale bars = 20µM.

Estradiol treatment successfully induced GUS expression in all cell types of XVE:GUS roots (Figure 5). Spatiotemporal analysis of xylem transdifferentiation in estradiol-treated VND7ox roots revealed that VND7-induced xylem transdifferentiation (depicted by secondary cell wall thickenings) never appears to occur in the columella root cap, epidermis, meristematic zone, transition zone and it was less evident in the late differentiation zone (Figure 6).

In all hormone conditions, estradiol-induced overexpression of *VND7* induced the transdifferentiation of various non-vascular cell types into xylem vessel cells. The control VND7ox roots showed high levels of transdifferentiated cells whereas interestingly, BR and auxin-treated roots showed reduced levels of VND7-induced xylem transdifferentiation. On the other hand, in CK-treated VND7ox roots, estradiol-induced *VND7* overexpression appeared to result in similar levels of transdifferentiation of non-vascular cell types into xylem vessel cells as the hormone-free control VND7ox roots (Figure 7).

VND7ox;H2B::YFP roots after 7 days of induction and phytohormone treatment still showed a fluorescent signal from YFP in the nucleus of cells with secondary cell wall thickenings (Figure 8).

3.3 The effect of loss of function of histone modifying enzymes on tracheary element differentiation

Specific chromatin changes have been associated with TE differentiation according to preliminary data obtained from chromatin-immunoprecipitation sequencing analyses on pluripotent cells and cells committed to TE differentiation. De Lucas (unpublished) found that in fully differentiated TEs, the net genomic coverage of active chromatin marks such as H3K4me3, H3K36me2 and H3K36me3 decreased whereas the net genomic coverage of repressive chromatin marks such as H3K27me3 and H3R2me2 increased (Appendix 7). Based on these results, it can be hypothesised that if chromatin structure guides TE differentiation, differences should be observed in this differentiation process when studying mutants impaired in chromatin remodelling processes.

To test this hypothesis, an experimental induction system recently developed by Saito et al. (2017) was used, which employs an inhibitor of GLYCOGEN SYNTHASE KINASE 3 (GSK3) proteins, bikinin, to induce TE transdifferentiation. BR-INSENSITIVE 2 (BIN2) is an example of a GSK3-like kinase inhibited by bikinin and it is a known suppressor of xylem differentiation from procambial cells (Kondo et al., 2014). BIN2 is activated by TRACHEARY ELEMENT DIFFERENTIATION INHIBITORY FACTOR (TDIF), which binds specifically to putative TDIF RECEPTOR (TDR)/PHLOEM INTERCALATED WITH XYLEM (PXY) and suppresses the differentiation of procambial cells into xylem cells by phosphorylation-dependent inhibition of BES1 in procambial cells (Kondo et al., 2014; Hirakawa et al., 2008; Fisher and Turner, 2007). BIN2 inhibition by upstream BR signalling is required to induce proper xylem cell differentiation (Kondo et al., 2014) and this concept has formed the basis of some *in vitro* induction experimental systems (Kondo et al., 2015; Saito et al., 2017).

In this study *Arabidopsis* leaf discs of loss-of-function mutants in histone modifying enzymes were cultured with auxin, CK and bikinin for 3 days, and the transdifferentiation of mesophyll cells into TEs was studied to identify the key histone modifying enzymes associated with xylem cell fate.

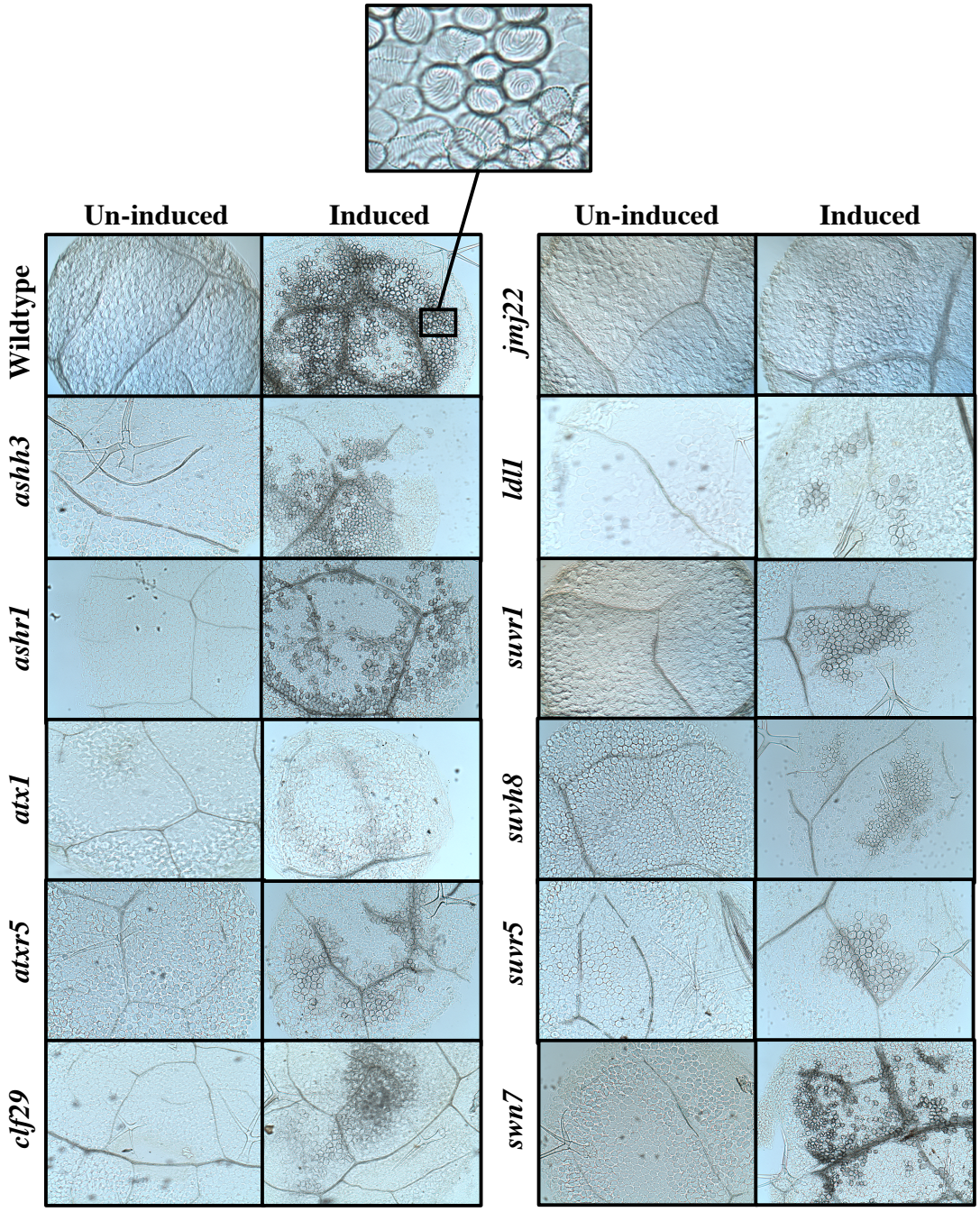

Figure 9: Xylem differentiation induction in leaves of histone modifying enzyme mutants. Un-induced and bikinin-induced xylem differentiation in 3-4-week-old wildtype and histone modifying enzyme mutant seedlings.

Transdifferentiation of mesophyll cells into TEs was induced in all histone modifying mutants (Figure 9).

3.4 Identifying the molecular interactions between histone modifying enzymes and hormone signalling genes

More than thirty independent histone post-transcriptional modifications control chromatin architecture, and hundreds of enzymes contribute to this complex regulatory mechanism. To date, knowledge of the specific function of each histone modification process in regulating chromatin architecture is limited. A few examples exist in literature whereby hormone signalling components interact with chromatin modifying enzymes and together regulate key developmental processes (Zhang et al., 2014b; Yu et al., 2008). Furthermore, mutants in auxin and CK signalling (Dello Ioio et al., 2008) exhibit phenotypic similarities with chromatin remodelling enzymes mutants which have defects in cell differentiation (Ikeuchi et al., 2015a). It is therefore plausible that hormone signalling integrates with chromatin remodelling during plant cell differentiation.

To begin to understand how hormone signals guide chromatin changes during cell differentiation, a yeast two-hybrid (Y2H) protein-protein interaction assay was performed to screen for interactions between histone modifying enzymes and the BR signalling negative regulator and known suppressor of xylem cell differentiation, BIN2. Y2H protein-protein interaction assays involve fusing proteins-of-interest, known as bait and prey, to the DNA binding domain (BD) or activation domain (AD) of a fragmented transcription factor. If these proteins interact with one another, the DNA-binding and activation domains get close enough to one another to form a functional transcription unit which activates the transcription of reporter genes (Fields and Song, 1989). Activation of reporter genes typically enables yeast to grow on selective medium and/or changes the colour of yeast colonies.

A large proportion of the work conducted in this study involved the generation of a Y2H library of 30% of the predicted histone modifying enzymes (Table 20), including both writers and erasers. This library was screened for interactions with BIN2 to get a better idea of how hormone signalling may guide chromatin remodelling during xylem cell differentiation.

Table 20: The histone remodelling enzymes screened for interactions with BR signalling component, BIN2

Accession Number	Name	Function
AT1G26760	ATXR1	histone-lysine methyltransferase
AT5G09790	ATXR5	histone-lysine methyltransferase
AT5G24330	ATXR6	histone-lysine methyltransferase
AT1G76710	ASHH1	histone-lysine methyltransferase
AT2G30580	BMI1A	Histone-lysine E3 ubiquitin ligase
AT1G06770	BMI1B	Histone-lysine E3 ubiquitin ligase
AT2G23380	CLF	histone-lysine methyltransferase
AT5G51230	EMF2	histone-lysine methyltransferase
AT3G20740	FIE	histone-lysine methyltransferase
AT2G31650	ATX1	histone-lysine methyltransferase
AT1G05830	ATX2	histone-lysine methyltransferase
AT1G62310	JMJ	histone-lysine demethylase
AT1G30810	JMJ18	histone-lysine demethylase
AT1G78280	JMJ21	histone-lysine demethylase
AT5G06550	JMJ22	histone-arginine demethylase
AT4G00990	JMJ27	histone-lysine demethylase
AT3G20810	JMJ30	histone-lysine demethylase
AT5G17690	LHP1	Maintains methylated state
AT1G62830	LDL1	histone-lysine demethylase
AT3G13682	LDL2	histone-lysine demethylase
AT5G58230	MSI1	histone-lysine methyltransferase
AT1G08620	PKDM7D	histone-lysine demethylase
AT1G04870	PRMT10	histone-arginine methyltransferase
AT2G19670	PRMT1A	histone-arginine methyltransferase
AT4G29510	PRMT1b	histone-arginine methyltransferase
AT4G31120	PRMT5	histone-arginine methyltransferase
AT4G16570	PRMT7	histone-arginine methyltransferase
AT5G44280	RING1A	Histone-lysine E3 ubiquitin ligase
AT1G03770	RING1B	Histone-lysine E3 ubiquitin ligase
AT2G33290	SUVH2	histone-lysine methyltransferase
AT2G35160	SUVH5	histone-lysine methyltransferase
AT3G04380	SUVR4	histone-lysine methyltransferase
AT2G23740	SUVR5	histone-lysine methyltransferase
AT4G02020	SWN	histone-lysine methyltransferase
AT4G16845	VRN2	histone-lysine methyltransferase

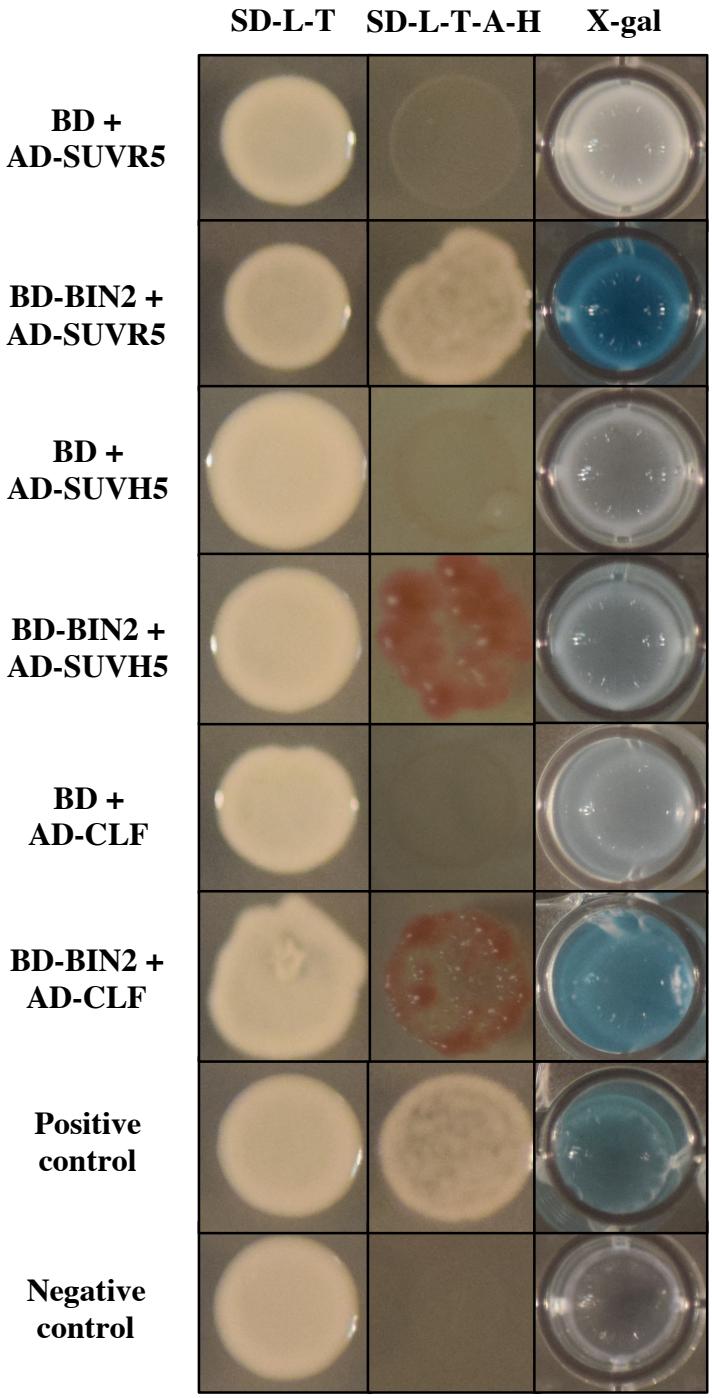

Figure 10: Yeast two-hybrid assay for protein-protein interactions between histone modifying enzymes and BIN2. Y2H screen for protein-protein interactions between BIN2 and SUVR5, SUVH5 and CLF, with BD-BIN2 + AD-BZR1 as a positive control and BD-BIN2 + AD as a negative control. *Saccharomyces cerevisiae* strains were growth tested on SD-L-T (non-selective) and SD-L-T-A-H (selective) media incubated at 30ºC for 2-4 days. Colonies cultured on SD–L-T were also assayed for β-galactosidase activity (X-Gal). See Table 20 for list of histone modifying enzymes assayed for interactions with BIN2.

All strains grew successfully on SD-L/T. This indicates that the strain has been successfully transformed with both pGADT7 and pGBKT7 plasmids which contain *LEU2* and *TRP1* genes that are required for the synthesis of leucine and tryptophan respectively (Figure 10).

Growth on SD–L/T/A/H and presence of blue colour indicate expression of the three reporter genes, *ADE2* and *HIS3,* which are required for synthesis of adenine and histidine respectively, and *MEL1,* which encodes β-galactosidase that interacts with X-gal and turns cells blue in colour. A Y2H interaction was considered positive if at least two of the reporter genes are activated. This Y2H screen therefore revealed positive interactions between hormone signalling protein, BIN2, and histone modifying enzymes, SUVR5, SUVH5 and CLF (Figure 10).

3.5 Verifying interactions between histone modifying enzymes and hormone signalling genes *in vivo*

Having identified positive protein-protein interactions between hormone signalling protein, BIN2, and histone modifying enzymes, SUVR5, SUVH5 and CLF by Y2H assay, next these interactions needed to be validated in vivo by bimolecular fluorescence complementation (BiFC). Validation of protein-protein interactions by BiFC entailed fusing the two putative interaction partners with the N-terminal and C-terminal fragments of YFP (YN and YC). Positive interactions between the proteins of interest bring the two YFP fragments in close proximity resulting in the formation of a bimolecular fluorescent complex. This results in an appearance of the fluorescence signal (reviewed in Kerppola, 2008). There was only time in this study to generate BiFC plasmids encoding BIN2, BZR1, SUVR5 and CLF proteins fused to YFP fragments to validate the interaction between BIN2 and SUVR5 and CLF.

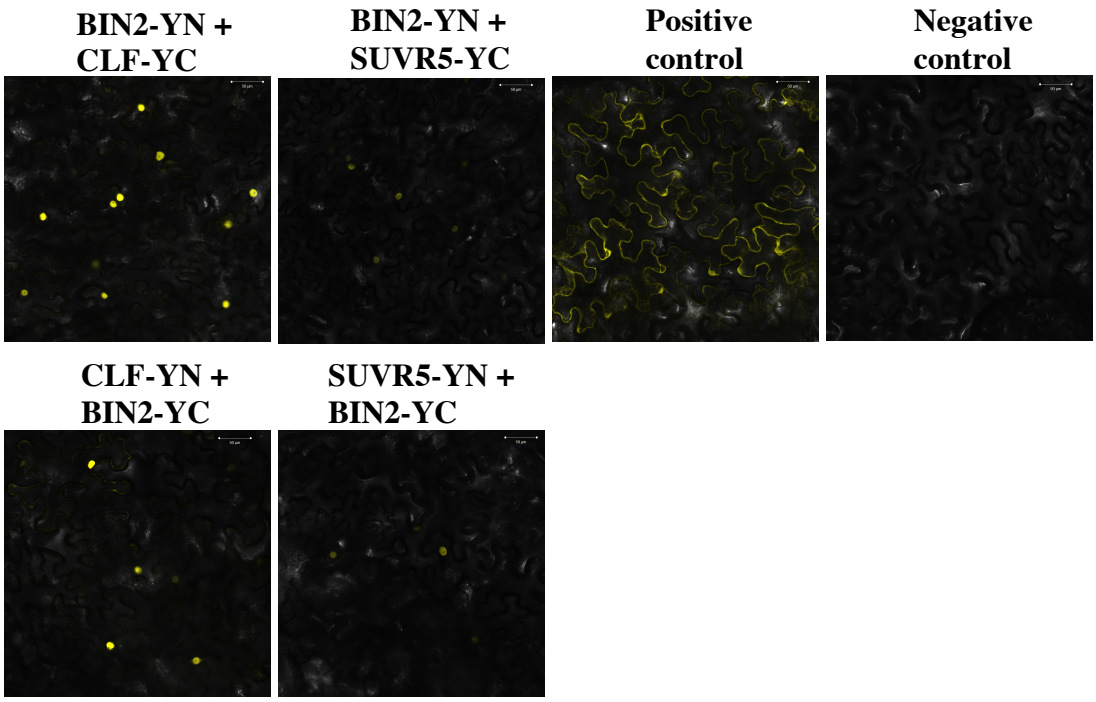

Figure 11: Validating putative interactions from yeast two-hybrid screening *in vivo* by BiFC. BiFC interaction assays were conducted in *Nicotiana benthamiana* leaf epidermal cells. Confocal micrographs were taken 3d post-infiltration. BIN2-YN + BZR1-YC and BIN2-YN + BIN2-YC are the positive and negative controls, respectively. Scale bars = 50μM.

Strong fluorescence was observed in the nucleus of *Nicotiana benthamiana* cells infiltrated with a combination of successfully cloned BiFC plasmids containing the genes of interest (Figure 11), verifying that BIN2 interacts with SUVR5 and CLF.

3.6 Expression analyses of a candidate gene associated with cell division that is regulated by brassinosteroid signalling and SUVR5

Thus far, SUVR5 has been shown to play an important role in regulating meristematic cell division and the transition from cell division to cell elongation based on meristem size analysis. Y2H analysis also revealed that SUVR5 interacts with hormone signalling component BIN2. To begin to elucidate the specific role of SUVR5 during differentiation, this study set out to identify candidate genes associated with cell proliferation and cell differentiation which are regulated by BR signalling and SUVR5.

Caro et al. (2012) identified SUVR5 as a SET histone methyltransferase which facilitates DNA methylation–independent deposition of the repressive histone mark H3K9me2 to induce gene silencing. Caro et al. (2012) isolated a T-DNA mutant in SUVR5, *suvr5-1,* which shows an overall decrease in heterochromatic H3K9me2 levels and analysed its transcriptome by mRNA sequencing (mRNA-Seq). They compiled a list of genes significantly upregulated in the *suvr5-1* mutant, which is likely due to a decrease in H3K9me2 levels. This list was compared to a list of common genes up-regulated after bikinin and BL treatment, up-regulated in the *bzr1-1d* mutant and down-regulated in the *bri1-116* mutant (Nemhauser, 2004; Goda, 2004; De Rybel et al., 2009; Sun et al., 2010). This comparison highlighted 23 candidate genes regulated by BRs and upregulated in *suvr5-1*.

On this list of candidate genes was a gene which encodes for atypical E2F transcription factor E2Fe/DEL1. E2Fe controls the expression of an anaphase-promoting complex/cyclosome (APC/C) activator gene and is a negative regulator of cell endocycle onset and cell cycle progression in proliferating cells (Lammens et al., 2008). The transition from the mitotic cell cycle to the endocycle is associated with termination of cell division and initiation of cell elongation in the transition zone and later differentiation (Hayashi et al., 2013). The role of endoreduplication in xylem differentiation however is yet to be studied in depth. Nonetheless, Heyman et al. (2017) recently used transcriptional *GUS* reporter lines to determine the expression patterns of *E2Fe/DEL1* in the *Arabidopsis* root. *E2Fe/DEL1* expression was found to be high in the meristematic zone whereby cells show high cell division activity yet expression levels were low in the differentiation zone. This suggests that E2Fe may negatively regulate cell differentiation initiation by promoting and maintaining cell division.

Moreover, González-García et al. (2011) found that BRs regulate *Arabidopsis* root meristem size by promoting cell cycle progression and differentiation. Gain-of-function BR-related mutants and BL-treated plants underwent a premature cell cycle exit resulting in early differentiation of meristematic cells, which reduces the meristem size. The BR signalling pathway is therefore essential for normal cell-cycle progression and to maintain the balance between cell division and cell differentiation.

Based on these studies, it was hypothesised that BRs and SUVR5 may regulate *E2Fe* expression and subsequently cell cycle progression and cell differentiation initiation. The protein-protein interaction assays suggest that SUVR5 could be a phosphorylation target of BIN2. It was therefore postulated that when BR levels are high and BIN2 is inhibited, SUVR5 would not be phosphorylated and potentially inactivated by BIN2 and so can actively deposit the repressive mark, H3K9me2, onto *E2Fe* loci resulting in premature cell endocycle onset and early differentiation of meristematic cells.

To test this hypothesis, *E2Fe* expression levels were measured by qPCR analysis in undifferentiated cells and fully differentiated TEs as well as in wildtype and *suvr5* loss of function mutant seedlings treated with BL and the BR inhibitor, BRZ.

Table 21: Descriptive statistics for the relative expression of *E2Fe* in undifferentiated cells and TEs

Cells	**N**	**Mean**	**Standard Error of the Mean (SEM)**
Undifferentiated	2	0.0040	0.00297
TEs	2	0.0078	0.00323

Table 22: T-test statistics for the effect of differentiation stage of a cell on relative expression of *E2Fe*

	T critical value	**Degrees of freedom (df)**	**p-value**
Undifferentiated cells vs. TEs	-0.873	2	P = 0.475

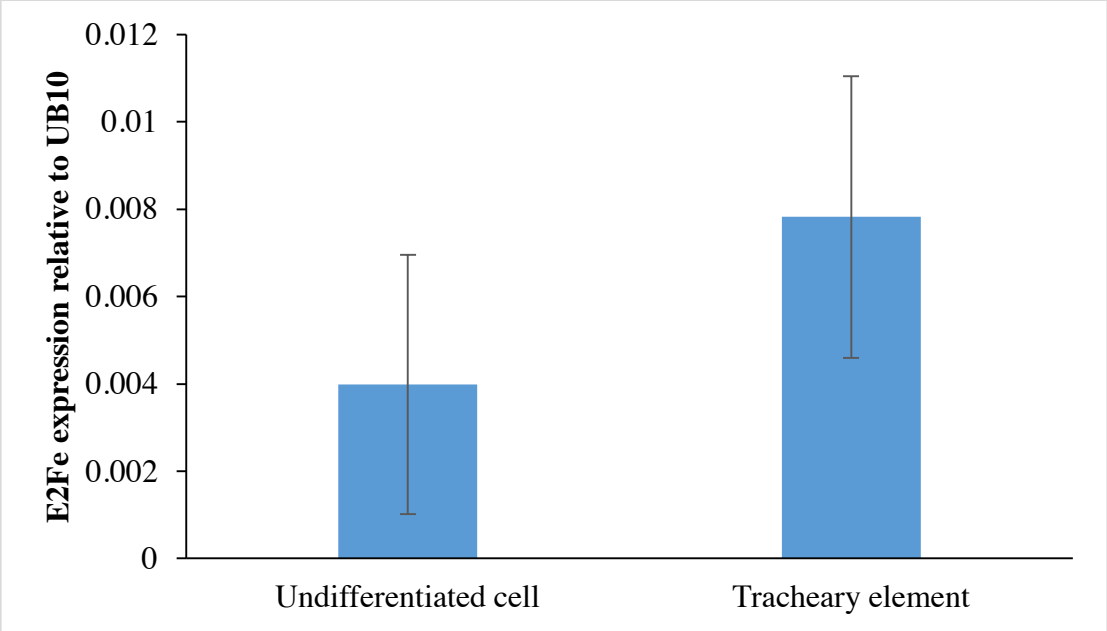

Figure 12: The relative expression of *E2Fe* in undifferentiated cells and tracheary elements. qPCR analysis of the expression of *E2Fe* relative to the expression of reference gene *UB10* in undifferentiated cells and TEs. Error bars represent the mean +/- 1 SEM for two biological and three technical repeats.

Table 23: Descriptive statistics for the relative expression of *E2Fe* in mock-treated, brassinolide (BL)-treated and brassinazole (BRZ)-treated wildtype and *suvr5* mutant seedlings

Treatment	Plant	N	Mean	Standard Error of the Mean (SEM)
Mock	Col0	3	0.0027	0.00076
	suvr5	3	0.0037	0.00078
BR	Col0	3	0.0029	0.00040
	suvr5	3	0.0047	0.00155
BRZ	Col0	3	0.0022	0.00026
	suvr5	2	0.0026	0.00198

Table 24: T-test statistics for the effect of loss of function of SUVR5 on relative expression of *E2Fe* in mock-treated, brassinolide (BL)-treated and brassinazole (BRZ)-treated seedlings

Treatment	Plant	T critical value	Degrees of freedom (df)	p-value
Mock	Col0 vs. *suvr5*	-0.856	4	P = 0.440
BR	Col0 vs. *suvr5*	-1.141	4	P = 0.317
BRZ	Col0 vs. *suvr5*	-0.185	1.033	P = 0.883

Table 25: T-test statistics for the effect of brassinolide (BL) treatment and brassinazole (BRZ) treatment on relative expression of *E2Fe* in wildtype and *suvr5* seedlings.

Plant line	Treatment	T critical value	Degrees of freedom (df)	p-value
Col0	Mock vs. BR	-0.144	4	P = 0.892
	Mock vs. BRZ	0.616	4	P = 0.571
suvr5	Mock vs. BR	-0.588	4	P = 0.588
	Mock vs. BRZ	0.588	3	P = 0.598

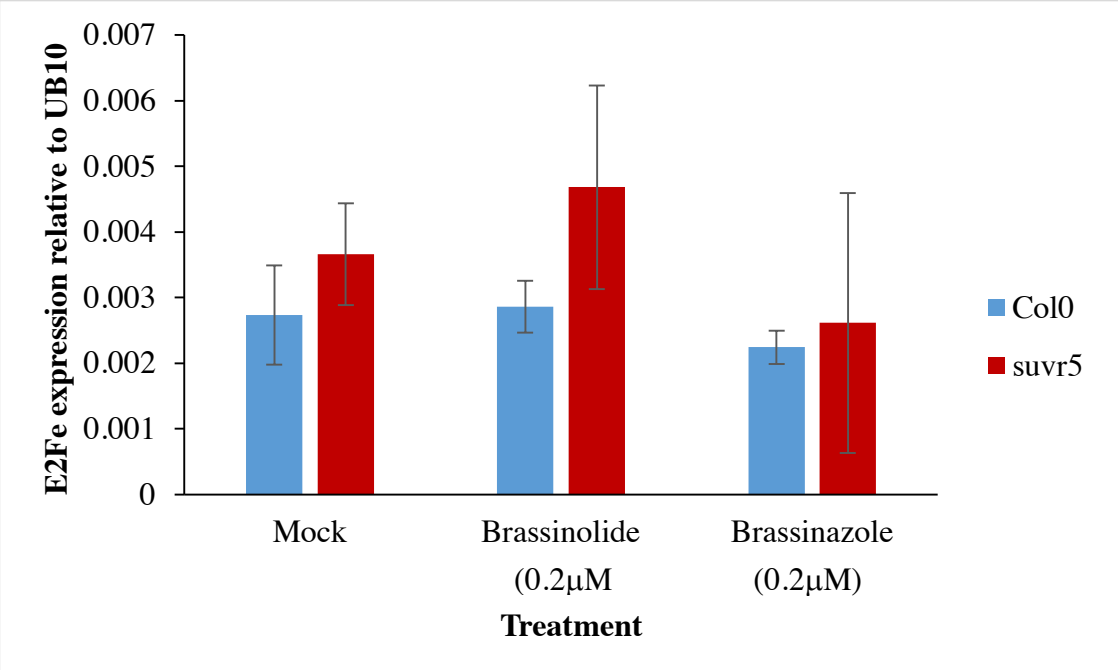

Figure 13: The effect of brassinosteroid treatment on the expression of *E2Fe* in wildtype and *suvr5* seedlings. Quantitative real-time PCR analysis of the expression of *E2Fe* relative to the expression of reference gene *UB10* in 5-d-old wildtype and *suvr5* mutant seedlings treated for 16h with brassinolide (0.2μM), brassinazole (0.2μM), or mock control. Error bars represent the mean +/- 1 SEM from three biological and three technical repeats.

Statistical analysis showed that there was no significant difference between the mean relative expression of *E2Fe* in undifferentiated cells and TEs (Tables 21 and 22, Figure 12). There was also no significant difference between mean relative expression of *E2Fe* in mock-treated, BL-treated and BRZ-treated wildtype and *suvr5* mutant seedlings (Tables 23, 24 and 25, Figure 13). See Appendices 8 and 9 for figures depicting fold change of *E2Fe* expression levels.

3.7 The effect of loss of function of SUVR5 and CLF on brassinosteroid response

Next, this study aimed to determine the biological meaning of the positive protein-protein interactions identified and validated by Y2H and BiFC analyses between BIN2 and SUVR5, CLF and SUVH5. BRs have been shown to play a crucial role in regulating hypocotyl length. Whilst BL treatment drastically increases hypocotyl length and the length of hypocotyl cells in light-grown seedlings, treatment with BRZ suppresses the length of hypocotyl cells (Tanaka et al., 2003). Furthermore, overexpression of BR-biosynthesis gene *DWARF4* resulted in a dramatic increase in hypocotyl length of light-grown seedlings (Choe et al., 2001). BRs therefore have been shown to promote hypocotyl elongation by regulating cell enlargement in hypocotyls of light-grown plants.

If BRs regulate hypocotyl elongation and BR signalling integrates with SUVR5, CLF and SUVH5 via BIN2, it was hypothesised that loss of function of SUVR5, CLF and SUVH5 would impact upon BR response and thus hypocotyl length. To test this, loss-of-function mutants that were available for SUVR5 and CLF were treated with BL and BRZ and the hypocotyl length was measured.

Table 26: Descriptive statistics for the mean hypocotyl length of mock-treated, brassinolide (BL)-treated and brassinazole (BRZ)-treated wildtype, *suvr5* and *clf29* seedlings

Treatment	Plant line	N	Mean (mm)	Standard Error of the Mean (SEM) (mm)
Mock	Col0	95	1.56	0.0254
	suvr5	50	1.60	0.0286
	clf29	17	1.49	0.0965
BL	Col0	54	2.66	0.101
	suvr5	37	3.02	0.0868
	clf29	18	2.75	0.179
BRZ	Col0	74	1.26	0.0273
	suvr5	37	1.30	0.0462
	clf29	21	1.27	0.0319

Table 27: T-test statistics for the effect of brassinosteroid treatment on mean hypocotyl length of loss of function *suvr5* and *clf29* seedlings relative to wildtype.

Treatment	**Plant line**	**T critical value**	**Degrees of freedom (df)**	**p-value**
Mock	Col0 vs. *suvr5*	-1.06	143	P = 0.291
	Col0 vs. *clf29*	0.715	18.3	P = 0.483
BL	Col0 vs. *suvr5*	-2.66	88.8	P < 0.05
	Col0 vs. *clf29*	-0.401	70	P = 0.689
BRZ	Col0 vs. *suvr5*	-0.812	109	P = 0.419
	Col0 vs. *clf29*	-0.330	93	P = 0.742

Table 28: T-test statistics for the effect of brassinosteroid treatment on mean hypocotyl length of wildtype, *suvr5* and *clf29* seedlings

Plant	**Treatment**	**T critical value**	**Degrees of freedom (df)**	**p-value**
Col0	Mock vs. BL	-10.6	59.8	P < 0.001
	Mock vs. BRZ	8.11	167	P < 0.001
suvr5	Mock vs. BL	-15.5	43.9	P < 0.001
	Mock vs. BRZ	5.64	62.2	P < 0.001
clf29	Mock vs. BL	-6.17	26.0	P < 0.001
	Mock vs. BRZ	2.12	19.5	P < 0.05

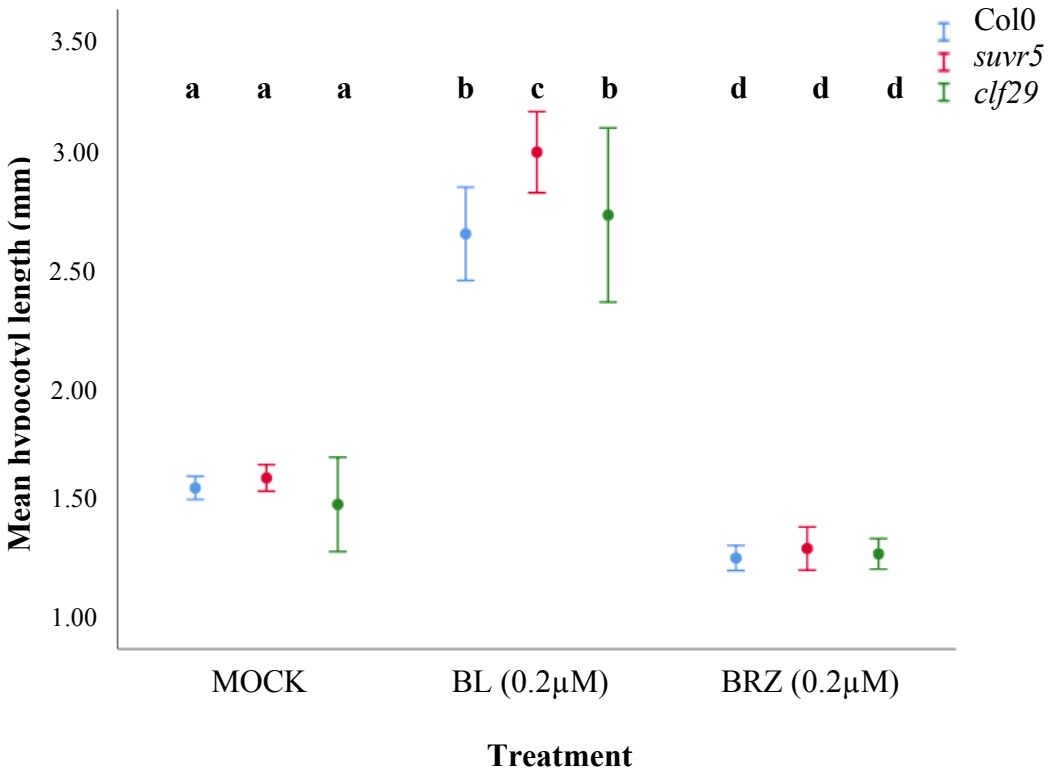

Figure 14: The effect of loss of function of SUVR5 and CLF on brassinosteroid response and mean hypocotyl length. Mean hypocotyl length of 2-d-old wildtype, *suvr5* and *clf29* seedlings treated for 3d with mock, brassinolide (BL) (0.2µM) and brassinazole (BRZ) (0.2µM). Error bars represent ± 1 SEM. Letters denote significant differences between groups when α=0.005. Groups denoted by the same letter are not significantly different from each other. See Table 26 for sample sizes (N).

Statistical analysis showed that the mean hypocotyl length of BL-treated *suvr5* seedlings is significantly higher than BL-treated wildtype seedlings (Tables 26 and 27, Figure14). There was no significant difference between the mean hypocotyl length in BL-treated wildtype seedlings and BL-treated *clf29* seedlings. In addition, the mean hypocotyl length in BRZ-treated *suvr5* and *clf29* seedlings was not significantly different from BRZ-treated wildtype seedlings (Tables 26 and 27, Figure 14).

Wildtype, *suvr5* and *clf29* seedlings all have a significantly higher mean hypocotyl length in BL-treated seedlings compared to mock-treated seedlings (Tables 26 and 28, Figure 14). On the other hand, wildtype, *suvr5* and *clf29* all have a significantly lower mean hypocotyl length in BRZ-treated seedlings compared to mock-treated seedlings (Tables 26 and 28, Figure 14).

4. Discussion

4.1 Cytokinin signalling guides histone modifying enzymes which regulate cell differentiation initiation

Key epigenetic regulators such as PcG and trxG proteins have been shown to play a crucial role in regulating meristematic activity and the balance between cell proliferation and cell differentiation (Aichinger et al., 2011). In this study, loss of function of SET domain methyltransferases ASHH3, ASHR1 and SUVR1, the H3K27 monomethyltransferase ATXR5, the H3K27 trimethyltransferase CLF, the H3K9 dimethyltransferase SUVR5, the H3K4 demethylase LDL1, and finally the H4R3me2 demethylase JMJ22 (Table 15), impacted upon root meristem size and cytokinin (CK) response. This suggests that these histone modifying enzymes have an important role in regulating the expression of genes involved in cell differentiation and their activity is potentially modulated by CK.

Firstly, mock-treated *ashh3, ashr1, atxr5, clf29, jmj22* and *ldl1* mutants had a significantly lower mean meristem cell number compared to mock-treated wildtype. Contrastingly, in mock-treated *suvr1* and *suvr5* mutants, the mean meristem cell number was significantly higher than mock-treated wildtype (Figure 4). Reduced cell number in the root meristem can either be representative of there being fewer cells due to a reduction in the division potential of meristematic transit-amplifying cells, or as a result of prolonged cell cycle duration and thus delayed transition from cell division to cell elongation (De Ioio et al., 2008; Li et al., 2017). An increase in meristem size, on the other hand, may be due to an increase in meristem activity and the expression of root stem cell and meristem marker genes as found by Aichinger et al. (2011). These changes in root meristem size relative to the wildtype in loss-of-function mutants suggests that the specific histone modifying enzymes inactivated in these mutants may be associated with regulating cell proliferation and the transition to cell differentiation.

Alongside identifying the key histone modifying enzymes associated with cell differentiation, this study aimed to test the hypothesis that hormone signals guide the

activity of histone modifying enzymes to modulate cellular decisions during differentiation. In *Arabidopsis* roots, CK promotes cell differentiation such that exogenous application of CK decreases the number of meristematic cells (Dello Ioio et al., 2007; Dello Ioio et al., 2008). If the hypothesis is correct, loss-of-function mutants in key histone modifying enzymes may therefore show differences in their response to CK. Root meristem size analysis did reveal that *ashh3*, *ashr1*, *atxr5*, *clf29*, *suvr5, ldl1* and *jmj22*, were insensitive to CK-induced differentiation as there was no significant difference between the mean meristem cell number in untreated and CK-treated roots (Figure 4). These results agree with the initial hypothesis that hormone signals such as CK signalling guide histone modifying enzymes during cell differentiation initiation.

Altogether the results suggest that CK signalling may activate SUVR5 activity, as CK treatment reduces meristem size in wildtype seedlings yet *suvr5* loss-of-function mutants have a larger meristem size compared to wildtype and are also insensitive to CK. On the other hand, CK signalling may inactivate ATXR5, CLF, LDL1 and JMJ22 activity as similarly to CK-treated wildtype seedlings, loss-of-function mutants *atxr5*, *clf29, ldl1* and *jmj22* have a shorter meristem size compared to wildtype and are also insensitive to CK.

This control of histone modifying enzyme activity by CK signalling can be put into the context of cell differentiation. Activation of SUVR5 by CK signalling may result in deposition of the repressive mark H3K9me2 on root stem cell and meristem marker genes or auxin signalling genes, which would result in reduced mitotic activity and initiation of cell differentiation. Aichinger et al. (2011) showed this to be the case for PcG-mediated H3K27me3. On the other hand, inactivation of ATXR5 by CK signalling may reduce the deposition of repressive mark H3K27me1 on genes involved in cell-cycle progression, thus promoting initiation of cell differentiation. A study by Raynaud et al. (2006) supports this as ATXR5 was found to accumulate during the S phase of the cell cycle whereby S phase progression is important in both proliferating cells and cells undergoing endoreduplication and entering differentiation (Inzé, 2005). Furthermore, inactivation of LDL1 by CK signalling may prevent removal of the active mark H3K4me(1/2/3) from similar cell-cycle genes, promoting

the transition from meristematic cell proliferation to differentiation. Finally, CK signalling-mediated inactivation of JMJ22 may prevent removal of the repressive H4R3me2 mark from genes involved in meristematic cell division and maintenance, enabling the transition from cell division to cell elongation.

In this study, the root meristem size analysis showed that *clf29* mutants had a shorter meristem compared to the wildtype and were insensitive to CK signalling, leading one to believe that CK signalling activates CLF. However, a number of studies have demonstrated that loss of function of CLF results in a larger meristem size (Aichinger et al., 2011; De Lucas et al., 2016) as seen with *suvr5* in this study. This instead suggests that CLF may actually be activated by CK signalling. The conflicting result obtained for *clf29* in this study is likely due to experimental error. This may perhaps be as a result of differences in seed germination between *clf29* and wildtype seedlings used in this study which could be due to different seed harvesting times. There is no reason to doubt the meristem size for the other mutant lines however since observations made in this study for CLF disagree with what has previously been published, the experiment should be repeated with new sets of *clf29* and Col0 seeds and on more individual seedlings.

Overall, the root meristem size analysis conducted in this study suggests that chromatin remodelling processes play a critical role in regulating cell differentiation. Moreover, hormone signalling is thought to regulate the activity of histone modifying enzymes during cell differentiation. In future, the specific effect of mutating key histone modifying enzymes on root meristem activity could be tested by analysing the expression of a G_2/M transition marker, *CYCLIN B1,* to determine whether the cell proliferation is compromised in loss-of-function mutants as in Napsucialy-Mendivil et al. (2014). Furthermore, also similarly to Napsucialy-Mendivil et al. (2014), the effect of loss of function of histone modifying enzymes on the transition from cell division to cell elongation in cells entering differentiation could be analysed. A way to do this could be to measure the number of cells that start to elongate during a set time period in mutants and compare this to the wildtype. It would also be interesting to look at the root meristem size phenotype of *SUVR5, ATXR5, CLF, LDL1* and *JMJ22* overexpression lines. If the hypothesis is correct, *SUVR5* and *CLF* overexpression is

expected to result in a short meristem whereas overexpression of *ATXR5, LDL1* and *JMJ22* should result in a longer meristem.

4.2 Specific hormonal signals are required to promote tracheary element differentiation

Having demonstrated that specific histone modifying enzymes are associated with cell differentiation initiation and are controlled by CK signalling, this study next aimed to clarify the role of hormonal signalling in guiding cell fate. Tracheary element (TE) differentiation was used as a model system whereby the experimental system used induced TE differentiation independently of hormones by overexpressing the master transcription factor VND7. Knowing that a combination of auxin, CK and brassinosteroids (BRs) is required for proper TE differentiation (Fukuda, 2004), it was hypothesised that a specific balance of those hormones might control VND7 transdifferentiation activity. If that is the case, VND7-induced xylem transdifferentiation may be impeded in scenarios where the hormone balance does not favour xylem differentiation.

This hypothesis was tested first by looking at the spatiotemporal pattern of VND7-induced xylem transdifferentiation. The secondary cell wall deposition of cells both along the longitudinal axis of the whole root and across different cell types after 3 days of VND7 induction was analysed. This revealed that secondary cell wall deposition did not occur in the columella root cap, meristematic zone, transition zone and was reduced in the late differentiation zone. In addition, secondary cell wall deposition was never seen in epidermal cells throughout the root. However, ectopic transdifferentiation of various non-vascular cell types into xylem vessel cells was observed in the elongation zone and most of the differentiation zone (Figure 6). Estradiol-induced GUS expression was equally distributed across all cell types of XVE:GUS roots (Figure 5), which eliminated the possibility that estradiol treatment might affect the spatial pattern of VND7-induced xylem transdifferentiation. The differentiation stage of the cell may determine to some extent the transdifferentiation-potential of a cell as overexpression of *VND7* was unable to induce young meristematic or fully differentiated cells to transdifferentiate into xylem vessels.

Furthermore, the absence of transdifferentiation in epidermal cells suggests positional information influences VND7 activity. Knowing this, VND7ox plant lines were then pre-treated with auxin, CK or BRs for 24hrs before induction and during 3 days of induction in order to perturb the hormone balance, and the ratio of VND7-induced transdifferentiated xylem cells was analysed in order to evaluate the importance of specific hormonal scenarios in controlling VND7 activity.

Regardless of hormonal treatment, estradiol-induced overexpression of *VND7* was found to induce the transdifferentiation of numerous non-vascular cell types into xylem cells which were identified by secondary cell wall deposition (Figure 7). However, BR and auxin-treated roots showed a reduction in TE differentiation levels (Figure 7). Thus treatment with auxin and BRs appears to impair VND7-inducible xylem transdifferentiation. This suggests that specific hormonal contexts may be required for proper TE transdifferentiation to occur.

To further analyse the role of these phytohormones in guiding VND7-induced xylem differentiation on a cell-type specific level, *VND7* overexpressor plant lines were crossed with H2B::YFP lines to mark nuclei and then pre-treated with phytohormones before induction as before. Escamez and Tuominen (2014) reviewed evolutionary and molecular studies and came to the conclusion that during TE differentiation, programmed cell death and autolysis, which result in the loss of cell contents including nuclei, are directly regulated by VND7 and VND6. Secondary cell wall deposition and lignification were thought to have evolved later to improve the efficacy of the water-transport system and be regulated by transcription factors, such as MYB46 and MYB83, that are downstream of VND7 and VND6. However, in this study it was found that after 7 days of induction of *VND7* overexpression in VND7ox;H2B::YFP roots, a fluorescent signal from YFP was still detected in the nucleus of cells with secondary cell wall thickenings (Figure 8). This indicates that secondary cell wall deposition, autolysis and programmed cell death constitute separate TE differentiation programmes with separate regulation whereby the master regulator VND7 may only control secondary cell wall deposition. Therefore, detecting the presence or absence of nuclei according to fluorescence signals may not be a valid system to confirm the xylem transdifferentiation of different cell lines. Instead,

lignified tissues could be stained with fuschin in the future to more clearly see the effect of phytohormones on VND7-induced xylem transdifferentiation detected by lignification.

In this study, different hormone scenarios were indeed found to affect the ratio of VND7-induced transdifferentiated xylem cells identified by secondary cell wall deposition. This is in line with the original hypothesis that specific hormonal contexts may be required to promote TE differentiation. Braszewska-Zalewska et al. (2013) provided evidence for distinct levels of histone and DNA modifications across root meristematic tissues in *Hordeum vulgare*. For example, the active chromatin mark H4K5ac was observed at a high level in vascular tissues and low level in the epidermis and it was concluded that vascular tissue-specific H4K5ac levels may be associated with regulating vascular tissue differentiation. In addition, De Lucas et al. (2016) observed that PRC2, which catalyses the repressive mark H3K27me3, regulates genes in a cell-type specific fashion. Whilst *VND7* is expressed in vascular cells, localised deposition of H3K27me3 mediates specific repression of *VND7* in nonvascular cells. It is therefore possible that specific hormone signalling contexts mediate localised chromatin remodelling processes, which regulate the accessibility of DNA to VND7 that in turn controls xylem cell differentiation. In future, it would be interesting to repeat this experiment and treat VND7ox plant lines with different hormone-combinations such as auxin:CK, auxin:BRs, and CK:BRs to examine the effect this has on VND7-induced xylem transdifferentiation. In addition, whole-mount immunostaining using histone mark-specific antibodies could be performed on VND7ox roots treated with different hormone-combinations. The histone mark distribution could then be compared to the VND7-induced xylem transdifferentiation pattern to determine if there is any correlation.

4.3 Histone modifying enzymes and tracheary element differentiation

In order to test whether histone modifying enzymes play an important role in TE differentiation, an *in vitro* experimental system was used. Leaf discs of loss-of-function mutants in histone modifying enzymes were cultured with auxin, cytokinin and bikinin for 3 days to induce xylem cell differentiation (Saito et al., 2017). If the

initial hypothesis is true, histone modifying enzyme mutants should have defects in bikinin-induced TE differentiation.

In this study, wildtype and all the loss-of-function histone modifying enzyme mutants tested showed differentiation of a large number of mesophyll cells to TEs having cultured leaf discs for 3 days with auxin, CK and bikinin (Figure 9). These results do not necessarily disprove the initial hypothesis that histone modifying enzymes regulate xylem cell fate, instead, it likely demonstrates the redundancy of function observed amongst histone modifying enzymes such that loss of one enzyme is substituted by another. For example, SUVR5 is known to function redundantly with KRYPTONITE (KYP)/SUVH5/SUVH6 in depositing H3K9me2 in heterochromatin (Caro et al., 2012), and CLF has been found to function partially redundantly with its homolog SWN (Chanvivattana et al., 2004). Furthermore, SUVR5 and LDL1 have been shown to interact and form a repressor complex whereby their H3K9 methyltransferase and H3K4 demethylase activities combined repress gene expression (Caro et al., 2012). This experiment should therefore be repeated using double and triple loss-of-function histone modifying mutants to determine whether chromatin remodelling modulates cell identity, specifically during TE differentiation.

4.4 Histone modifying enzymes SUVR5, CLF and SUVH5 interact with a cell differentiation-regulating hormone signalling gene, BIN2

To investigate how hormone signalling integrates with chromatin remodelling processes during cell differentiation, a yeast two-hybrid (Y2H) protein-protein interaction assay was performed to screen for interactions between a library of 30% of histone modifying enzymes and a key negative regulator of BR signalling, BIN2.

BIN2 is inhibited by upstream BR signalling. This BR signalling pathway begins with BRs binding to and being perceived by a cell-surface receptor kinase, BR INSENSITIVE1 (BRI1) (Belkhadir and Chory, 2006). This activates BRI1 kinase activity (Wang, 2001) and BRI1 goes on to phosphorylate BR-SIGNALLING KINASE1 (BSK1), promoting binding of BSK1 to BRI1-SUPPRESSOR1 (BSU1) (Kim et al., 2009). BSU1 inactivates the GSK3-like kinase BIN2 by

dephosphorylating a conserved tyrosine residue (Kim et al., 2009) and the E3 ubiquitin ligase, KIB1, mediates ubiquitination and degradation of BIN2 (Zhu et al., 2017). Inactivation of BIN2 results in dephosphorylation of BZR1 and BES1 family of transcription factors allowing them to move into the nucleus and bind directly to the promoters of their target genes to activate or repress gene expression and mediate BR responses (Zhao et al., 2002; Wang et al., 2002; Yin et al., 2002; He et al., 2002).

As is the case in the BR signalling pathway, many known BIN2 substrates are transcription factors (Li and Nam, 2002; Vert et al., 2008; Cho et al., 2014; Bernardo-García et al., 2014; Zhang et al., 2014c). However, the Y2H assay conducted in this study revealed that BIN2 also interacts with histone methyltransferases SUVR5, SUVH5 and CLF (Figure 10), which mediate deposition of repressive chromatin marks H3K9me2 and H3K27me3 via their catalytic SET and SET and RING finger Associated (SRA) domains (Caro et al., 2012; Johnson et al., 2007; Ebbs and Bender, 2006; Cao et al., 2002). A Y2H interaction was considered positive if at least two of the reporter genes were activated and thus if cells could grow on plates lacking adenine and histidine and/or yeast colonies turned blue in the presence of X-Gal. Some colonies appeared dark red in colour when grown on medium with low amounts of adenine due to poor synthesis of adenine suggesting these proteins may be less stable or have a weaker interaction with BIN2. Furthermore, for some positive protein-protein interactions no blue signal was observed in the presence of X-gal. This will be because the X-gal assay is time dependent and therefore at one time point the blue signal may be present for a particular protein-protein interaction, but it may not be seen at other time points. Nonetheless, the positive interactions between BIN2 and SUVR5 and CLF were validated *in vivo* by BiFC as a strong fluorescent signal was observed (Figure 11). The BIN2 interaction with SUVH5 was not analysed by BiFC due to unsuccessful cloning of a SUVH5 fusion protein into BiFC plasmid vectors within the time available.

Previously in this study and according to literature, both SUVR5 and CLF have been shown to be associated with regulating meristem activity and the transition from cell division to cell elongation/differentiation. Furthermore, BR signalling has also been implicated with controlling the same processes (Chaiwanon and Wang, 2015;

González-García et al., 2011) as well as playing a crucial role in TE differentiation (Iwasaki and Shibaoka, 1991; Yamamoto et al., 1997) of which BIN2 is a suppressor (Kondo et al., 2015). Therefore, the positive protein-protein interactions between BIN2 and SUVR5, SUVH5 and CLF identified by Y2H suggests that BR signalling may guide chromatin architecture via these histone modifying enzymes during cell differentiation. Further research is required however to fully understand the context and biological meaning of these interactions.

4.5 Brassinosteroid signalling and histone methyltransferase SUVR5 regulate common genes involved in cell differentiation initiation

To start unravelling the specific role of BR signalling in guiding SUVR5 activity during differentiation, a list of candidate genes significantly upregulated in the *suvr5-1* mutant (Caro et al., 2012) and regulated by BRs (Nemhauser, 2004; Goda, 2004; De Rybel et al., 2009; Sun et al., 2010) was compiled. *E2Fe* was selected from this list of candidate genes for further investigation as similarly to BR signalling, it has been implicated in regulating cell cycle progression and the transition from cell division and cell differentiation (Lammens et al., 2008; González-García et al., 2011). It was hypothesised that BR signalling guides SUVR5-mediated chromatin remodelling, which may regulate *E2Fe* expression and subsequently cell differentiation initiation.

However, results from qPCR analysis investigating the expression levels of *E2Fe* in undifferentiated cells and TEs as well as in untreated, BL-treated and BRZ-treated wildtype and *suvr5* seedlings, did not agree with the initial hypothesis. There was no significant difference between the mean relative expression of *E2Fe* in undifferentiated cells and TEs, nor between untreated, BL-treated and BRZ-treated wildtype and *suvr5* mutant seedlings. Whilst endocycle initiation has been associated with the transition from cell division to cell elongation and differentiation (Hayashi et al., 2013), the role of endoreduplication in TE differentiation remains largely unknown.

In future, BR-treating the seedlings for 3 days as opposed to overnight (16h) may have more obvious implications on *E2Fe* relative expression in Col0 and *suvr5* roots. It may also prove more informative to conduct transcriptional analysis on BR biosynthesis and signalling loss- and gain-of-function mutants such as *de-etiolated2-1* (*det2-1*) (Chory et al., 1991), *bri1*-1 (Clouse et al., 1996), *bsu1-1D* (Mora-García et al., 2004), *dwf4* (Choe et al., 2001), *bin2-1* (Li and Nam, 2002), to get a more robust idea of the role of BR signalling in regulating *E2Fe* expression via SUVR5.

4.6 Brassinosteroid signalling may inactivate SUVR5

To further investigate the biological meaning of the molecular interactions between BIN2 and SUVR5, CLF and SUVH5, next this study analysed the BR response of the *suvr5* and *clf29* loss of function mutants that were available to use in this study. Since BR signalling is a known key regulator of hypocotyl elongation (Tanaka et al., 2003) and BR signalling integrates with the histone modifying enzymes SUVR5, CLF and SUVH5 via BIN2, it was hypothesised that loss-of-function mutants in SUVR5 and CLF would show differences in their BR response and therefore hypocotyl length.

Tanaka et al. (2003) showed that BL-treatment increases hypocotyl length in light-grown seedlings whilst BRZ-treatment decreases hypocotyl length. Similarly to the wildtype seedlings, the hypocotyl length of loss of function *clf29* and *suvr5* mutants significantly increased upon treatment with BL and significantly decreased upon treatment with BRZ. *suvr5* mutants appeared more sensitive to BL treatment as statistical analysis revealed that the mean hypocotyl length of BL-treated loss of function *suvr5* mutant seedlings was significantly higher than BL-treated wildtype seedlings. This suggests that BR signalling may modulate hypocotyl elongation by inactivating SUVR5 and therefore loss of function of SUVR5 confers hypersensitivity of hypocotyl elongation to BL.

Zhang et al. (2014a) discovered that the chromatin remodelling factor PICKLE/ ENHANCED PHOTOMORPHOGENIC 1 (PKL/EPP1) directly interacts with BR signalling positive regulator, BZR1, and promotes hypocotyl elongation by repressing H3K27me3 at cell-elongated related genes. This demonstrated a role for BR signalling

in inhibiting repressive mark H3K27me3 at loci involved in cell elongation and regulating hypocotyl length. Therefore, SUVR5-mediated H3K9me2 deposition at cell-elongated related genes may also be repressed by BR signalling to promote hypocotyl elongation, explaining the hypersensitivity of *suvr5* mutants to BL and thus longer hypocotyls. This suggests a role for BR signalling in guiding SUVR5-mediated histone marks during plant development.

4.7 Conclusions

Chromatin remodelling is a complex process whereby histone modifications are dynamically regulated by histone writers and erasers and interact with each other both antagonistically and synergistically to modulate gene expression during plant development. Investigating the specific role of histone modifying enzymes in regulating cell differentiation can therefore be met by some challenges. Namely, extensive redundancy of function is observed amongst chromatin remodelling enzymes (Caro et al., 2012; Chanvivattana et al., 2004). Furthermore, complex crosstalk exists between histone modifications (Lee et al., 2010) which can interact with multiple effector protein complexes to mediate dynamic chromatin states (Berger, 2007).

Despite these challenges, the results from this study can be drawn together to propose a model for the role of BR signalling in regulating histone modifying enzymes during cell differentiation, in particular, when to switch from cell division to cell differentiation. Meristem size analysis conducted in this study and previous research (Aichinger et al., 2011; De Lucas et al., 2016) have demonstrated that loss-of-function of SUVR5 and CLF increases meristem size suggesting a role for these histone modifying enzymes in regulating meristem activity. Furthermore, BR-insensitive *bri1* mutants exhibit a reduced meristem size which suggests balanced BR signalling is required to maintain meristem size (González-García et al., 2011; Hacham et al., 2011). Therefore, BR signalling may regulate meristem size by affecting the stability and activity of SUVR5 and CLF. Analysis of the BR response of *suvr5* and *clf29* mutants indeed revealed that *suvr5* mutants are hypersensitive to BL suggesting that BR signalling may inactivate SUVR5. Furthermore, SUVR5 and CLF were found to

interact with negative regulator of BR signalling, BIN2, in this study. BIN2 has previously been shown to positively regulate substrates by phosphorylating and stabilising them as is the case for the transcription factor ABSCISIC ACID INSENSITIVE5 (ABI5) to modulate ABA response; in addition to the transcription factors myeloblastosis family transcription factor like-2 (MYBL2) and homeodomain-leucine zipper protein 1 (HAT1) to inhibit BR-repressed gene expression (Hu and Yu, 2014; Ye et al., 2012; Zhang et al., 2014b). Moreover, studies have shown that loss of function of CLF and gain of function of BIN2 result in contrasting phenotypes. Whilst *clf* loss-of-function mutants show hyponastic leaves, early flowering and increased apical dominance (Goodrich et al., 1997), gain-of-function mutations in *BIN2* gene result in round and epinastic leaves, late flowering, and reduced apical dominance (Li et al., 2001). Knowing all this, the results of this study, supported by previous research, can be used to propose a model whereby BIN2 activity in the absence of BR signalling may function in phosphorylating and stabilising SUVR5 and CLF perhaps via their shared catalytic SET domain to regulate meristem size.

In addition, the interaction between BIN2 and SUVR5, CLF and SUVH5 may also be important in regulating xylem cell differentiation. In this study, disturbing the balance of hormones by treating VND7ox seedlings with BRs caused defects in VND7-induced transdifferentiation into TEs. Localised deposition of histone marks has been found to control *VND7* expression (De Lucas et al., 2016) and therefore specific hormonal signals may guide the spatial pattern of histone marks to control *VND7* expression and TE differentiation. However, in this study bikinin-induced transdifferentiation was not impeded in loss-of-function mutants in histone modifying enzymes, but this may be explained by redundancy of function between histone modifying enzymes. Nonetheless, the suppressor of xylem differentiation, BIN2, was found to interact with SUVR5 and CLF. Altogether, this research suggests that BIN2 could guide SUVR5 and CLF activity to regulate deposition of repressive marks H3K9me2 and H3K27me3 on master regulators such as VND7 to suppress TE differentiation yet further research is required.

4.8 Future work

Alongside the ideas already mentioned throughout the discussion, there remain a number of opportunities for further research. In future, a priority would be to try overcome the challenges that accompany the complexity of chromatin remodelling such as redundancy of function between histone modifying enzymes. This could include conducting experiments on double and triple loss-of-function histone modifying enzyme mutants, or on plants overexpressing the histone modifying enzyme of interest under the control of a 35SCaMV promoter. The phenotype of these mutants could then be compared to the single loss-of-function mutants to see if it is more severe.

In order to further elucidate the level and context of the molecular interactions identified between BIN2 and SUVR5, CLF and SUVH5, a number of other experiments could be conducted in the future. Phosphorylation assays could be carried out on SUVR5, CLF and SUVH5 incubated with BIN2 to see if the histone methyltransferases are phosphorylated in the presence of BIN2. If the phosphorylation of SUVR5, CLF and SUVH5 incubated with BIN2 decreases in the presence of bikinin, this would suggest that observed phosphorylation of SUVR5, CLF and SUVH5 is indeed catalysed by BIN2. Furthermore, the stability of SUVR5, CLF and SUVH5 upon treatment with BL, BRZ and bikinin could be analysed by western blot. This altogether would test whether BIN2 phosphorylates and stabilises SUVR5, CLF and SUVH5 as hypothesised in the proposed model.

In addition, the downstream consequences of BIN2 activity over SUVR5, CLF and SUVH5 should be studied at a number of levels. This could involve looking at H3K27me3 and H3K9me3 abundance and genome wide distribution in wildtype, *clf29* and *suvr5* seedlings treated with BL and BRZ and evaluating the transcription of key regulators of cell differentiation in these treated seedlings.

It would also be useful to perform more Y2H screens for interactions between histone modifying enzymes and other BR signalling components as well as CK and auxin signalling genes and conduct similar follow up analysis as aforementioned. This

would provide a more in depth idea of the role of hormone signalling and chromatin remodelling during cell differentiation.

5. Bibliography

Achard, P., Gusti, A., Cheminant, S., Alioua, M., Dhondt, S., Coppens, F., Beemster, G.T.S., and Genschik, P. (2009). Gibberellin signaling controls cell proliferation rate in *Arabidopsis*. *Curr*. *Biol*.; **19**: 1188–1193.

Aichinger, E., Villar, C.B.R., Di Mambro, R., Sabatini, S., and Köhler, C. (2011). The CHD3 Chromatin Remodeler PICKLE and Polycomb Group Proteins Antagonistically Regulate Meristem Activity in the *Arabidopsis* Root. *The Plant Cell*; **23**: 1047–1060.

Alonso, J.M., Stepanova, A.N., Leisse, T.J., Kim, C.J., Chen, H., Shinn, P., Stevenson, D.K., Zimmerman, J., Barajas, P., Cheuk, R., Gadrinab, C., Heller, C., Jeske, A., Koesema, E., Meyers, C.C., Parker, H., Prednis, L., Ansari, Y., Choy, N., Deen, H., Geralt, M., Hazari, N., Hom, E., Karnes, M., Mulholland, C., Ndubaku, R., Schmidt, I., Guzman, P., Aguilar-Henonin, L., Schmid, M., Weigel, D., Carter, D.E., Marchand, T., Risseeuw, E., Brogden, D., Zeko, A., Crosby, W.L., Berry, C.C., and Ecker, J.R. (2003). Genome-Wide Insertional Mutagenesis of *Arabidopsis thaliana*. *Science*; **301**: 653-657.

Alvarez-Venegas, R., Pien, S., Sadder, M., Witmer, X., Grossniklaus, U., and Avramova, Z. (2003). ATX-1, an *Arabidopsis* homolog of trithorax, activates flower homeotic genes. *Curr*. *Biol*.*;* **13**: 627–637.

Aoto, T., Saitoh, N., Ichimura, T., Niwa, H., and Nakao, M. (2006). Nuclear and chromatin reorganisation in the MHC-Oct3/4 locus at developmental phases of embryonic stem cell differentiation. *Dev*. *Biol*.; **298**: 354-367.

Argyros, R.D., Mathews, D.E., Chiang, Y.H., Palmer, C.M., Thibault, D.M., Etheridge, N., Argyros, D.A., Mason, M.G., Kieber, J.J., and Schaller, G.E. (2008). Type B response regulators of *Arabidopsis* play key roles in CK signaling and plant development. *Plant Cell*; **20**: 2102–2116.

Arents, G., Burlingame, R.W., Wang, B.C., Love, W.E., and Moudrianakis, E.N. (1991). The nucleosomal core histone octamer at 3.1 A resolution: A tripartite protein assembly and a left-handed superhelix. *PNAS USA*; **88**: 10148-10152.

Arents, G., and Moudrianakis, E.N. (1995). The histone fold: a ubiquitous architectural motif utilized in DNA compaction and protein dimerization. *PNAS*; **92**(24): 11170–11174.

Bannister, A.J. and Kouzarides, T. (2011). Regulation of chromatin by histone modifications. *Cell research*; **21**: 381-395.

Bannister, A.J., Schneider, R. and Kouzarides, T. (2002). Histone methylation: dynamic or static? *Cell;* **109**: 801–806.

Bartova, E., Galiova, G., Krejci, J., Harnicarova, A., Strasak, L., and Kozubek, S. (2008). Epigenome and chromatin structure in human embryonic stem cells undergoing differentiation. *Dev. Dyn.*; **237**: 3690-3702.

Baum, S.F, Aloni, R., and Peterson, C.A. (1991). The role of CK in vessel regeneration in wounded Coleus internodes. *Ann. Bot.*; **67**: 543-548.

Belda-Palazón, B., Ruiz, L., Martí, E., Tárraga, S., Tiburcio, A.F., Culiáñez, F., Farràs, R., Carrasco, P., and Ferrando, A. (2012). Aminopropyltransferases Involved in Polyamine Biosynthesis Localise Preferentially in the Nucleus of Plant Cells. *PLoS ONE*; **7**(10): e46907.

Belkhadir, Y. and Chory, J. (2006). BR signaling: A paradigm for steroid hormone signaling from the cell surface. *Science*; **314**: 1410–1411.

Berger, S.L. (2007). The complex language of chromatin regulation during transcription. *Nature*; **447**: 407–412.

Bernardo-García, S., De Lucas, M., Martínez, C., Espinosa-Ruiz, A., Davière, J-M., and Prat, S. (2014). BR-dependent phosphorylation modulates PIF4 transcriptional activity and shapes diurnal hypocotyl growth. *Genes Dev.*; **28**(15): 1681–1694.

Berr, A., Shafiq, S., and Shen W.-H. (2011). Histone modifications in transcriptional activation during plant development. *Biochimica et Biophysica Acta*; **1809:** 567–576.

Bishopp, A., Help, H., El-Showk, S., Weijers, D., Scheres, B., Friml, J., Benková, E., Mähönen, A.P., Helariutta, Y. (2011). A mutually inhibitory interaction between auxin and CK specifies vascular pattern in roots. *Curr. Biol.;* **21**: 917–926.

Blilou, I., Xu, J., Wildwater, M., Willemsen, V., Paponov, I., Friml, J., Heidstra, R., Aida, M., Palme, K., and Scheres, B. (2005). The PIN auxin efflux facilitator network controls growth and patterning in Arabidopsis roots. *Nature*; **433**(7021): 39-44.

Boisnard-Lorig, C., Colon-Carmona, A., Bauch, W., Hodge, S., Doerner, P., Bancharel, E., Dumas, C., Haseloff, J., and Berger, F. (2001). Dynamic analyses of the expression of the HISTONE::YFP fusion protein in *Arabidopsis* show that syncytial endosperm is divided in mitotic domains. *Plant Cell*; **13**: 495–509.

Boland, M.J., Nazor, K.L. and Loring, J.F. (2014). Epigenetic Regulation of Pluripotency and Differentiation**.** *Circulation Research*; **115**: 311-324.

Braszewska-Zalewska, A.J., Wolny, E.A., Smialek, L., and Hasterok, R. (2013). Tissue-Specific Epigenetic Modifications in Root Apical Meristem Cells of Hordeum vulgare. *PLoS ONE*; **8**(7): e69204.

Byrd, K.N. and Shearn, A. (2003). ASH1, a *Drosophila* trithorax group protein, is required for methylation of lysine 4 residues on histone H3. *PNAS*; **100**(20): 11535–11540.

Caño-Delgado, A., Yin, Y., Yu, C., Vafeados, D., Mora-Garc, S., Cheng, J.C., Nam, K.H., Li, J., and Chory, J. (2004). BRL1 and BRL3 are novel BR receptors that function in vascular differentiation in *Arabidopsis*. *Development*; **131**: 5341–5351.

Cao, R., Wang, L., Wang, H., Xia, L., Erdjument-Bromage, H., Tempst, P., Jones, R.S. and Zhang, Y. (2002). Role of histone H3 lysine 27 methylation in polycomb-group silencing. *Science*; **298**: 1039–1043.

Caro, E., Stroud, H., Greenberg, M.V.C., Bernatavichute, Y.V., Feng, S., Groth, M., Vashisht, A.A., Wohlschlegel, J. and Jacobsen, S.E. (2012). The SET-Domain Protein SUVR5 Mediates H3K9me2 Deposition and Silencing at Stimulus Response Genes in a DNA Methylation–Independent Manner. *PLoS Genet;* 8(10): e1002995.

Causier, B., Ashworth, M., Guo, W. and Davies, B. (2012). The TOPLESS interactome: A framework for gene repression in *Arabidopsis*. *Plant Physiol*; **158**: 423–438.

Chaiwanon, J. and Wang, Z-Y. (2015). Spatiotemporal BR Signaling and Antagonism with Auxin Pattern Stem Cell Dynamics in *Arabidopsis* Roots. *Current Biology*; **25**(8): 1031-1042.

Chanvivattana, Y., Bishopp, A., Schubert, D., Stock, C., Moon, Y.H., Sung, Z.R., and Goodrich, J. (2004). Interaction of Polycomb-group proteins controlling flowering in *Arabidopsis*. *Development*; **131**: 5263–5276.

Chen, Z., Zang, J., Whetstine, J., Hong, X., Davrazou, F., Kutateladze, T.G., Simpson, M., Mao, Q., Pan, C-H., Dai, S., Hagman, J., Hansen, K., Shi, Y., and Zhang, G. (2006). Structural Insights into Histone Demethylation by JMJD2 Family Members. *Cell*; **125**: 691–702.

Cho, J-N., Ryu, J-Y., Jeong, Y-M., Park, J., Song, J-J., Amasino, R.M., Noh, B., and Noh, Y-S. (2012). Control of Seed Germination by Light-Induced Histone Arginine Demethylation Activity. *Developmental Cell*; **22**(4): 736-748.

Cho, H., Ryu, H., Rho, S., Hill, K., Smith, S., Audenaert, D., Park, J., Han, S., Beeckman, T., Bennett, M.J., Hwang, D., De Smet, I., and Hwang, I. (2014). A secreted peptide acts on BIN2-mediated phosphorylation of ARFs to potentiate auxin response during lateral root development. *Nature Cell Biology*; **16**(1): 66-76.

Choe, S., Fujioka, S., Noguchi, T., Takatsuto, S., Yoshida, S., and Feldmann, K.A. (2001). Overexpression of DWARF4 in the BR biosynthetic pathway results in increased vegetative growth and seed yield in *Arabidopsis*. *Plant J*.; **26**: 573 – 582.

Choe, S.W., Noguchi, T., Fujioka, S., Takatsuto, S., Tissier, C.P., Gregory, B.D., Ross, A.S., Tanaka, A., Yoshida, S., Tax, F.E., and Feldmann, K.A. (1999). The *Arabidopsis* dwf7/ste1 mutant is defective in the Delta(7) sterol C-5 desaturation step leading to BR biosynthesis. *Plant Cell*; **11**: 207–221.

Chory, J., Nagpal, P., and Peto, C.A. (1991). Phenotypic and genetic analysis of *det2*, a new mutant that affects light-regulated seedling development in *Arabidopsis*. *Plant Cell*; **3**:445–459.

Clouse, S.D., Langford, M., and McMorris, T.C. (1996). A BR-insensitive mutant in *Arabidopsis thaliana* exhibits multiple defects in growth and development. *Plant Physiol.;* **111**(3):671-678.

Coego, A., Brizuela, E., Castillejo, P., Ruíz, S., Koncz, C., del Pozo, J.C., Piñeiro, M., Jarillo, J.A., Paz-Ares, J., León, J.; TRANSPLANTA Consortium. (2014). The TRANSPLANTA collection of *Arabidopsis* lines: a resource for functional analysis of transcription factors based on their conditional overexpression. *Plant J*.; **77**(6): 944-53.

Coiro, M and Truernit, E. (2017). Xylem Characterisation Using Improved Pseudo-Schiff Propidium Iodide Staining of Whole Mount Samples and Confocal Laser-Scanning *Microscopy*. *Methods Mol Biol*.; **1544**: 127-132.

Cooper, G.M. (2000) *Cell Proliferation in Development and Differentiation*. The Cell: A Molecular Approach. 2nd edition. Sunderland (Massachusetts): Sinauer Associates.

Davey, C.A., Sargent, D.F., Luger, K., Maeder, A.W., and Richmond, T.J. (2002). Solvent Mediated Interactions in the Structure of the Nucleosome Core Particle at 1.9 Å Resolution. *Journal of Molecular Biology*; **319**(5): 1097-1113.

De Lucas, M., Pu, L., Turco, G.M., Gaudinier, A., Marao, A.K., Hiroshima, H., Kim, D., Ron, M., Sugimoto, K., Roudier, F.M., and Brady, S.M. (2016). Transcriptional regulation of *Arabidopsis* Polycomb Repressive Complex 2 coordinates cell type proliferation and differentiation., *Plant cell*.; **28**(10): 2616-2631.

De Rybel, B., Audenaert, D., Vert, G., Rozhon, W., Mayerhofer, J., Peelman, F., Coutuer, S., Denayer, T., Jansen, L., Nguyen, L., Vanhoutte, I., Beemster, G.T., Vleminckx, K., Jonak, C., Chory, J., Inzé, D., Russinova, E., and Beeckman, T. (2009). Chemical inhibition of a subset of *Arabidopsis thaliana* GSK3-like kinases activates BR signalling. *Chem. Biol*.; **16**: 594–604.

Dello Ioio, R., Linhares, F.S., Scacchi, E., Casamitjana-Martinez, E., Heidstra, R., Costantino, P., and Sabatini, S. (2007). CKs determine *Arabidopsis* root-meristem size by controlling cell differentiation. *Curr Biol;* **17**: 678–682.

Dello Ioio, R., Nakamura, K., Moubayidin, L., Perilli, S., Taniguchi, M., Morita, M.T., Aoyama, T., Costantino, P., and Sabatini, S. (2008). A genetic framework for the auxin/CK control of cell division and differentiation in the root meristem. *Science;* **322**: 1380–1384.

Di Mambro, R., De Ruvo, M., Pacifici, E., Salvi, E., Sozzani, R., Benfey, P.N., Busch, W., Novak, O., Ljung, K., Di Paola, L., Marée, A.F.M., Costantino, P., Grieneisen, V.A., and Sabatini, S. (2017). Auxin minimum triggers the developmental switch from cell division to cell differentiation in the *Arabidopsis* root. *PNAS*; **114**(36): e7641-e7649.

Dolan, L., Janmaat, K., Willemsen, V., Linstead, P., Poethig, S., Roberts, K. and Scheres, B. (1993). Cellular organisation of the *Arabidopsis thaliana* root. *Development*; **119**: 71–84.

Dorighi, K.M., and Tamkun, J.W. (2013). The trithorax group proteins Kismet and ASH1 promote H3K36 dimethylation to counteract Polycomb group repression in *Drosophila*. *Development;* **140**(20): 4182–4192.

Ebbs, M.L. and Bender, J. (2006). Locus-Specific Control of DNA Methylation by the *Arabidopsis* SUVH5 Histone Methyltransferase. *The Plant Cell*; **18**: 1166–1176.

Escamez, S. and Tuominen, H. (2014). Programmes of cell death and autolysis in tracheary elements: when a suicidal cell arranges its own corpse removal. *Journal of Experimental Botany*; **65**(5): 1313–1321.

Espinosa-Ruiz, A., Martıńez, C., de Lucas, M., Fabregas, N., Bosch, N., Caño-Delgado, A.I. and Prat, S. (2017). TOPLESS mediates BR control of shoot boundaries and root meristem development in *Arabidopsis thaliana*. *Development*; **144**: 1619-1628.

Fields, S. and Song, O. (1989) A novel genetic system to detect protein-protein interactions. *Nature;* **340**: 245–246.

Fisher, K. and Turner, S. (2007). PXY, a receptor-like kinase essential for maintaining polarity during plant vascular-tissue development. *Curr. Biol.*; **17**: 1061–1066.

Fromm, M. and Avramova, Z. (2014). ATX1/AtCOMPASS and the H3K4me3 marks: How do they activate *Arabidopsis* genes? *Curr Opin Plant Biol;* **21**: 75–82.

Fu, C., Donovan, W.P., Shikapwashya-Hasser, O., Ye, X., and Cole, R.H. (2014). Hot Fusion: An Efficient Method to Clone Multiple DNA Fragments as Well as Inverted Repeats without Ligase. *PLoS ONE*; **9**(12): e115318.

Fukuda, H. (1996). Xylogenesis: initiation, progression, and cell death. *Annu. Rev. Plant Physiol. Plant Mol. Biol.;* **47**: 299-325.

Fukuda, H. (1997). Tracheary element differentiation. *Plant Cell*; **9**: 1147–1156.

Fukuda, H. (2004). Signals that control plant vascular cell differentiation. *Nat. Rev. Mol. Cell Biol.;* **5:** 379–391.

Fukuda, H. and Komamine, A. (1980). Establishment of an experimental system for the tracheary element differentiation from single cells isolated from the mesophyll of *Zinnia elegans*. *Plant Physiol*.; **65**: 57-60.

Gälweiler, L., Guan, C., Müller, A., Wisman, E., Mendgen, K., Yephremov, A., and Palme, K. (1998). Regulation of polar auxin transport by AtPIN1 in *Arabidopsis* vascular tissue. *Science*; **282**: 2226–2230.

Geisler, S.J. and Paro R. (2015). Trithorax and Polycomb group-dependent regulation: a tale of opposing activities. *Development;* **142**: 2876-2887.

Goda, H., Sawa, S., Asami, T., Fujioka, S., Shimada, Y., and Yoshida, S. (2004). Comprehensive Comparison of Auxin-Regulated and BR-Regulated Genes in *Arabidopsis*. *Plant Physiology*; **134**(4): 1555–1573.

Goldberg, A.D., David Allis, C., and Bernstein, E. (2007). Epigenetics: A Landscape Takes Shape. *Cell*; **128**(4): 635-638.

González-García, M.P., Vilarrasa-Blasi, J., Zhiponova, M., Divol, F., Mora-García, S., Russinova, E., Caño-Delgado, A.I. (2011). BRs control meristem size by promoting cell cycle progression in *Arabidopsis* roots. *Development;* **138**: 849–859.

Goodrich, J., Puangsomlee, P., Martin, M., Long, D., Meyerowitz, E.M. and Coupland, G. (1997). A Polycomb-group gene regulates homeotic gene expression in *Arabidopsis*. *Nature;* **386**: 44–51.

Grossniklaus, U., Vielle-Calzada, J.P., Hoeppner, M.A., and Gagliano, W.B. (1998). Maternal control of embryogenesis by MEDEA, a polycomb group gene in *Arabidopsis*. *Science;* **280**(5362): 446-450.

Guo, L., Yu, Y., Law, J.A. and Zhang, X. (2010). SET DOMAIN GROUP2 is the major histone H3 lysine 4 trimethyltransferase in *Arabidopsis*. *PNAS USA*; **107**: 18557–18562.

Hacham, Y., Holland, N., Butterfield, C., Ubeda-Tomas, S., Bennett, M.J., Chory, J., and Savaldi-Goldstein, S. (2011). BR perception in the epidermis controls root meristem size. *Development; **138***(5): 839–848.

Hale, C.J., Potok, M.E., Lopez, J., Do, T., Liu, A., Gallego-Bartolome, J., Michaels, S.D., and Jacobsen, S.E. (2016). Identification of Multiple Proteins Coupling Transcriptional Gene Silencing to Genome Stability in *Arabidopsis thaliana*. *PLoS Genetics*; **12**(6): e1006092.

Hardtke, C.S. and Berleth, T. (1998). The *Arabidopsis* gene MONOPTEROS encodes a transcription factor mediating embryo axis formation and vascular development. *EMBO J*.; **17**: 1405–1410.

Hayashi, K., Hasegawa, J. and Matsunaga, S. (2013). The boundary of the meristematic and elongation zones in roots: endoreduplication precedes rapid cell expansion. *Sci. Rep.*; **3**: 2723.

He, J.X., Gendron, J.M., Yang, Y., Li, J., and Wang, Z.Y. (2002). The GSK3-like kinase BIN2 phosphorylates and destabilises BZR1, a positive regulator of the BR signaling pathway in *Arabidopsis*. *PNAS USA.;* **99**: 10185–10190.

Heyman, J., Polyn, S., Eekhout, T., and De Veylder, L. (2017). Tissue-Specific Control of the Endocycle by the Anaphase Promoting Complex/Cyclosome inhibitors UVI4 and DEL1. *Plant Physiol*.; **175**(1): 303-313.

Hirakawa, Y., Shinohara, H., Kondo, Y., Inoue, A., Nakanomyo, I., Ogawa, M., Sawa, S., Ohashi-Ito, K., Matsubayashi, Y., and Fukuda, H. (2008). Non-cell-autonomous control of vascular stem cell fate by a CLE peptide/receptor system. *Proc. Natl Acad. Sci. USA*; **105**: 15208–15213.

Hobbie, L., McGovern, M., Hurwitz, L.R., Pierro, A., Liu, N.Y., Bandyopadhyay, A. and Estelle, M. (2000). The axr6 mutants of *Arabidopsis thaliana* define a gene involved in auxin response and early development. *Development*; **127**: 23–32.

Hu, Y. and Yu, D. (2014). BR INSENSITIVE2 Interacts with ABSCISIC ACID INSENSITIVE5 to Mediate the Antagonism of BRs to Abscisic Acid during Seed Germination in *Arabidopsis*. *Plant Cell;* **26**(11): 4394-4408.

Huang, H., Sabari, B.R., Garcia, B.A., Allis, C.D., and Zhao, Y. (2014). SnapShot: Histone Modifications. *Cell*; **159**: 458-458.

Ikeuchi, M., Iwase, A., Rymen, B., Harashima, H., Shibata, M., Ohnuma, M., Breuer, C., Morao, A.K., de Lucas, M., De Veylder, L., Goodrich, J., Brady, S.M., Roudier, F. and Sugimoto, K. (2015b). PRC2 represses dedifferentiation of mature somatic cells in *Arabidopsis*. *Nat. Plants*; **1**: 15089.

Ikeuchi, M., Iwase, A. and Sugimoto, K. (2015a). Control of plant cell differentiation by histone modification and DNA methylation. *Current Opinion in Plant Biology*; **28**: 60–67.

Inzé, D. (2005). Green light for the cell cycle. *The EMBO Journal*; **24**(4): 657–662.
Iwasaki, T. and Shibaoka, H. (1991). BRs act as regulators of tracheary-element differentiation in isolated *Zinnia* mesophyll cells. *Plant Cell Physiol*.; **32**: 1007–1014.

Jacob, Y., Feng, S., LeBlanc, C.A., Bernatavichute, Y.V., Stroud, H., Cokus, S., Johnson, L.M., Pellegrini, M., Jacobsen, S.E., and Michaels, S.D. (2009). ATXR5 and ATXR6 are H3K27 monomethyltransferases required for chromatin structure and gene silencing. *Nat. Struct. Mol. Biol.;* **16**(7): 763-768.

Jaillais, Y., and Chory, J. (2010). Unraveling the paradoxes of plant hormone signalling integration. *Nature Structural & Molecular Biology*; 17: 642-645.

Jenuwein T. and Allis, C.D. (2001). Translating the histone code. *Science*; **293**: 1074–1080.

Jenuwein, T., Laible, G., Dorn, R. and Reuter, G. (1998). SET domain proteins modulate chromatin domains in eu- and heterochromatin. *Cell Mol. Life Sci.;* **54**: 80–93.

Jiang, D., Wang, Y., Wang, Y., and He, Y. (2008). Repression of FLOWERING LOCUS C and FLOWERING LOCUS T by the *Arabidopsis* Polycomb repressive complex 2 components. *PLoS ONE*; **3**: e3404.

Jiang, D., Yang, W., He, Y., and Amasino, R.M. (2007). *Arabidopsis* Relatives of the Human Lysine-Specific Demethylase1 Repress the Expression of FWA and FLOWERING LOCUS C and Thus Promote the Floral Transition. *The Plant Cell*; **19**(10): 2975–2987.

Johnson, L.M., Bostick, M., Zhang, X., Kraft, E., Henderson, I., Callis, J., and Jacobsen, S.E. (2007). The SRA methyl-cytosine-binding domain links DNA and histone methylation. *Curr. Biol.*; **17**: 379–384.

Jürgens, G., Mayer, U., Torres Ruiz, R. A., Berleth, T. and Miséra, S. (1991). Genetic analysis of pattern formation in the *Arabidopsis* embryo. *Development*; **11**: 27-38.

Kim, T-W., Guan, S., Sun, Y., Deng, Z., Tang, W., Shang, J-X., Sun, Y., Burlingame, A.L. and Wang, Z-Y. (2009). BR signal transduction from cell-surface receptor kinases to nuclear transcription factors**.** *Nature Cell Biology;* **11**: 1254 –1260.
Kerppola, T. K. (2008). Bimolecular Fluorescence Complementation (BiFC) analysis as a probe of protein interactions in living cells. *Annual Review of Biophysics*; **37**: 465–487.

Kondo, Y., Fujita, T., Sugiyama, M., and Fukuda, H. (2015). A novel system for xylem cell differentiation in *Arabidopsis thaliana*. *Molecular plant;* **8**: 612–621.

Kondo, Y., Ito, T., Nakagami, H., Hirakawa, Y., Saito, M., Tamaki, T., Shirasu, K. and Fukuda, H. (2014). Plant GSK3 proteins regulate xylem cell differentiation downstream of TDIF–TDR signalling. *Nature Communications*; **5**: 3504.

Koornneef, M., and Meinke, D. (2010). The development of *Arabidopsis* as a model plant. *Plant Journal*; **61**: 909-921.

Kornet, N. and Scheres, B. (2009). Members of the GCN5 histone acetyltransferase complex regulate PLETHORA-mediated root stem cell niche maintenance and transit amplifying cell proliferation in *Arabidopsis*. *Plant Cell*; **21**: 1070–1079.

Kouzarides, T. (2002). Histone methylation in transcriptional control. *Curr. Opin. Genet. Dev.*; **12**: 198–209.

Kouzarides, T. (2007). Chromatin Modifications and Their Function. *Cell;* **128**: 13.

Krejci, J., Uhlirova, R., Galiova, G., Kozubek, S., Smigova, J., and Bartova, E. (2009). Genome-wide reduction in H3K9 acetylation during human embryonic stem cell differentiation. *J. Cell Physiol*.; **219**: 677-687.

Kubo, M., Udagawa, M., Nishikubo, N., Horiguchi, G., Yamaguchi, M., Ito, J., Mimura, T., Fukuda, H. and Demura, T. (2005). Transcription switches for protoxylem and metaxylem vessel formation. *Genes Dev*.; **19**(16): 1855-1860.

Kumar, R., Ichihashi, Y., Kimura, S., Chitwood, D.H., Headland, L.R., Peng, J., Maloof, J.N. and Sinha, N.R. (2012) A high-throughput method for Illumina RNA-Seq library preparation. *Front. Plant Sci.;* **3**(202).

Kurihara, D., Yoko, M., Yoshikatsu, S., and Tetsuya, H. (2015). ClearSee: a Rapid Optical Clearing Reagent for Whole-Plant Fluorescence Imaging. *Development;* **142**(23): 4168–4179.

Kuzmichev, A., Nishioka, K., Erdjument-Bromage, H., Tempst, P., and Reinberg, D. (2002). Histone methyltransferase activity associated with a human multiprotein complex containing the Enhancer of Zeste protein. *Genes Dev*.; **16**: 2893-2905.

Lammens, T., Boudolf, V., Kheibarshekan, L., Zalmas, L.P., Gaamouche, T., Maes, S., Vanstraelen, M., Kondorosi, E., La Thangue, N.B., Govaerts, W., Inzé, D. and De Veylder, L. (2008). Atypical E2F activity restrains APC/$C^{CCS52A2}$ function obligatory for endocycle onset. *PNAS USA*; **105**: 14721-14726.

Lee, J.H., Hart, S.R., and Skalnik, D.G. (2004). Histone deacetylase activity is required for embryonic stem cell differentiation. *Genesis*; **38**:32-38.

Lee, J.S., Smith, E., and Shilatifard, A. (2010). The language of histone crosstalk. *Cell*; **142**: 682–685.

Lelli, K.M., Slattery, M., and Mann, R.S. (2012) Disentangling the many layers of eukaryotic transcriptional regulation. *Annual Review of Genetics*; **46**: 43–68.

Li, H., Torres-Garcia, J., latrasse, D., Benhamed, M., Schilderink, S., Zhou, W., Kulikova, O., Hirt, H., and Bisseling, T. (2017). Plant-specific Histone Deacetylases HDT½ Regulate GIBBERELLIN 2-OXIDASE 2 Expression to Control *Arabidopsis* Root Meristem Cell Number. *The Plant Cell Online*; **29**(8): tpc.00366.2017.

Li, J. M. and Nam, K. H. (2002). Regulation of BR signaling by a GSK3/SHAGGY-like kinase. *Science;* **295**(5558): 1299–1301.

Li, J., Nam, K.H., Vafeados, D., and Chory, J. (2001) *BIN2*, a New BR-Insensitive Locus in Arabidopsis. *Plant Physiology*; **127**(1): 14–22.

Long, J.A., Ohno, C., Smith, Z.R. and Meyerowitz, E.M. (2006). TOPLESS regulates apical embryonic fate in *Arabidopsis*. *Science*; **312**: 1520–1523.

Lucas, W.J., Groover, A., Lichtenberger, R., Furuta, K., Yadav, S.R., Helariutta, Y., He, X.Q., Fukuda, H., Kang, J., Brady, S.M., Patrick, J.W., Sperry, J., Yoshida, A., Lopez-Millan, A.F., Grusak, M.A. and Kachroo, P. (2013). The plant vascular system: evolution, development and functions. *J. Integr. Plant Biol.*; **55**: 294–388.

Mähönen, A.P., Bishopp, A., Higuchi, M., Nieminen, K.M., Kinoshita, K., Törmäkangas, K., Ikeda, Y., Oka, A., Kakimoto, T., and Helariutta, Y. (2006b). CK signaling and its inhibitor AHP6 regulate cell fate during vascular development. *Science*; **311**: 94–98.

Mähönen, A.P., Bonke, M., Kauppinen, L., Riikonen, M., Benfey, P., Helariutta, Y. (2000). A novel two-component hybrid molecule regulates vascular morphogenesis of the *Arabidopsis* root. *Genes Dev.*; **14**: 2938–2943.

Mähönen, A.P., Higuchi, M., Törmäkangas, K., Miyawaki, K., Pischke, M.S., Sussman, M.R., Helariutta, Y., and Kakimoto, T. (2006a). CKs regulate a bidirectional phosphorelay network in *Arabidopsis*. *Curr. Biol.*; **16**: 1116–1122.

Mattout, A. and Meshorer, E. (2010). Chromatin plasticity and genome organisation in pluripotent embryonic stem cells. *Current Opinion in Cell Biology;* **22**: 334–341.

Mayer, U., Torres-Ruiz, R.A., Berleth, T., Miséra, S. and Jürgens, G. (1991). Mutations affecting body organisation in the *Arabidopsis* embryo. *Nature*; **353**: 402–407.

Meshorer, E. and Misteli, T. (2006). Chromatin in pluripotent embryonic stem cells and differentiation. *Nat. Rev. Mol. Cell Biol.*; **7**(7): 540-546.

McManus, M.T. and Veit, B.E. (2002) Meristematic tissues in plant growth and development. Sheffield: Sheffield Academic Press.

Möckli, N. and Auerbach, D. (2004). Quantitative β-galactosidase assay suitable for high-throughput applications in the yeast two- hybrid system. *BioTechniques;* **36**: 872-876.

Mora-García, S., Vert, G., Yin, Y., Caño-Delgado, A., Cheong, H., and Chory, J. (2004). Nuclear protein phosphatases with Kelch-repeat domains modulate the response to BRs in *Arabidopsis*. *Genes & Development*; **18**(4): 448–460.

Morales, V., Giamarchi, C., Chailleux, C., Moro, F., Marsaud, V., Le Ricousse, S., and Richard-Foy, H. (2001). Chromatin structure and dynamics: Functional implications. *Biochimie*; **83:** 1029–1039.

Moubayidin, L., Perilli, S., Dello Ioio, R., Di Mambro, R., Costantino, P., and Sabatini, S. (2010). The rate of cell differentiation controls the *Arabidopsis* root meristem growth phase. *Curr. Biol.*; **20**: 1138–1143.

Muller, J., Hart, C.M., Francis, N.J., Vargas, M.L., Sengupta, A., Wild, B., Miller, E.L., O'Connor, M.B., Kingston, R.E., and Simon, J.A. (2002). Histone methyltransferase activity of a Drosophila polycomb group repressor complex. *Cell*; **111**: 197-208.

Napsucialy-Mendivil, S., Alvarez-Venegas, R., Shishkova, S. and Dubrovsky, J.G. (2014). *Arabidopsis* homolog of trithorax1 (ATX1) is required for cell production, patterning, and morphogenesis in root development. *J. Exp. Bot.*; **65**: 6373–6384.

Nemhauser, J.L., Mockler, T.C., and Chory, J. (2004). Interdependency of BR and Auxin Signaling in *Arabidopsis*. *PLoS Biol*; **2**(9): e258.

Nieminen, K., Blomster, T., Helariutta, Y., and Mähönen, A.P. (2015). Vascular Cambium Development. *The Arabidopsis Book*; **11**: e0177.

Niu, L., Zhang, Y., Pei, Y., Liu, C., and Cao, X. (2008). Redundant requirement for a pair of PROTEIN ARGININE METHYLTRANSFERASE4 homologs for the proper regulation of *Arabidopsis* flowering time. *Plant Physiol.*; **148**: 490–503.

Ng, S.S., Yue, W.W., Oppermann, U., and Klose, R.J. (2009). Dynamic protein methylation in chromatin biology. *Cellular and Molecular Life Sciences;* **66**(3): 407–422.

Oda, Y., Iida, Y., Kondo, Y., and Fukuda, H. (2010). Wood Cell-Wall Structure Requires Local 2D-Microtubule Disassembly by a Novel Plasma Membrane-Anchored Protein. *Current Biology*; **20**: 1197–1202.

Oda, Y., Mimura, T., and Hasezawa, S. (2005). Regulation of secondary cell wall development by cortical microtubules during tracheary element differentiation in *Arabidopsis* cell suspensions. *Plant Physiol.;* **137**: 1027–1036.

Ohashi-Ito, K. and Fukuda, H. (2010). Transcriptional regulation of vascular cell fates. *Current Opinion in Plant Biology*; **13:** 670–676.

Ohashi-Ito, K., Oda, Y., and Fukuda, H. (2010). *Arabidopsis* VASCULAR-RELATED NAC-DOMAIN6 directly regulates the genes that govern programmed cell death and secondary wall formation during xylem differentiation. *Plant Cell;* **22**: 3461–3473.

Perilli, S. and Sabatini, S. (2010). Analysis of root meristem size development. *Methods Mol. Biol.;* **655**: 177-187.

Perilli, S., Di Mambro, R., and Sabatini, S. (2012). Growth and development of the root apical meristem. *Current Opinion in Plant Biology*; **15**: 17–23.

Pesquet, E., Korolev, A.V., Calder, G., and Lloyd, C.W. (2010). The microtubule-associated protein AtMAP70-5 regulates secondary wall patterning in *Arabidopsis* wood cells. *Curr. Biol.;* **20**: 744–749.

Pi, L., Aichinger, E., van der Graaff, E., Llavata-Peris, C.I., Weijers, D., Hennig, L., Groot, E., and Laux, T. (2015). Organiser-derived WOX5 signal maintains root columella stem cells through chromatin- mediated repression of CDF4 expression. *Dev. Cell*; **8**: 576-588.

Pien, S., Fleury, D., Mylne, J.S., Crevillen, P., Inzé, D., Avramova, Z., Dean, C., and Grossniklaus, U. (2008). ARABIDOPSIS TRITHORAX1 Dynamically Regulates FLOWERING LOCUS C Activation via Histone 3 Lysine 4 Trimethylation. *The Plant Cell*; **20**: 580–588.

Ralston, A. and Shaw, K. (2008) Gene expression regulates cell differentiation. *Nature Education*; **1**(1): 127.

Raynaud, C., Sozzani, R., Glab, N., Domenichini, S., Perennes, C., Cella, R., Kondorosi, E. and Bergounioux, C. (2006). Two cell-cycle regulated SET-domain proteins interact with proliferating cell nuclear antigen (PCNA) in *Arabidopsis*. *The Plant Journal*; **47**: 395–407.

Rieu, I., Eriksson, S., Powers, S.J., Gong, F., Griffiths, J., Woolley, L., Benlloch, R., Nilsson, O., Thomas, S.G., Hedden, P., and Phillips, A.L. (2008). Genetic analysis reveals that C19-GA 2-oxidation is a major gibberellin inactivation pathway in *Arabidopsis*. *The Plant cell*; **20**: 2420-2436.

Rohland, N. and Reich, D. (2012). Cost-effective, high-throughput DNA sequencing libraries for multiplexed target capture. *Genome Research*; **22**(5): 939–946.

Rosa, S., Ntoukakis, V., Ohmido, N., Pendle, A., Abranches, R., and Shaw, P. (2014). Cell differentiation and development in *Arabidopsis* are associated with changes in histone dynamics at the single-cell level. *Plant Cell*; **26**: 4821–4833.

Ruzicka, K., Simásková, M., Duclercq, J., Petrásek, J., Zazímalová, E., Simon, S., Friml, J., Van Montagu, M.C., and Benková, E. (2009). CK regulates root meristem activity via modulation of the polar auxin transport. *Proc. Natl. Acad. Sci. USA.*; **106**: 4284–4289

Ryu, H., Cho, H., Bae, W., and Hwang, I. (2014). Control of early seedling development by BES1/TPL/HDA19-mediated epigenetic regulation of ABI3. *Nat Commun.*; **5**: 4138.

Sabatini, S., Beis, D., Wolkenfelt, H., Murfett, J., Guilfoyle, T., Malamy, J., Benfey, P., Leyser, O., Bechtold, N., Weisbeek, P., and Scheres, B. (1999) An auxin-dependent distal organizer of pattern and polarity in the Arabidopsis root. *Cell*; **99**(5): 463-472.

Saito, M., Nurani, A.M., Kondo, Y. and Fukuda, H. (2017). Tissue Culture for Xylem Differentiation with *Arabidopsis* Leaves. Xylem: Methods and Protocols. *Methods in Molecular Biology*; **1544**: 59-65.

Scheres, B., and Wolkenfelt, H. (1998). The *Arabidopsis* root as a model to study plant development. *Plant Physiology and Biochemistry*; **36**: 21-32.

Schubert, D., Primavesi, L., Bishopp, A., Roberts, G., Doonan, J., Jenuwein, T., and Goodrich, J. (2006). Silencing by plant Polycomb-group genes requires dispersed trimethylation of histone H3 at lysine 27. *EMBO J*; **25**: 4638–4649.

Sessions, A., Burke, E., Presting, G., Aux, G., McElver, J., Patton, D., Dietrich, B., Ho, P., Bacwaden, J., Ko, C., Clarke, J.D., Cotton, D., Bullis, D., Snell, J., Miguel, T., Hutchison, D., Kimmerly, B., Mitzel, T., Katagiri, F., Glazebrook, J., Law, M., and Goff, S.A. (2002). A high-throughput *Arabidopsis* reverse genetics system. *Plant Cell*; **14**: 2985–2985.

Shi, Y., Lan, F., Matson, C., Mulligan, P., Whetstine, J.R., Cole, P.A., Casero, R.A., and Shi, Y. (2004). Histone demethylation mediated by the nuclear amine oxidase homolog LSD1. *Cell*; **119**: 941-953.

Srivastava, R., Singh, U.M. and Dubey, N.K. (2016). Histone Modifications by different histone modifiers: insights into histone writers and erasers during chromatin modification. *J. Biol. Sci. Med.*; **2**(1): 45-54.

Stange, L. (1965) Plant Cell Differentiation. *Annu. Rev. Plant. Physiol.*; **16**(1): 119–140.

Steinmann, T., Geldner, N., Grebe, M., Mangold, S., Jackson, C.L., Paris, S., Gälweiler, L., Palme, K. and Jürgens, G. (1999). Coordinated polar localisation of auxin efflux carrier PIN1 by GNOM ARF GEF. *Science*; **286**: 316– 318.

Strahl, B.D. and Allis, C.D. (2000). The language of covalent histone modifications. *Nature*; **403:** 41-45.

Struhl, K. (1998). Histone acetylation and transcriptional regulatory mechanisms. *Genes Dev.*; **12**: 599-606.

Sun, Y., Fan, X.-Y., Cao, D.-M., He, K., Tang, W., Zhu, J.-Y., He, J-X., Bai, M-Y., Zhu, S., Oh, E., Patil, S., Kim, T-W., Ji, H., Wong, W.H., Rhee, S.Y., and Wang, Z-Y. (2010). Integration of BR Signal Transduction with the Transcription Network for Plant Growth Regulation in *Arabidopsis*. *Developmental Cell*; **19**(5): 765–777.

Szekeres, M., Nemeth, K., Koncz-Kalman, Z., Mathur, J., Kauschmann, A., Altmann, T., Redei, G.P., Nagy, F., Schell, J., and Koncz, C. (1996). BRs rescue the deficiency of CYP90, a cytochrome P450 controlling cell elongation and de-etiolation in *Arabidopsis*. *Cell*; **85**: 171–182.

Szemenyei, H., Hannon, M. and Long, J.A. (2008). TOPLESS mediates auxin-dependent transcriptional repression during *Arabidopsis* embryogenesis. *Science*; **319**: 1384–1386.

Takatsuka, H., and Umeda, M. (2014). Hormonal control of cell division and elongation along differentiation trajectories in roots. *Journal of Experimental Botany*; **65**: 2633-2643.

Tanaka, K., Nakamura, Y., Asami, T., Yoshida, S., Matsuo, T., and Okamoto, S. (2003). Physiological roles of BRs in early growth of *Arabidopsis*: BRs have a synergistic relationship with gibberellin as well as auxin in light-grown hypocotyl elongation. *Journal of Plant Growth Regulation*; **22**: 259-271.

Thies, J.E. and Grossman, J.M. (2006). The Soil Habitat and Soil Ecology. Biological Approaches to Sustainable Soil Systems. *CRC Press*, Boca Raton, p. 70.

Townsley, B.T., Covington, M.F., Ichihashi, Y., Zumstein, K. and Sinha, N.R. (2015). BrAD-seq: Breath Adapter Directional sequencing: a streamlined, ultra-simple and fast library preparation protocol for strand specific mRNA library construction. *Front. Plant Sci.*; **6**: 366.

Tsankova, N., Renthal, W., Kumar, A. and Nestler, E.J. (2007). Epigenetic regulation in psychiatric disorders. *Nature Reviews Neuroscience*; **8**: 355-367.

Tsukada, Y., Fang, J., Erdjument-Bromage, H., Warren, M.E., Borchers, C.H., Tempst, P., and Zhang, Y. (2006). Histone demethylation by a family of JmjC domain-containing proteins. *Nature*; **439**: 811–816.

Turner, S., Gallois, P., and Brown, D. (2007). Tracheary element differentiation. *Annu. Rev. Plant Biol.;* **58**: 407-433.

Ubeda-Tomas, S., Federici, F., Casimiro, I., Beemster, G.T., Bhalerao, R., Swarup, R., Doerner, P., Haseloff, J., and Bennett, M.J. (2009). Gibberellin signaling in the endodermis controls *Arabidopsis* root meristem size. *Current biology*; **19**: 1194-1199.

Van den Berg, C., Willemsen, V., Hendriks, G., Weisbeek, P., and Scheres, B. (1997). Short-range control of cell differentiation in the *Arabidopsis* root meristem. *Nature*; **390**: 287-289.

Vert, G., Walcher, C.L., Chory, J., and Nemhauser, J.L. (2008). Integration of auxin and BR pathways by Auxin Response Factor 2. *PNAS USA*; **105**(28): 9829-9834.

Vragović, K., Sela, A., Friedlander-Shani, L., Fridman, Y., Hacham, Y., Holland, N., Bartom, E., Mockler, T.C., and Savaldi-Goldstein, S. (2015). Translatome analyses capture of opposing tissue-specific BR signals orchestrating root meristem differentiation. *PNAS*; **112**(3): 923–928.

Walhout, A.J.M., and Vidal, M. (2001). "High-Throughput Yeast Two-Hybrid Assays for Large-Scale Protein Interaction Mapping." *Methods;* 24(3): 297–306.

Wang, C., Shang, J-X., Chen, Q-X., Oses-Prieto, J.A., Bai, M-Y., Yang, Y., Yuan, M., Zhang, Y-L., Mu, C-C., Deng, Z., Wei, C-Q, Burlingame, A.L., Wang, Z-Y, and Sun, Y. (2013). Identification of BZR1-interacting Proteins as Potential Components of the BR Signaling Pathway in *Arabidopsis* Through Tandem Affinity Purification. *Mol Cell Proteomics*; **12**(12): 3653–3665.

Wang, H., Liu, C., Cheng, J., Liu, J., Zhang, L., He, C., Shen, W-H., Jin, H., Xu, L., Zhang, Y. (2016). *Arabidopsis* Flower and Embryo Developmental Genes are Repressed in Seedlings by Different Combinations of Polycomb Group Proteins in Association with Distinct Sets of Cis-regulatory Elements. *PLoS Genet*.; **12**(1): e1005771.

Wang, X., Zhang, Y., Ma, Q., Zhang, Z., Xue, Y., Bao, S., and Chong, K. (2007). SKB1-mediated symmetric dimethylation of histone H4R3 controls flowering time in *Arabidopsis*. *EMBO J.;* **26**: 1934–1941

Wang, Z.Y., Nakano, T., Gendron, J., He, J., Chen, M., Vafeados, D., Yang, Y., Fujioka, S., Yoshida, S., Asami, T., and Chory, J. (2002). Nuclear-localised BZR1 mediates BR-induced growth and feedback suppression of BR biosynthesis. *Dev. Cell;* **2**: 505–513.

Wang, Z.Y., Seto, H., Fujioka, S., Yoshida, S., and Chory, J. (2001). BRI1 is a critical component of a plasma-membrane receptor for plant steroids. *Nature*; **410**: 380–383.

Weiste, C. and Dröge-Laser, W. (2014). The *Arabidopsis* transcription factor bZIP11 activates auxin-mediated transcription by recruiting the histone acetylation machinery. *Nat. Commun*.; **5**: 3883.

Wysocka, J., Swigut, T., Milne, T.A., Dou, Y., Zhang, X., Burlingame, A.L., Roeder, R.G., Brivanlou, A.H., and Allis, C.D. (2005). WDR5 Associates with Histone H3 Methylated at K4 and Is Essential for H3 K4 Methylation and Vertebrate Development. *Cell*; **121**(6): 859–872.

Xiao, J., Jin, R., Yu, X., Shen, M., Wagner, J. D., Pai, A., & Song, C., Zhuang, M., Klasfeld, S., He, C., Santos, A.M., Helliwell, C., Pruneda-Paz, J.L., Kay, S.A., Lin, X., Cui, S., Fernandez Garcia, M., Clarenz, O., Goodrich, J., Zhang, X., Austin, R.S., Bonasio, R., and Wagner, D. (2017). Cis and trans determinants of epigenetic silencing by Polycomb repressive complex 2 in *Arabidopsis*. *Nature Genetics;* **49**(10): 1546-1552.

Yamaguchi, M., Goue, N., Igarashi, H., Ohtani, M., Nakano, Y., Mortimer, J.C., Nishikubo, N., Kubo, M., Katayama, Y., Kakegawa, K., Dupree, P., and Demura, T. (2010a). VASCULAR-RELATED NAC-DOMAIN6 and VASCULAR-RELATED NAC-DOMAIN7 effectively induce transdifferentiation into xylem vessel elements under control of an induction system. *Plant Physiol*; **153**: 906–914.

Yamaguchi, M., Kubo, M., Fukuda, H. and Demura, T. (2008). Vascular-related NAC-DOMAIN7 is involved in the differentiation of all types of xylem vessels in *Arabidopsis* roots and shoots. *Plant J*.; **55**(4): 652-664.

Yamaguchi, M., Ohtani, M., Mitsuda, N., Kubo, M., Ohme-Takagi, M., Fukuda, H., and Demura, T. (2010b). VND-INTERACTING2, a NAC domain transcription factor, negatively regulates xylem vessel formation in *Arabidopsis*. *The Plant Cell*; **22**: 1249–1263.

Yamamoto, R., Demura, T., and Fukuda, H. (1997). BRs induce entry into the final stage of tracheary element differentiation in cultured *Zinnia* cells. *Plant and Cell Physiology*; **38**: 980–983.

Yao, X., Feng, H., Yu, Y., Dong, A. and Shen, W-H. (2013). SDG2-mediated H3K4 methylation is required for proper *Arabidopsis* root growth and development. *PLOS ONE*; **8**: e56537.

Ye, H., Li, L., Guo, H., and Yin, Y. (2012). MYBL2 is a substrate of GSK3- like kinase BIN2 and acts as a corepressor of BES1 in BR signaling pathway in *Arabidopsis*. *PNAS*; **109**: 20142–20147.

Ye, Z.H. (2002). Vascular tissue differentiation and pattern formation in plants. *Annu. Rev. Plant Biol.*; **53**: 183–202.

Yin, Y., Wang, Z.Y., Mora-Garcia, S., Li, J., Yoshida, S., Asami, T., and Chory, J. (2002). BES1 accumulates in the nucleus in response to BRs to regulate gene expression and promote stem elongation. *Cell;* **109**: 181–191.

Yoshida, S., Iwamoto, K., Demura, T. and Fukuda, H. (2009). Comprehensive analysis of the regulatory roles of auxin in early transdifferentiation into xylem cells. *Plant Mol. Biol.*; **70**: 457-469.

Yoshida, S., Kuriyama, H., and Fukuda, H. (2005). Inhibition of transdifferentiation into tracheary elements by polar auxin transport inhibitors through intracellular auxin depletion. *Plant Cell Physiol.*; **46**: 2019–2028.

Yu, X., Li, L., Li, L., Guo, M., Chory, J. and Yin, Y. (2008). Modulation of BR-regulated gene expression by jumonji domain-containing proteins ELF6 and REF6 in *Arabidopsis*. *PNAS*; **105**(21): 7618-7623.

Yue, M., Li, Q., Zhang, Y., Zhao, Y., Zhang, Z., and Bao, S. (2013). Histone H4R3 Methylation Catalysed by SKB1/PRMT5 Is Required for Maintaining Shoot Apical Meristem. *PLoS ONE*; **8**(12): e83258.

Zentner, G.E. and Henikoff, S. (2013). Regulation of nucleosome dynamics by histone modifications. *Nat. Struct. Mol. Biol.*; **20**: 259-266.

Zhang, D., Jing, Y., Jiang, Z., and Lin, R. (2014a). The Chromatin-Remodeling Factor PICKLE Integrates BR and Gibberellin Signaling during Skotomorphogenic Growth in *Arabidopsis*. *The Plant Cell*; **26**: 2472–2485.

Zhang, D., Ye, H., Guo, H., Johnson, A., Lin, H., and Yin, Y. (2014c). Transcription factors involved in BR repressed gene expression and their regulation by BIN2 kinase. *Plant Signal Behav.*; 9(1): e27849.

Zhang, D., Ye, H., Guo, H., Johnson, A., Zhang, M., Lin, H., and Yin, Y. (2014b). Transcription factor HAT1 is phosphorylated by BIN2 kinase and mediates BR repressed gene expression in *Arabidopsis*. *Plant J.*; 77(1): 59-70.

Zhang, X., Bernatavichute, Y.V., Cokus, S., Pellegrini, M. and Jacobsen, S.E. (2009). Genome-wide analysis of mono-, di- and trimethylation of histone H3 lysine 4 in *Arabidopsis thaliana*. *Genome Biol*.; **10**: R62.

Zhang, X., Clarenz, O., Cokus, S., Bernatavichute, Y.V., Pellegrini, M., Goodrich, J., and Jacobsen, S.E. (2007). Whole-genome analysis of histone H3 lysine 27 trimethylation in *Arabidopsis*. *PLoS Biol*; **5**(5): e129.

Zhang, X., Germann, S., Blus, B.J., Khorasanizadeh, S., Gaudin, V., and Jacobsen, S.E. (2007). The *Arabidopsis* LHP1 protein colocalises with histone H3 Lys27 trimethylation. *Nat*. *Struct*. *Mol*. *Biol*.; **14**: 869–871.

Zhao, J., Peng, P., Schmitz, R.J., Decker, A.D., Tax, F.E., and Li, J. (2002). Two putative BIN2 substrates are nuclear components of BR signaling. *Plant Physiol*.; **130**(3): 1221-1229.

Zhu, J.Y., Li, Y., Cao, D.M., Yang, H., Oh, E., Bi, Y., Zhu, S., and Wang, Z.Y. (2017). The F-box Protein KIB1 Mediates BR-Induced Inactivation and Degradation of GSK3-like Kinases in *Arabidopsis*. *Mol*. *Cell*.; **66**(5): 648-657.

Zuo, J., Niu, Q.W., and Chua, N.H. (2000) Technical advance: An estrogen receptor-based transactivator XVE mediates highly inducible gene expression in transgenic plants. *Plant J;* **24**: 265–273.

6. Appendices

Appendix 1: List of suppliers of all chemicals and reagents used in this study

Reagent	**Suppliers**
2-(N-morpholino)ethanesulfonic acid (MES)	Melford
2-Mercaptoethanol	VWR
2X SYBR Green PCR Mix Lo-ROX	PCR Biosystems
3-Indolacetic Acid (IAA)	Duchefa Biochemie
5-Bromo-4-chloro-3-indolyl-ß-D-galactoside (X-GAL)	Melford
5X First Reaction Buffer	Thermo Fisher Scientific
5X Phusion HF Buffer	PCR Biosystems
Acetic Acid	Thermo Fisher Scientific
Acetone	Scientific Laboratory Supplies
Acetosyringone	Sigma Aldrich
Advance seed and modular compost plus sand	Levington
Agar	Melford
Agarose	Bioline
Ammonium Sulphate	Melford
Bikinin	Selleckchem
Brassinazole (BRZ)	Sigma Aldrich
Bromophenol Blue	Sigma Aldrich
Calcofluor White/ Fluorescent Brightener 28	Sigma Aldrich
Carbenicillin Disodium	Melford
Carboxyl-modified Sera-Mag Magnetic Speed-beads	Thermo Fisher Scientific
Chloral Hydrate	Acros Organics
D-Glucose	Thermo Fisher Scientific
Dimethyl Sulphoxide (DMSO)	Melford
DNA Gel Loading Dye (6X)	Thermo Fisher Scientific
dNTPs	Thermo Fisher Scientific
DTT	Melford
Epibrassinolide (BL)	Sigma Aldrich
Ethanol (EtOH)	Thermo Fisher Scientific
Ethidium Bromide	Thermo Fisher Scientific
Ethylenediamine Tetraacetic Acid (EDTA)	Thermo Fisher Scientific
Gentamycin Sulphate	Melford
Glycerol	Melford
Hydrochloric acid (HCl)	Thermo Fisher Scientific
Hygromycin	Melford
Hyperladder 1kb	Bioline
Kanamycin Monosulphate	Melford
LB Agar High Salt Granulated	Melford
LB Broth High Salt Granulated	Melford
Lithium Acetate (LiAc)	Sigma Aldrich
Murashige & Skoog Medium	Duchefa Biochemie

NTI binding buffer	Macherey-Nagel
Paraformaldehyde	Agar Scientific
PEG 8000	Melford
Periodic acid	Honeywell
Phusion DNA polymerase	Thermo Fisher Scientific
Potassium Ferricyanide	Sigma Aldrich
Potassium Ferrocyanide	Sigma Aldrich
Potassium hydroxide (KOH)	Melford
Propidium Iodide	Sigma Aldrich
Random primers	Thermo Fisher Scientific
RiboLock RNase Inhibitor	Thermo Fisher Scientific
Rifampicin	Melford
Sc Dropout minus Leu	Formedium
Sc Dropout minus Trp	Formedium
Sheared Salmon Sperm DNA	Invitrogen
Sodium Chloride (NaCl)	Scientific Laboratory Supplies
Sodium Deoxycholate	Sigma
Sodium Dodecil Sulfate (SDS)	Melford
Sodium Hydroxide (NaOH)	Melford
Sodium Metabisulphite ($Na_2S_2O_5$)	Thermo Fisher Scientific
ß-estradiol	Sigma Aldrich
Streptavidin Magnetic Beads	New England Biolabs
Sucrose	Melford
RevertAid Reverse Transcriptase	Thermo Fisher Scientific
Synthetic Complete (Sc) Dropout minus ADE, HIS, LEU, TRP	Formedium
Taq Mix Red	PCR Biosystems
Trans-Zeatin	Sigma Aldrich
Tris pH 7.6	Melford
Tris-HCl pH8	Scientific Laboratory Supplies
Triton TX-100	Sigma Aldrich
Tween 20	Melford
Urea	Melford
X-alpha-gal	Apollo Scientific
Xylene Cyanol FF	Thermo Fisher Scientific
Xylitiol	Sigma
Yeast Extract Peptone Dextrose (YEPD)	Formedium
Yeast Nitrogen Base (w/o amino acids)	Formedium
Zirconium silica beads	Thistle Scientific

Appendix 2: Primers used for genotyping PCR

Mutant	Primer Name	Primer sequences
ashh3	LB	ATTTTGCCGATTTCGGAAC
	LP	GTGTCGTATCTTGCTCGCTTC
	RP	TCAAGGCCAAAACAAATCTTG
ashr1	LB	ATTTTGCCGATTTCGGAAC
	LP	TGATCCTTTTGGATCGTAACG
	RP	AGTGCAATAACATGGTGTCGG
atx1	LB	ATTTTGCCGATTTCGGAAC
	LP	AATGAAAGCATGCGGATACAC
	RP	TCCGTGTTGACTGGAAAGATC
atxr5	LB	ATTTTGCCGATTTCGGAAC
	LP	TTTCTCTTGTCCGGTGAAATG
	RP	CCTGCAACAATCAGTGTGATG
clf29	LB	ATTTTGCCGATTTCGGAAC
	LP	AAGAAACTTGCTAGTTCCGCC
	RP	GAGGCATTGACTTTGATTTGC
jmj22	LB	GCTTCCTATTATATCTTCCCAAATTACCAATACA
	LP	TCTTTGCTTGGTGTATTTGCC
	RP	TCGGTTTCATTTCAAGATTCG
ldl1	LB	ATTTTGCCGATTTCGGAAC
	LP	TGTTTCCGTGTAACTTCTGGG
	RP	TTGTTCTTGACGACGACTGTG
suvh8	LB	ATTTTGCCGATTTCGGAAC
	LP	CTGGCAAGTGACAGGAAAATC
	RP	AAACAAAAACAAACACCACGG
suvr1	LB	ATTTTGCCGATTTCGGAAC
	LP	TGGAATCTCGATCAAGTTTGC
	RP	AAACAACGAATTTGCATTTGC
suvr5	LB	ATTTTGCCGATTTCGGAAC
	LP	CATCATCGACGACACAAATTG
	RP	TTGGAAATTCATGTGGAGGAG
swn7	LB	ATTTTGCCGATTTCGGAAC
	LP	TGATTATTGCTCCGTTTCCAC
	RP	CGAGGAATTTTCTAATTCCGG

Gene	Primer sequences
XVE	GCAGGAAGAGGAAGAAGGGT TCAAATCCACAAAGCCTGGC
mGFP5	TTCTTCAAGGACGACGGGAA CCATGTGTAATCCCAGCAGC

Appendix 3: Primers used for hot fusion cloning analysis

Gene	Vector	Primer Sequences
ATXR1	pGADT7	GTACCAGATTACGCTCATATGAGAGGAGAGCAATTCGAGC ATTCATCTGCAGCTCGATTACTCTATGCCAAGAAGAGTC
ATXR5	pGADT7	GTACCAGATTACGCTCATATGGCCACATGGAACGCATCCT ATTCATCTGCAGCTCGATCAGAGGAAGTGATGAGTAGGA
ATXR6	pGADT7	GTACCAGATTACGCTCATATGGTGGCTGTGAGGCGAAGGA ATTCATCTGCAGCTCGATTATACAAAATGTTCAGTTGGA
ASHH1	pGBKT7	CAGAGGAGGACCTGCATATGCAATTTTCTTGTGATCCTG GCTAGTTATGCGGCCGCTCATTTGGCTTCCAAGAGTTTA
BMI1A	*pGADT7*	GTACCAGATTACGCTCATATGGAAGGAGACATGGTGGCTA ATTCATCTGCAGCTCGATTAGTTGTTGCATTCAGGGAGC
	pGBKT7	CAGAGGAGGACCTGCATATGGAAGGAGACATGGTGGCTA GCTAGTTATGCGGCCGCTTAGTTGTTGCATTCAGGGAGC
BMI1B	*pGADT7*	GTACCAGATTACGCTCATATGATGATTAAGGTGAAGAAGG ATTCATCTGCAGCTCGATTACATGTTGCACTCTGGTAGC
	pGBKT7	CAGAGGAGGACCTGCATATGATGATTAAGGTGAAGAAGG GCTAGTTATGCGGCCGCTTACATGTTGCACTCTGGTAGC
CLF	*pGADT7*	GTACCAGATTACGCTCATATGGCGTCAGAAGCTTCGCCTT ATTCATCTGCAGCTCGACTAAGCAAGCTTCTTGGGTCTA
	pGBKT7	CAGAGGAGGACCTGCATATGGCGTCAGAAGCTTCGCCTT GCTAGTTATGCGGCCGCCTAAGCAAGCTTCTTGGGTCTA
EMF2	*pGADT7*	GTACCAGATTACGCTCATATGCCAGGCATTCCTCTTGTTA ATTCATCTGCAGCTCGATCAAATTTGGAGCTGTTCGAGA
	pGBKT7	CAGAGGAGGACCTGCATATGCCAGGCATTCCTCTTGTTA GCTAGTTATGCGGCCGCTCAAATTTGGAGCTGTTCGAGA
FIE	*pGADT7*	GTACCAGATTACGCTCATATGTCGAAGATAACCTTAGGGA ATTCATCTGCAGCTCGACTACTTGGTAATCACGTCCCAG
	pGBKT7	CAGAGGAGGACCTGCATATGTCGAAGATAACCTTAGGGA GCTAGTTATGCGGCCGCCTACTTGGTAATCACGTCCCAG
ATX1	pGADT7	GTACCAGATTACGCTCATATGGCGTGTTTTTCTAACGAAA ATTCATCTGCAGCTCGATTATTCTGCGGTCCAGTCTATT
ATX2	pGADT7	GTACCAGATTACGCTCATATGATTTCAATGTCGTGTGTCC ATTCATCTGCAGCTCGATCAGGACTCTGTCCACTCTTTT
JMJ	pGADT7	GTACCAGATTACGCTCATATGGATTCTGGAGTTAAATTGG ATTCATCTGCAGCTCGATCAAAGAGATAAAAGACTTGCC
	pGBKT7	CAGAGGAGGACCTGCATATGGATTCTGGAGTTAAATTGG GCTAGTTATGCGGCCGCTCAAAGAGATAAAAGACTTGCC
JMJ18	pGADT7	GTACCAGATTACGCTCATATGGAAAATCCTCCATTAGAAT ATTCATCTGCAGCTCGATTACATCAAATCTACTCCGAAA
	pGBKT7	CAGAGGAGGACCTGCATATGGAAAATCCTCCATTAGAAT GCTAGTTATGCGGCCGCTTACATCAAATCTACTCCGAAA
JMJ21	pGADT7	GTACCAGATTACGCTCATATGGATTCTGGAGTTAAATTGG ATTCATCTGCAGCTCGATCAAAGAGATAAAAGACTTGCC
	pGBKT7	CAGAGGAGGACCTGCATATGGATTCTGGAGTTAAATTGG GCTAGTTATGCGGCCGCTCAAAGAGATAAAAGACTTGCC
JMJ22	pGADT7	GTACCAGATTACGCTCATATGCCAAAGTGCAAGAATCTGT ATTCATCTGCAGCTCGATTAGAAAGAAAACTTGAAAGTA
	pGBKT7	CAGAGGAGGACCTGCATATGCCAAAGTGCAAGAATCTGT GCTAGTTATGCGGCCGCTTAGAAAGAAAACTTGAAAGTA
JMJ27	pGADT7	GTACCAGATTACGCTCATATGGAGAAAATGAGAGGGAAGC ATTCATCTGCAGCTCGATTAGGTATCACTGCGTCGGGAG
JMJ30	pGADT7	GTACCAGATTACGCTCATATGTCAGGAGCTACCACCGCTT ATTCATCTGCAGCTCGACTACGAGCTAGAAGATTCTGCT
	pGBKT7	CAGAGGAGGACCTGCATATGTCAGGAGCTACCACCGCTT GCTAGTTATGCGGCCGCCTACGAGCTAGAAGATTCTGCT
LHP1	*pGADT7*	GTACCAGATTACGCTCATATGAAAGGGGCAAGTGGTGCTG ATTCATCTGCAGCTCGATTAAGGCGTTCGATTGTACTTG

	pGBKT7	CAGAGGAGGACCTGCATATGAAAGGGGCAAGTGGTGCTG GCTAGTTATGCGGCCGCTTAAGGCGTTCGATTGTACTTG
	pGADT7	GTACCAGATTACGCTCATATGTCAACAGAGACTAAAGAAA ATTCATCTGCAGCTCGACTAATCAAAGATCTGTCGATTC
LDL1	pGBKT7	CAGAGGAGGACCTGCATATGTCAACAGAGACTAAAGAAA GCTAGTTATGCGGCCGCCTAATCAAAGATCTGTCGATTC
LDL2	pGADT7	GTACCAGATTACGCTCATATGAATTCTCCGGCGTCGGATG ATTCATCTGCAGCTCGATCAATTAAAATGCAGGGGGTTT
	pGADT7	GTACCAGATTACGCTCATATGGGGAAAGACGAAGAGGAAA ATTCATCTGCAGCTCGACTAAGAAGCTTTTGATGGTTCT
MSI1	*pGBKT7*	CAGAGGAGGACCTGCATATGGGGAAAGACGAAGAGGAAA GCTAGTTATGCGGCCGCCTAAGAAGCTTTTGATGGTTCT
PKDM7D	pGADT7	GTACCAGATTACGCTCATATGGGGACAGAGCTAATGAGAA ATTCATCTGCAGCTCGATCAGCGACGGTTCTGGATCTCT
PRMT10	pGADT7	GTACCAGATTACGCTCATATGAGGAGCTCCCAAAACGGCG ATTCATCTGCAGCTCGATCACTCTATGAAGTAAGTCTTC
PRMT1A	pGADT7	GTACCAGATTACGCTCATATGACTAGTACGGAGAACAACA ATTCATCTGCAGCTCGATTAGCGCATCTTATAGAAGTGG
PRMT1b	pGADT7	GTACCAGATTACGCTCATATGACTAAGAACAGTAACCACG ATTCATCTGCAGCTCGATTAACGCATTTTGTAGTGTTGG
	pGADT7	GTACCAGATTACGCTCATATGCCGCTCGGAGAGAGAGGAG ATTCATCTGCAGCTCGACTAAAGGCCAACCCAGTACGAA
PRMT5	pGBKT7	CAGAGGAGGACCTGCATATGCCGCTCGGAGAGAGAGGAG GCTAGTTATGCGGCCGCCTAAAGGCCAACCCAGTACGAA
	pGADT7	GTACCAGATTACGCTCATATGTCGCCTCTGTCTTCTCTTC ATTCATCTGCAGCTCGATCAAGAAATAGTATGAGTGACG
PRMT7	pGBKT7	CAGAGGAGGACCTGCATATGTCGCCTCTGTCTTCTCTTC GCTAGTTATGCGGCCGCTCAAGAAATAGTATGAGTGACG
RING1A	*pGADT7*	GTACCAGATTACGCTCATATGTCTGTCAAGAATAATAGCT ATTCATCTGCAGCTCGATCACTCAGTTTGCTTCTTCCGG
	pGBKT7	CAGAGGAGGACCTGCATATGTCTGTCAAGAATAATAGCT GCTAGTTATGCGGCCGCTCACTCAGTTTGCTTCTTCCGG
RING1B	*pGADT7*	GTACCAGATTACGCTCATATGCCTTCCTTGAAGAGCTTCT ATTCATCTGCAGCTCGACTACGCGATTTGCTTTCTCCGG
	pGBKT7	CAGAGGAGGACCTGCATATGCCTTCCTTGAAGAGCTTCT GCTAGTTATGCGGCCGCCTACGCGATTTGCTTTCTCCGG
	pGADT7	GTACCAGATTACGCTCATATGAGTACATTGTTACCATTTC ATTCATCTGCAGCTCGACTAGTTGCAGATGGCGAGCTTG
SUVH2	pGBKT7	CAGAGGAGGACCTGCATATGAGTACATTGTTACCATTTC GCTAGTTATGCGGCCGCCTAGTTGCAGATGGCGAGCTTG
SUVH5	pGADT7	GTACCAGATTACGCTCATATGGTACATTCAGAGTCATCAA ATTCATCTGCAGCTCGATTAGTAGAGCCTACCACTACAC
SUVR4	pGADT7	GTACCAGATTACGCTCATATGATCAGTCTCTCCGGACTAA ATTCATCTGCAGCTCGATCATTTGCGCTTTTTAGACA
SUVR5	pGADT7	GTACCAGATTACGCTCATATGGAAGTTAAAATGGATGAGT ATTCATCTGCAGCTCGACTAACTTAAGAGACCTCTGCAA
	pGADT7	GTACCAGATTACGCTCATATGGTGACGGACGATAGCAACT ATTCATCTGCAGCTCGATCAATGAGATTGGTGCTTTCTG
SWN	*pGBKT7*	CAGAGGAGGACCTGCATATGGTGACGGACGATAGCAACT GCTAGTTATGCGGCCGCTCAATGAGATTGGTGCTTTCTG
	pGADT7	GTACCAGATTACGCTCATATGTGTAGGCAGAATTGTCGCG ATTCATCTGCAGCTCGATTACTTGTCTCTGCTGTTATTG
VRN2	*pGBKT7*	CAGAGGAGGACCTGCATATGTGTAGGCAGAATTGTCGCG GCTAGTTATGCGGCCGCTTACTTGTCTCTGCTGTTATTG

Plasmids in italics were generated by Dr. De Lucas using Gateway LR clonase technology (Invitrogen).

Appendix 4: Primers used for colony PCR

Primer name	**Sequence**
T7 Promoter Forward	TAATACGACTCACTATAGGG
3'AD Reverse	AGATGGTGCACGATGCACAG
3'BD Reverse	TAAGAGTCACTTTAAAATTTGTATC

Appendix 5: Primers used for BiFC analysis

Gene	**Primer sequences**
BIN2	GGAGGTGGATCTCTTGGCATGGCTGATGATAAGGAGATGC GGCCGCTCTAGAACTAGTACGATTCATCTGCAGCTCGAG
SUVR5	GGAGGTGGATCTCTTGGCATGGAAGTTAAAATGGATGAGT GGCCGCTCTAGAACTAGTACGATTCATCTGCAGCTCGAG
CLF	GGAGGTGGATCTCTTGGCATGGCGTCAGAAGCTTCGCCTT GGCCGCTCTAGAACTAGTACGATTCATCTGCAGCTCGAG
BZR1	GGAGGTGGATCTCTTGGCATGACTTCGGATGGAGCTACGT GGCCGCTCTAGAACTAGTACGATTCATCTGCAGCTCGAG

Appendix 6: Primers used for qPCR

Gene	**Primer Sequences**
UB10	GGCCTTGTATAATCCCTGATGAATAAG AAAGAGATAACAGGAACGGAAACATAGT
E2Fe/DEL1	CCAATCTTCAGATCCCTCCA TCATAAAGCCGCCTCACTTT

Appendix 7: Number of differentially regulated chromatin regions in undifferentiated cells and TEs.

Histone mark	**Undifferentiated cell**	**TE**
H3K4me3	11913	9632
H3K36me2	7289	6006
H3K36me3	10313	7758
H3K27me3	4839	5762
H3R2me3	3472	6295

Appendix 8: Fold change in expression of *E2Fe* in undifferentiated cells and TEs.

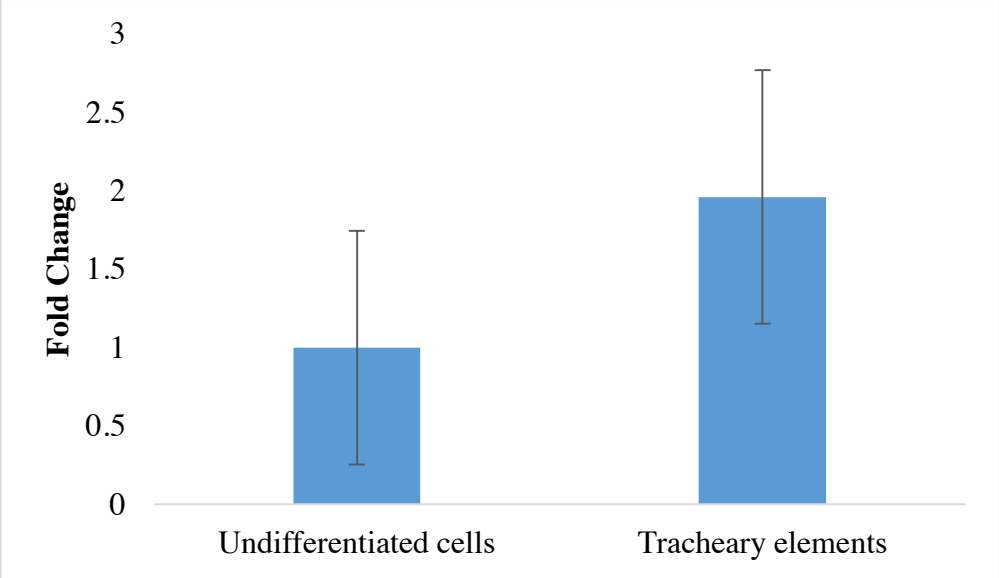

Quantitative real-time PCR analysis of the fold change in expression of *E2Fe* relative to the expression of reference gene *UB10* in undifferentiated and differentiated TEs. Error bars represent the mean +/- SE from three biological and three technical repeats.

Appendix 9: The effect of BR treatment on fold change in expression of *E2Fe* in wildtype Col0 and *suvr5*.

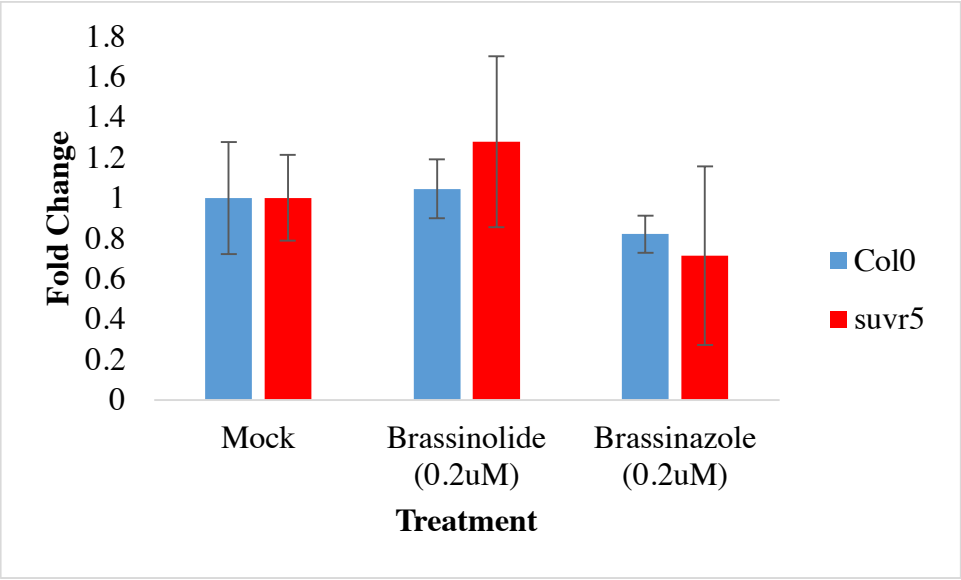

Quantitative real-time PCR analysis of the fold change in expression of *E2Fe* relative to the expression of reference gene *UB10* in brassinolide (BL) and brassinazole (BRZ)-treated wildtype and *suvr5* roots. Error bars represent the mean +/- SE from three biological and three technical repeats.